Development of Performance Properties of Ternary Mixtures: Phase I Final Report

National Concrete Pavement Technology Center

Final Report
December 2007

Sponsored through
Federal Highway Administration;
FHWA Pooled Fund Study TPF-5(117):
California, Illinois, Iowa (lead state), Kansas, Mississippi, New Hampshire, Pennsylvania, Wisconsin, and Utah;
the Portland Cement Association;
Headwaters Resources;
the American Coal Ash Association; and
the Slag Cement Association

ctre
Center for Transportation Research and Education

Iowa State University

The University of Utah

About the National Concrete Pavement Technology Center

The mission of the National Concrete Pavement Technology Center is to unite key transportation stakeholders around the central goal of advancing concrete pavement technology through research, tech transfer, and technology implementation.

Disclaimer Notice

The contents of this report reflect the views of the authors, who are responsible for the facts and the accuracy of the information presented herein. The opinions, findings and conclusions expressed in this publication are those of the authors and not necessarily those of the sponsors.

The sponsors assume no liability for the contents or use of the information contained in this document. This report does not constitute a standard, specification, or regulation.

The sponsors do not endorse products or manufacturers. Trademarks or manufacturers' names appear in this report only because they are considered essential to the objective of the document.

Nondiscrimination Statement

Iowa State University does not discriminate on the basis of race, color, age, religion, national origin, sexual orientation, gender identity, sex, marital status, disability, or status as a U.S. veteran. Inquiries can be directed to the Director of Equal Opportunity and Diversity, (515) 294-7612.

Technical Report Documentation Page

1. Report No. Pooled Fund Study TPF-5(117)	**2. Government Accession No.**	**3. Recipient's Catalog No.**	
4. Title and Subtitle Development of Performance Properties of Ternary Mixtures: Phase I Final Report		**5. Report Date** December 2007 **6. Performing Organization Code**	
7. Author(s) Paul Tikalsky, Vernon Schaefer, Kejin Wang, Barry Scheetz, Tyson Rupnow, Alison St. Clair, Mohamed Siddiqi, and Stephanie Marquez		**8. Performing Organization Report No.**	
9. Performing Organization Name and Address Center for Transportation Research and Education Iowa State University 2711 South Loop Drive, Suite 4700 Ames, IA 50010-8634		**10. Work Unit No. (TRAIS)** **11. Contract or Grant No.**	
12. Sponsoring Organization Name and Address Federal Highway Administration U.S. Department of Transportation 400 7th Street SW, HIPT-20 Washington, DC 20590		**13. Type of Report and Period Covered** Final Report, Phase I **14. Sponsoring Agency Code**	
15. Supplementary Notes Visit www.ctre.iastate.edu for color PDF files of this and other research reports.			

16. Abstract

This report summarizes the findings of Phase I of the research project. The project is a comprehensive study of how supplementary cementitious materials (SCMs), can be used to improve the performance of concrete mixtures. The initial stages of this project consider several sources of each type of supplementary cementitious material (fly ash, slag, and silica fume) so that the material variability issues can also be addressed. Several different sources of portland cement (PC) and blended cement are also used in the experimental program. The experimental matrix includes 110–115 different mixtures; hence, the project is being conducted in three different phases. This report contains a brief literature study to summarize the state of the practice in ternary mixtures. The literature study includes the efforts by state departments of transportation (DOTs) that have utilized ternary mixtures in field work (for example, Ohio DOT, New York State DOT, Pennsylvania DOT, Iowa DOT) to discuss practical concerns about field applications. The initial phase covered in this report is a study with a large scope to identify materials combinations that will likely perform adequately in Phases II and III. Phase I of the study consisted of a 24-month laboratory program that studied the influence of multiple combination and proportions of cement, slag, silica fume, and fly ash on specific performance properties of mortar specimens. Test results are presented in this report. Chemical admixtures (water reducers, air-entraining agents, and accelerators) were included in this phase of the study to compare the effects of ternary mixtures on setting time, water demand, and air content. Phase I results have created the architecture for predicting the performance of ternary systems based on the material properties of the total cementitious system.

17. Key Words Fly ash—slag—silica fume—portland cement—ternary mixtures		**18. Distribution Statement** No restrictions.	
19. Security Classification (of this report) Unclassified.	**20. Security Classification (of this page)** Unclassified.	**21. No. of Pages** 130	**22. Price** NA

DEVELOPMENT OF PERFORMANCE PROPERTIES OF TERNARY MIXES: PHASE I FINAL REPORT

Phase I Final Report
December 2007

Co-Principal Investigators
Vernon R. Schaefer
Professor of Civil, Construction, and Environmental Engineering
Iowa State University

Paul J. Tikalsky
Professor of Civil and Environmental Engineering
University of Utah

Kejin Wang
Associate Professor of Civil, Construction, and Environmental Engineering
Iowa State University

Authors
Paul Tikalsky, Vernon Schaefer, Kejin Wang, Barry Scheetz, Tyson Rupnow, Alison St. Clair, Mohamad Siddiqi, and Stephanie Marquez

Sponsored through
Federal Highway Administration;
FHWA Pooled Fund Study TPF-5(117): California, Illinois, Iowa (lead state), Kansas, Mississippi, New Hampshire, Pennsylvania, Wisconsin, Utah;
The Portland Cement Association; Headwaters Resources; the American Coal Ash Association; and the Slag Cement Association

A report from
National Center for Concrete Pavement Technology
Iowa State University
2711 South Loop Drive, Suite 4700
Ames, IA 50010-8664
Phone: 515-294-5879
Fax: 515-294-0467
www.cptech.org

TABLE OF CONTENTS

LIST OF FIGURES

LIST OF TABLES

ACKNOWLEDGMENTS

This research was conducted under Federal Highway Administration Pooled Fund Study TPF-5(117), involving the following State Departments of Transportation:

- California Department of Transportation
- Illinois Department of Transportation
- Iowa Department of Transportation (lead state)
- Kansas Department of Transportation
- Mississippi Department of Transportation
- New Hampshire Department of Transportation
- Pennsylvania Department of Transportation
- Wisconsin Department of Transportation
- Utah Department of Transportation

The researchers recognize the following partners for sponsoring this research:

- American Coal Ash Association
- Headwaters Resources
- Portland Cement Association
- Slag Cement Association

Finally, the researchers recognize the following companies for their in-kind contributions to this research:

- BASF Admixtures
- Elkem
- Engelhard
- Geneva Rock
- Giant Cement
- Holcim Cement
- Keystone Cement
- Lafarge Cement

EXECUTIVE SUMMARY

Supplementary cementitious materials (SCMs) such as fly ash, ground granulated blast-furnace slag (GGBFS), calcined kaolinite, natural pozzolans, and silica fume, have become common parts of modern concrete practice (PCA 2002; Transportation Research Board 1990). The blending of two or three cementitious materials to optimize durability, strength, or economics provides owners, engineers, materials suppliers, and contractors with substantial advantages over mixtures containing only portland cement (PC). However, these advances in concrete technology and engineering have not been adequately captured in the specification of concrete. Usage is often curtailed because of prescriptive concerns or historical comparisons about how such materials should perform. In addition, SCMs can exhibit significant variation in chemical and physical properties, both within a given source and, more commonly, between sources. Hence, current literature contains contradictory reports concerning the "optimal use" of SCMs. Users need specific guidance to assist them in defining the performance requirements for a concrete application and the selection of optimal proportions of the cementitious materials needed to produce the required durable concrete. The selection process is complicated by the fact that blended cements are currently available in selected regions (ACI 2007). Both portland and blended cements have already been optimized by the manufacturer to provide specific properties (i.e., setting time, shrinkage, strength gain). The addition of SCMs (as binary, ternary, or even more complex mixtures) can alter these properties, and hence, has the potential to impact the overall performance of the concrete.

The project presented herein provides the quantitative information needed to make sound engineering judgments pertaining to the selection and use of SCMs in conjunction with portland or blended cement. This report summarizes the results of Phase I of a three-phase project. The initial phase focused on the paste and mortar properties of 114 ternary mixtures. The results quantify the shrinkage, sulfate resistance, alkali silica reaction (ASR) mitigation, strength development, chemical and physical properties of SCMs, heat signature, and sensitivity to sucrose-based water-reducing admixtures. The result of this work was the identification of 48 cementitious combinations for use in Phase II of the project.

INTRODUCTION

SCMs, such as fly ash, GGBFS, natural pozzolans, calcined kaolinite, and silica fume have become common parts of modern concrete practice (PCA 2002; Transportation Research Board 1990; ACI 2007). The blending of two or three cementitious materials to optimize durability, strength, or economics provides owners, engineers, materials suppliers, and contractors with substantial advantages over mixtures containing only PC. However, these advances in concrete technology and engineering have not been adequately captured in the specifications for concrete. Usage is often curtailed because of prescriptive concerns or historical comparisons about how such materials should perform. In addition, SCMs can exhibit significant variability in chemical and physical properties, both within a given source and, more commonly, between sources. Hence, current literature contains contradictory reports concerning the "optimal use" of SCMs. Users need specific guidance to assist them in defining the performance requirements for a concrete application and the selection of optimal proportions of the cementitious materials needed to produce the required durable concrete. The selection process is complicated by the fact that blended cements are currently available in selected regions. Both portland and blended cements have already been optimized by the manufacturer to provide specific properties (i.e., setting time, shrinkage, strength gain). The addition of SCMs (as binary, ternary, or even more complex mixtures) can alter these properties, and, hence, has the potential to impact the overall performance of concrete. Research is needed to identify and quantify the major factors that govern the performance of mixtures containing multiple SCMs. The focus of the research should be directed at providing tools so users can increase the probability that these various materials will always have a positive impact on the overall durability of the concrete.

Project Goals

The goal of this project is to provide the quantitative information needed to make sound engineering judgments pertaining to the selection and use of SCMs in conjunction with portland or blended cement. This information will lead to a more effective utilization of supplementary materials and/or blended cements enhancing the life-cycle performance and cost of transportation pavements and structures. The efforts of this project will be directed at producing test results that support the following specific goals:

- Provide quantitative guidance for ternary mixtures that can be used to enhance the performance of structural and pavement concrete
- Provide a solution to the cold weather issues that are currently restricting the use of blended cements and/or SCMs
- Identify how to best use ternary mixes when rapid strength gain is needed
- Develop performance-based specifications for concrete used in transportation pavements and structures

Background

Engineers for DOTs throughout the United States have used fly ash and GGBFS (slag cement) as a partial replacement for PC in concrete production on a regular basis since the implementation

of the Resource Conservation and Recovery Act in 1986. The Texas DOT was one of the few DOTs that conducted work to optimize the use of fly ash or slag cement to produce concrete mixtures that meet specific performance objectives prior to 1990 (Tikalsky et al. 1988). For many years most states implemented a strategy that was meant to produce concrete mixtures that exhibit performance similar to mixtures employing only PC. With the growing availability of slag cement and silica fume, and the limited supply of high quality fly ash in some markets, the selection of materials for any given job has become more complicated.

SCMs have the potential to dramatically improve the overall performance of concrete by increasing the longevity of the transportation infrastructure and decreasing the life-cycle cost of that infrastructure. However, the introduction of fly ash, silica fume, or slag cement has periodically resulted in the following technical issues:

- Rapid slump loss
- Unstable air content or inability to retain air
- Uncontrolled cracking with late season paving
- Overpasted or sticky mixtures
- Inability to predict workability and set time in early or late season construction
- Scaling in mixtures containing high dosages of SCMs

Closer inspection of the list and the technical literature suggests that the root issues appear to be related to selection of material combinations, proportioning of cementitious materials, constructability, ambient weather problems, and materials variability problems. However, some detailed discussion with appropriate materials vendors is needed to clarify the reasons for the real or perceived problems and to design solutions that optimize multiple cementitious systems for transportation concrete.

There are currently several ongoing research projects in this area. The Pennsylvania DOT and an industrial consortium have been working with Pennsylvania State University on optimizing performance in bridge deck concrete, using both binary and ternary blends of SCM (Tikalsky et al. 2003). The Texas DOT has conducted detailed studies on optimizing fly ash and PC combinations for selected performance characteristics (Carrasquillo et al. 1986). On a national level, the Federal Highway Administration (FHWA) initiated a major project (Task 64) that will help simplify job-specific mixture design when multiple sources of materials are available. The National Cooperative Highway Research Program (NCHRP) has two projects that are currently in progress that deal with SCMs. The first project is entitled "Supplementary Cementitious Materials to Enhance Durability of Concrete Bridge Decks (Project 18-08A)." The second project is entitled "Improved Specifications and Protocols for Acceptance Tests on Processing Additions in Cement Manufacturing (Project 18-11)."

Outline of Study Phases

Phase I of this study consisted of laboratory experiments that examined the influence of multiple combinations and proportions of cement, slag, silica fume, calcined kaolinite, and fly ash on specific performance properties of mortar specimens. The Phase I testing program used a wide

range of different materials and many different dosage levels. Test results were evaluated to identify material combinations for potential optimums in the various performance responses. Chemical admixtures (water reducers, air-entraining agents, and accelerators) were included in this phase of the study to compare how setting time, water demand, and air content vary with ternary mixtures. Phase I results were used to help create the architecture for predicting the performance of ternary systems based on the material properties of the total cementitious system.

All of the materials used in the study were subjected to bulk chemical and physical testing in accordance with the appropriate American Society for Testing and Materials (ASTM) or American Association of State Highway and Transportation Officials (AASHTO) specifications. In addition, X-ray diffraction (XRD) was used to determine the minerals present in the bulk samples and selected paste specimens. Glass content of the various SCMs and blended cements was estimated using semi-quantitative XRD analysis.

Phase II of the study will use the information obtained from Phase I to select a range of materials and dosages to investigate the effects of cold, hot, and ambient environmental conditions for use in laboratory concrete mixtures. The thrust of Phase II is to apply the mortar study data from Phase I to concrete mixtures and the performance characteristics of pavement and structural concrete. The materials used in both phases will be identical so that the mortar test results can be directly compared to the test results obtained from concrete test specimens. This comparison is needed to provide information pertaining to the selection of appropriate mixture design and performance tests for specification development. It would be desirable to develop mixture design tests using the behavior of mortar specimens that translate well into the performance of concrete. The results of Phase II will be trial performance-based specifications for concrete in transportation applications.

Phase III will be a field demonstration phase where contractors and states will have on-site technical support for using ternary mixtures. After each trial, the performance-based specifications will be reviewed and revised if necessary. The National Concrete Pavement Technology Center's (CP Tech Center) mobile research laboratory will participate in at least one project for each participant state.

LITERATURE REVIEW

Concrete is the world's most used and versatile construction material. Modern concrete is composed of six main ingredients: (1) coarse aggregate, (2) sand, (3) PC, (4) SCMs, (5) chemical admixtures, and (6) water.

Lime-based cements have been used for concretes as early as 7000 BC. Natural cements have been manufactured in the US since the early 1800s with the first being in Rosendale, NY. The first use of portland cement concrete (PCC) in the United States was in the Erie Canal in 1818. Pozzolans have been in use for thousands of years and excellent historical summaries are readily available in the literature (Abdun-Nur 1961; Mielenz 1983; Helmuth 1987; Lea 1971; Massazza 1998).

With the current global demand for PC sustainability on the rise, combined with a need for long life pavements and structures, engineers have looked to alternative binders such as fly ash, silica fume, GGBFS, metakaolin, and rice husk ash to increase pavement durability while lowering life-cycle cost.

Cementitious Materials

The cementitious materials section of the literature review provides a brief background on the materials used in this study including: PC, Class C and Class F fly ash, GGBFS, silica fume, and metakaolin.

Portland Cement

PC is manufactured using several key ingredients including limestone, clay or shale, and gypsum. Limestone provides the necessary calcium oxide while clays and shale provide the iron-bearing aluminosilicates. The materials are pulverized and heated to 1400°C to produce the calcium silicates characteristic of PC. The finished product, clinker, is then ground in ball mills, with added gypsum to prevent false set, and stored in silos until ready for distribution (Lea 1971). ASTM C 150, C 595, and C 1157 specify the chemical and physical requirements of the different types of PCs in the United States.

Ground Granulated Blast Furnace Slag

GGBFS is a predominately glassy material from the iron metal industry and is produced in iron blast furnaces at a temperature of about 1500°C. The molten slag is granulated by rapidly quenching it as it is drawn off the metal. Then the granulated material is ground to a fine particle size prior to being incorporated in mortar or concrete with other hydraulic cements or appropriate activators. Slag is not a basic pozzolan; rather it is cementitious material with both cementitious and pozzolanic properties. The cementitious nature of the GGBFS is much less rapid than that exhibited by PC. GGBFS has been used as a SCM since the early 1900s (Tuthill

1978; Lea 1971). However, it is only during recent years that the material has become widely available nationally. In 2006, approximately 3.5 million tons of GGBFS were sold in the US.

The ASTM specification for GGBFS is C 989 (ASTM 2007). The specification classifies GGBFS into three grades of 80, 100, and 120, based on compressive strength of mortar cubes (slag activity index test). The increasing grades correspond to increasing levels of reactivity or a more rapid strength gain in the slag activity index test. Practical information concerning the use of GGBFS can be found in ACI 233R-95 (ACI 2007). Slag can be used to replace PC in many different mix designs including pavements, structural concrete, and bridge decks. The slag replacement level can vary significantly from about 20% to 60% in some cases. The lower replacement range is typically used when setting time or hardening constraints limit the mix design. Higher replacement rates are generally used when ASR or sulfate resistance is required.

Fly Ash

Fly ash is the most commonly used SCM. Fly ash is the residue collected from the flue gasses exiting the boiler of a pulverized coal-generating station. The fly ash particles are collected in electrostatic precipitators or bag houses and then transferred to a storage silo or sluice pond. Fly ash has a spherical morphology and exhibits a rather wide range of bulk chemical compositions. This wide range of chemical composition has resulted in the creation of two classes of fly ash in ASTM specifications (ASTM 2007), and three classes of fly ash in Canadian Standard Association (CSA) (CSA 1998).

The majority of electricity produced in the United States is produced from the combustion of coal at coal-fired utilities. As a result, over 117 million tons of coal combustion byproducts are produced per year (American Coal Ash Association 2003). The American Coal Ash Association (ACAA) (2003) estimates that 68 million tons of fly ash are produced in the U.S. per annum. The 68 million tons are broken down into the following categories and tonnages (ACAA 2003):

- Bottom ash is approximately 18.7 million tons.
- Boiler slag totals approximately 2.5 million tons.
- Other byproducts are approximated at 24.8 million tons.

ASTM Specifications break fly ash into two classes based on $SiO_2+Al_2O_3+Fe_2O_3$ content. Class F fly ash has a $SiO_2+Al_2O_3+Fe_2O_3$ of 70% or more. Class C fly ash has a $SiO_2+Al_2O_3+Fe_2O_3$ content between 50% and 70%. Class F ashes are typically pozzolanic; however, some authors have noted that they may occasionally exhibit some self-cementitious properties (Majko 1987). Class C fly ashes may exhibit self-cementitious properties (ASTM 2007); however, some authors have expressed concern that this is an oversimplification (Cain 1981; Diamond 1981).

CSA specifications break fly ash into three types based on bulk calcium content (expressed as the oxide CaO). Type F has less than 8% bulk CaO. Type CI fly ash has a CaO content from 8% to 20%. Type CH fly ash has a bulk CaO content greater than 20%. This categorization scheme was created to deal with the fact that many high-calcium fly ashes were not producing some of the beneficial properties normally associated with fly ash, such as increased resistance to sulfate

attack (Dikeou 1975; Dunstan 1980; Tikalsky et al. 1992) and reduction in expansion caused by alkali-silica reaction (ASR) (Manz 1998; Shehata 2002).

Chemical and Physical Properties of Fly Ash

ASTM C618 defines fly ash as the fine residue produced from the burning of ground or powdered coal. Fly ash is collected from the flue gas of coal-fired boilers by the means of an electrostatic precipitator or bag house. Fly ash color may vary from tan to gray (Misra 2000). Self-cementing, Class C fly ash is generally produced from burning low sulfur, subbituminous and lignite coals. Class F fly ash is generally produced from burning bituminous and anthracite coals.

Fly ash particles are typically spherical in nature and contain some crystalline as well as carbonaceous matter (Barnes 1997; Misra 2000). Misra (2000) noted that a large percentage of fly ash is in the form of silica, alumina, ferric oxide, and calcium oxide. ASTM C618 chemical requirements are shown in Table 1.

Barnes (1997) and Misra (2000) state that the pozzolinity of fly ash is mainly dependent upon the fineness of the ash, amounts of silica and alumina, and the presence of moisture and free lime. Winkerton and Pamukcu (1991) also state that density, amount of carbon, temperature, and age also affect the rate of pozzolanic reaction.

Table 1. ASTM C 618 chemical requirements for Class F and Class C fly ash

Oxide	ASTM C 618 Class C fly ash	ASTM C 618 Class F fly ash
SiO_2	Summation between 50% and 70%	Summation greater than 70%
Al_2O_2		
FeO_3		
CaO		
MgO		
Na_2O		
K_2O		
TiO_2		
SO_3	Maximum of 5%	Maximum of 5%
LOI	Maximum of 6%	Maximum of 6%

Mineralogical determinations indicate that fly ash is predominantly glass. In addition, mineralogical determinations via XRD do not suffer the discrepancies in categorization that were

previously mentioned. Typically, the minerals identified in a sample of fly ash give a good indication of the pozzolanic or cementitious nature of the fly ash. Class F (or Type F) fly ashes contain a silicate glass and only a few minerals (alpha-quartz, mullite, a ferrite spinel, and perhaps small amounts of anhydrite and free lime). This glass is relatively insoluble in hydrochloric acid (less than 15% soluble). Class C fly ashes can contain a wide variety of minerals (McCarthy et al. 1984; McCarthy et al. 1990), and several of the minerals hydrate rapidly when mixed with water. This helps explain their self-cementitious behavior. Class C fly ashes tend to be quite soluble in hydrochloric acid (about 70% soluble), and most of the soluble material is related to both the cementitious materials and a high-calcium glass phase. Also, Class C fly ash contains a pozzolanic glass similar to Class F fly ash. Hence, both the mineralogy and bulk chemistry of Class C fly ash tends to be much more complex than that observed for Class F fly ash.

Practical information concerning the use of fly ash can be found in ACI 232.2R-96 (ACI 2007). Other similar sources of information exist (FHWA 1995). Most common mix design procedures rely on strength as the desired output (Kosmatka, Kerkhoff and Panarese 2002). However, as is fully described in the American Concrete Institute (ACI) document, strength does not need to be the primary criterion. Often, one may choose to improve sulfate resistance or minimize expansion caused by ASR. Fly ash replacements vary widely depending on the needs of any given project. Most concrete mixtures formulated for pavements tend to use approximately 15% to 30% fly ash as a cement replacement (ACI 2007; Hanson 2003; Parry 2001). The upper limit appears to be related to scaling issues noted in laboratory research (Parry 2001) but not generally observed in the field. Hence, such constraints may not be critical to states with less severe exposure conditions.

Silica Fume

Silica fume is a byproduct production of the silicon or ferrosilicon metal (Malhotra, 1987; Fidjestol and Lewis 1998). The material may also be referred to as condensed silica fume or microsilica. Particles of silica fume are collected in the bag house exiting a submerged-arc furnace. Hence, silica fume is almost entirely composed of sub-micron sized particles of amorphous silica. The material has both ASTM (ASTM 2007) and CSA (Canadian Standards Association 1998) specifications that describe the tests and specification limits applicable to the material. Silica fume is probably the most expensive of the SCMs that are used in the study; hence, it is available throughout most of the US. Experts in the industry (Wolsiefer 1999) indicate that about 75,000–100,000 tons of silica fume are produced in the US and Canada each year. The production depends heavily on the demand for silicon metal and the number of furnaces that are operational.

Current ASTM C1240 and CSA specifications indicate that the bulk of SiO_2 in the material must be at least 85%. However, there are alloys that do not meet this criterion, and there is still considerable debate on the use of these “non-spec” materials. Silica fume behaves as a pozzolan when mixed with calcium hydroxide or PC. Hence, the chemical reactions that take place when silica fume is mixed with cement (or lime) are reasonably well-understood. The main issues of interest to concrete technology are its tremendous surface area (which requires the use of high-range water reducers, HRWR, in many instances), and the presence of carbon particles in the

material. Both of these properties may cause air-entrainment issues in concrete. Practical information concerning the use of silica fume can be found in ACI 234R-96 (ACI 2007). Silica fume is typically used at quantities between 3% and 8% of the total cementitious materials in high-performance concrete, while a common range for pavement concrete is about 3% to 5%.

Metakaolin

Metakaolin, a calcined kaolinite clay mineral, is a processed pozzolan that can be combined with calcium hydroxide in solution to form calcium silica hydrate. The modern use of metakaolin dates back to 1962 when it was used to supplement PC during construction of the Jupia Dam in Brazil (Pera 2001). During heating, adsorbed water is driven off at 100°C, and the kaolinite decomposes at about 500°C. At 500°C, the hydroxyl groups are lost in the form of water. At temperatures of greater than 900°C, the metakaolin undergoes further reactions forming crystalline compounds of free silica and mullite (Pera 2001; Sabir et al. 2001).

Metakaolin is generally used to enhance concrete properties (Potgieter-Vermaak and Potgieter 2006). Concrete property improvements include the following: increased compressive strength, improved sulfate resistance, suppressed ASR expansion (Ramlochan et al. 2000), and reduced permeability. Through research, Frias and others (2000) noted increased heat of hydration when incorporating metakaolin. The researchers noted that heat of hydration curves for metakaolin concrete can be obtained to closely match heat of hydration curves for PCC when the metakaolin is incorporated at amounts less than 10% by weight.

The use of metakaolin in concrete tends to increase the water demand requiring a larger dosage of water-reducing admixture (Zhang and Malhotra 1995; Sabir et al. 2001). Zhang and Malhotra (1995) also noted an increased demand for air-entraining admixture comparable to a silica fume concrete. Metakaolin is beneficial in reducing drying shrinkage when compared to silica fume concrete.

Optimum ranges for metakaolin addition depend upon desired properties. Research conducted by Vu et al. (2001) noted the optimum to be 15% to 25% for compressive strength. Ramlochan et al. (2000) noted that 15% replacement is sufficient to prevent deleterious ASR expansion.

Admixtures

Admixtures are defined in ASTM C 125 as ingredients used in concrete other than materials such as water, aggregates, cement, and fiber reinforcement (Mindess et al. 2003). Such admixtures provide benefits by reducing cost, achieving sought properties, and helping to maintain quality concrete. More extensive classifications of each admixture can be found in various ASTM specifications (Kosmatka et al. 2002).

Air Entraining Agents

Air-entraining agents are specifically used to improve durability in freeze-thaw conditions and environments that expose concrete to deicing chemicals, as well as to improve workability. The

agent stabilizes small air bubbles (0.002 to 0.05 inches in size) in concrete to help protect against damage induced by expansion of freezing pore water. Satisfactory frost protection can generally be obtained with an air content range of 4% to 8% by volume of concrete (Mindess et al. 2003).

Air-entraining admixtures consist of salts of wood resins (Vinsol resin), synthetic detergents, salts of sulfonated lignin, salts of petroleum acids, salts of proteinaceous material, fatty and resinous acids and their salts, alkylbenzene sulfonates, and salts of sulfonated hydrocarbons. These admixtures are defined in ASTM C 260 and AASHTO M 154.

Water Reducers

Water reducers lower the amount of water required to attain a given slump, or simply reduce the water demand (Mindess et al. 2003). Therefore, the use of this admixture can reduce the water-cement ratio which will essentially increase the strength but can also increase the drying shrinkage (Kosmatka et al. 2002).

There are three broad classifications for water reducers used by manufacturers: low-range, mid-range, and high-range. The regular or low-range water reducer can reduce the water content by approximately 5% to 8%, while the mid- and high-range water reducers have higher percentages of reduction. Materials for water-reducing admixtures can consist of lignosulfonates, melamines, hydroxylated carboxylic acids, or carbohydrates. Performance specifications for regular water reducers can be found in ASTM C 494.

Roberts and Taylor (2007), Sandberg and Roberts (2005), and Wang et al. (2006) have studied some interaction issues with the combined use of PC, SCMs, and admixtures. They suggest these problems are associated with low system sulfate contents which are insufficient to control aluminate reactions, which, at the same time, are accelerated by some water-reducing admixtures.

In depth, Roberts and Taylor (2007) indicate that high-calcium fly ashes may contain calcium aluminates, which require additional sulfates to control their reactions. Sandberg and Roberts (2005) also describe SCMs as having larger surface areas due to their fineness, which also effectively increases the amount of sulfate required. Sandberg and Roberts (2005) noted that increasing the rate of hydration requires a greater amount of soluble calcium sulfate to control the aluminate hydration. Roberts and Taylor (2007), Sandberg and Roberts (2005), and Wang et al. (2006) each conclude that the combined use of SCMs and admixtures can severely delay strength development within a concrete mixture.

Roberts and Taylor (2007) and Sandberg and Roberts (2005) compared the heat flow versus time for a plain Type I cement, a mix with 68% cement and 32% Class C fly ash, and the same binary mixture with 325mL/100kg cementitious Type A water reducer. These graphs were drawn to show silicate hydration which is the second peak in the heat flow versus time graph. The cement alone hydrated normally with the silicate hydration peak of 3.0 mW/g at eight hours. When the Class C fly ash was added there was a reduction in silicate hydration heat with a second peak of

1.25 mW/g at 12 hours. No visible silicate reaction was seen in the binary mixture with the Type A water reducer.

Wang et al. (2006) also looked at cement hydration for a Type I cement, a Type I cement and 20% Class F fly ash with 2.6mL/kg Type A water reducer and Type B retarder, and a Type I cement and 20% Class C fly ash with 0.04 oz./lb (2.6 mL/kg) Type A water reducer and Type B retarder. Each chemical was added on a cement mass basis and a cementitious mass basis. The plain Type I cement silicate hydration peak occurred around 5 mW/g at eight hours. The Class F fly ash peak with the chemicals added by a cement mass base occurred later with an energy release rate of 4 mW/g at 14 hours. The Class F fly ash with the admixtures added by a cementitious mass base had a lower peak with 3.25 mW/g at 17 ½ hours. The total hydration of heat for the mixture containing the Class C fly ash was significantly depressed compared to the other mixtures. The peak based on the cement mass had an energy release rate of 3.5mW/g at 17 hours while the peak based on the cementitious mass had a rate of 3 mW/g at 21 hours.

Roberts and Taylor (2007), Sandberg and Roberts (2005), and Wang et al. (2006) each suggest it is important for the producer of the mixture to stay within the recommended limits of admixture dosage rates. Roberts and Taylor (2007) describe doubling or even tripling a recommended dosage has been found to delay the silicate peak causing retardation. Dosages of mixtures combining SCMs and admixtures should be limited and may need to be reduced to avoid early strength development problems.

Engineering Properties

The engineering properties section of the literature review is composed of four main parts dealing with the effect of SCMs on workability, heat of hydration, durability, and strength development.

Workability

Fresh concrete properties are important to a contractor for ease of placement and finishing. It is important to ensure proper air entrainment, as well as the desired workability to achieve a durable concrete.

The use of certain SCMs has been found to enhance the workability properties of PCC through synergy. Kashima et al. (1992) noted that the use of high contents of slag and fly ash allowed for the longer flow distances and the longer retention in flowability required for underwater bridge footings. In a study where workability was a secondary variable, the mixtures containing fly ash and GGBFS were shown to have improved workability when compared to mixtures containing silica fume (Swamy and Laiw 1995).

In a study completed by Collepardi et al. (2000), material fineness and its effect on the workability of concrete was studied. The results showed that an increase in the cementitious materials' fineness required an increase in superplasticizer to achieve the desired workability.

The round fly ash particles are reported to have a plasticizing effect on concrete rheology. Results obtained by Bhanumathidas and Kumar Mehta (2001) note that for mixtures produced with 50% total replacement, 40% fly ash, and 10% rice husk ash, increasing the fly ash content produced a more workable concrete. Results also showed that bleeding was reduced significantly when rice husk ash was introduced.

Heat of Hydration

Through the course of cement hydration, a significant amount of heat is produced. The heat produced causes thermal expansion and subsequent contraction with cooling of the concrete structure, potentially leading to thermal cracking. Thermal cracking is an issue that is encountered most when dealing with large concrete mass structures.

Addition of SCMs, such as GGBFS and fly ash, lowers the heat generated during hydration, thus reducing the potential for thermal cracking. Kashima and others (1992) noted that ternary blended cement with GGBFS and fly ash adequately produced a concrete with a low adiabatic temperature rise of 47.9°C—about a 75% reduction when compared to a normal PCC mixture.

The Fancuo Hydropower Station located in China incorporated both fly ash and silica fume. Fly ash was incorporated to lower the heat of hydration while the silica fume was added to increase abrasion resistance and strength. Both materials reduced concrete permeability. Results showed a 25% fly ash replacement rate increased the setting time and greatly lowered the heat of hydration (Baoyu et al. 1989).

Frias et al. (2000) noted the increased heat of hydration when incorporating metakaolin. They noted that heat of hydration curves for metakaolin concrete can be obtained to closely match heat of hydration curves for PCC when the metakaolin is incorporated at amounts less than 10% by weight.

Durability

Research has shown that the use of SCMs has several benefits to PCC directly affecting durability, including refined pore structure, lower permeability, and increased strength. The refined pore structure and reduced permeability are attributed to the pozzolanic reaction products formed, leading to a more dense paste structure found by Torii and Kawamura (1992). Some of the negative aspects of SCM replacement associated with durability include increased tendency for plastic and thermal shrinkage cracks, increased carbonation, and an increase in deicer scaling at early ages. In a study completed by Khatri and Sirivivatnanon (2001), the optimum fly ash content for chloride resistance durability in aggressive environments was determined to be about 40% replacement rate. The replacement rate dropped to 30% in mild chloride environments.

While much literature is available noting the benefits of SCM replacement for a more durable concrete, it is important to note that other factors affect durability as well. Other factors affecting durability include: water to cementitious materials ratio (w/cm), mix proportions, construction sequence, and finishing techniques (Mehta 1998).

Talbot et al. (1995) note that the use of fly ash in high replacement rates can reduce resistance to deicer salt scaling, even with reduced water to cementitious materials ratios. Although Talbot et al. note decreased resistance to salt scaling when using high volume fly ash and GGBFS replacements, they observed a reduction in capillary pore structure inferring a reduced permeability. Results obtained by Bijen et al. (1989), and Papadakis (2000) showed carbonation rates proceeding quickly, but then slow rapidly due to a denser pore structure attributed to pozzolanic reactions.

Taylor et al. (1995) implemented a study to establish performance criteria for a smelter project in South Africa. Several mixes were produced over a range of w/cm and then subjected to durability testing after a short curing period. Materials included Type I PC, Type III PC, GGBFS, Class F fly ash, and silica fume in the powder and slurry form. Durability testing included Autoclam air permeability and chloride conductivity. The test results showed that there is no difference in durability when comparing the two forms of silica fume; and poor curing of the GGBFS and fly ash mixtures produced poor air permeability results, showing that curing is of utmost importance. Chloride permeability results showed that the silica fume mixtures outperformed all other mixtures for the limited curing provided.

A study conducted by Swamy and Laiw (1995) showed that w/cm has an effect on chloride ion penetration depth. The authors also noted that the chloride concentration profile is essentially the same shape for all concrete mixtures. Chloride penetration depth was shown to be reduced for those concretes with fly ash, GGBFS, or silica fume. The results showed that the silica fume concrete showed the greatest reduction in chloride penetration depth followed by the GGBFS concrete and fly ash concrete respectively. Similar results were obtained by Torii et al. (1995) for a study including calcium chloride. Ganesh Babu and Sree Rama Kumar (2001) investigated the effects of GGBFS in aggressive marine environments. The results showed that to produce a concrete containing GGBFS resistant to the harsh chloride environment, a 50% replacement rate was needed.

Ramezanianpour et al. (1998) studied the performance of concretes with SCMs under cyclic wetting and drying. Using a constant w/cm of 0.4 and a superplasticizer to keep a medium slump, several concrete mixtures were produced. SCMs included silica fume and GGBFS as well as diatomite and trass. Cyclic wetting and drying were used to simulate Persian Gulf conditions. Chloride and sulphate content were tested at four months to determine corrosion rates. The results showed that specimens subjected to the cyclic wetting and drying in sea water had higher chloride values; and the addition of SCMs improved the performance.

Environmental sulfate attack can damage concrete due to the formation of gypsum, ettringite, and thaumasite leading to spalling, strength reduction, and mass loss at low temperatures. Borsoi and others (2000) completed a study investigating the effects of a tricalcium aluminate-free PC with fly ash and GGBFS on thaumasite formation. The results showed that after five years of exposure to MgSO4, there appeared to be little to no surface damage. XRD analysis confirmed neither ettringite nor thaumasite were present near the concrete surface.

In a study completed by Lynsdale and Khan (2000), the effects of fly ash and silica fume on chloride and oxygen permeability were studied. PC was replaced by both fly ash and silica fume

to form a ternary system. The results showed that incorporation of fly ash and silica fume decreased the chloride permeability gradually from 7 to 90 days. Silica fume was shown to be better than fly ash at reducing permeability at later ages. The results showed that the ternary blends reduced permeability at both early and later ages. The oxygen permeability results showed that fly ash had little effect, but silica fume had a significant effect on the reduction of oxygen permeability.

Ramlochan, Thomas, and Gruber (2000) noted increased durability of concrete incorporating metakaolin. Results showed 10% to 15% replacement of PC with metakaolin may be sufficient to control deleterious ASR expansion. Results showed reduction in ASR expansion occurred due to entrapment of alkalis by the supplementary hydrates and a decrease in the pH of the pore solutions.

Gruber et al. (2001) showed incorporation of metakaolin decreased chloride permeability of concrete. The level of reduction averaged 50% to 60% for mixes containing 8% and 12% metakaolin, respectively.

Strength Development

Strength development of PCC is affected by several factors, including mixture proportions, cement and admixture chemistry, temperature, and curing conditions. Giergiczny (1992) noted that elevated curing temperatures and pressures produced elevated strengths when compared to low pressure steam curing.

The use of SCMs can significantly affect the strength development of PCC. Generally, the use of SCMs tends to slightly decrease the early-age strengths and increase the long-term strengths, as is the case with fly ashes and GGBFS. Silica fume and metakaolin on the other hand tend to increase the strength of PCC at all ages.

Kelham et al. (1995) tested several pastes and mortars for compressive strength development. The results showed a reduction in strength when ground limestone was added about equal to the percentage of limestone added. The GGBFS was shown to increase strengths after seven days while the fly ash did not contribute to strength development until greater than 28 days.

In a study undertaken by Collepardi et al. (2000) to establish the engineering properties of concrete containing combinations of Class F fly ash, silica fume in the powder form, and combinations of GGBFS and silica fume, compressive and flexural strength was measured. The testing results showed the fly ash-silica fume strengths lagged behind the GGBFS-silica fume strengths after one day. Swamy and Darwish (1998) noted that all fly ash–silica fume and GGBFS–silica fume samples attained the target strength of 40 MPa at seven days and 50 MPa at 28 days. The results also showed increase in flexural and compressive strength due to pozzolanic activity, except in those samples exposed to air. The authors noted that exposure to air caused cessation of pozzolanic activity.

Temperature plays an important factor in compressive strength gain, as shown in a study completed by Collepardi et al. (2000). Four concretes with up to 50% mass replacement of cement with fly ash and GGBFS were cured at 5°C and 20°C. The results showed higher strengths for those samples cured at 20°C. Strengths were found to increase slightly when incorporating ground fly ash when compared to normal fly ash and strengths improved more so when incorporating GGBFS.

A project completed in Olvarria, Argentina compared a normal PC to a limestone PC with a high activity GGBFS (Menedez et al. 2002). The limestone PC contained 18% ground limestone powder. The limestone powder is not a pozzolan, but provides nucleation sites for calcium hydroxide crystals. The limestone powder was used to improve early age strength while the GGBFS was used to improve long term strength. The results show addition of limestone powder and GGBFS improved the early and later age strengths. Addition of the GGBFS also increased slump retention providing a more workable concrete.

A study completed by Shiathas et al. (2003) compared the properties and durability of binary and ternary cementitious systems and found that metakaolin increased compressive strength rapidly and reduced chloride ion penetration. The results also showed GGBFS reduced early age strengths and exhibited higher permeability values at early ages, but showed later age values comparable to the control mixture of normal PC.

Literature points noted increased strengths when incorporating metakaolin as a mineral admixture (Zhang and Malhotra 1995; Wild et al. 1996; Curcio et al. 1998). Results showed faster compressive strength gain when compared to silica fume up to 28 days. Results obtained by Wild et al. (1996) showed an optimum replacement rate for metakaolin to be about 20% for long term strength gain.

METHODS

ASTM Standards

The following ASTM standards were used in determining the chemical characteristics of the cementitious materials and the physical characteristics of the sand used in this study:

- ASTM C 128 [Standard Test Method for Density, Relative Density (Specific Gravity), and Absorption of Fine Aggregate]
- ASTM C 150 [Standard Specification for Portland Cement]
- ASTM C 204 [Standard Test Method for Fineness of Hydraulic Cement by Air-Permeability Apparatus]
- ASTM C 311 [Standard Test Methods for Sampling and Testing Fly Ash or Natural Pozzolans for Use in Portland-Cement Concrete]
- ASTM C 595 [Standard Specification for Blended Hydraulic Cements]
- ASTM C 618 [Standard Specification for Coal Fly Ash and Raw or Calcined Natural Pozzolan for Use in Concrete]

- ASTM C 989 [Standard Specification for Ground Granulated Blast-Furnace Slag for Use in Concrete and Mortars]
- ASTM C 1240 [Standard Specification for Use of Silica Fume as a Mineral Admixture in Hydraulic Cement Concrete, Mortar, and Grout]

The following standards were used in the mixing and development of the performance properties of the ternary cementitious systems. Deviations from the standard are noted.

- ASTM C 109 / C 109M [Standard Test Method for Compressive Strength of Hydraulic Cement Mortars (Using 2-in. or [50-mm] Cube Specimens]
- ASTM C 157 / C 157M [Standard Test Method for Length Change of Hardened Hydraulic-Cement Mortar and Concrete]
- ASTM C 185 [Standard Test Method for Air Content of Hydraulic Cement Mortar] *Deviated by using a non-standard sand gradation
- ASTM C 187 [Standard Test Method for Normal Consistency of Hydraulic Cement]
- ASTM C 191 [Standard Test Method for Time of Setting of Hydraulic Cement by Vicat Needle]
- ASTM C 305 [Standard Practice for Mechanical Mixing of Hydraulic Cement Paste and Mortars of Plastic Consistency]
- ASTM C 403 / C 403M [Standard Test Method for Time of Setting of Concrete Mixtures by Penetration Resistance]
- ASTM C 1012 [Standard Test Method for Length Change of Hydraulic-Cement Mortars Exposed to a Sulfate Solution]
- ASTM C 1437 [Standard Test Method for Flow of Hydraulic Cement Mortar]
- ASTM C 1567 [Standard Test Method for Determining the Potential Alkali-Silica Reactivity of Combinations of Cementitious Materials and Aggregate (Accelerated Mortar-Bar Method

X-ray Diffraction (XRD) Testing Method

XRD was performed using a Bruker (SIEMENS) D 500 X-ray diffractometer. The instrument was configured with Bragg-Brentano geometry, 1° fixed divergence and 0.05° medium resolution detector slits, diffracted beam monochromater tuned to Cu K-alpha radiation, scintillation detector and a pulse-height analysis (PHA) circuit. The source operated at 27 kV / 50 mA and the target was a Cu fine focus with a 1.5kW maximum power side-window tube. The instrument consisted of a cavity mount specimen holder 25.4 mm diameter by 5 mm deep in dimensions. The sample was prepared as a power mount which was back-loaded on a frosted glass surface. Data results were collected by a step-scan mode which operated at 3 seconds / 0.05°2Θ. Jade 7.0 was used for analysis of the data.

XRF Testing Method

X-ray fluorescence (XRF) analyses were performed using a Panalytical (Philips) PW-2404 X-ray Spectrometer. The source target was an Rh end-window X-ray tube with maximum power of 4

kW. XRF analyses ran at a constant power of 3600 watts while changing the kV (mA) settings to optimize excitation of the various elements.

Two sample preparation techniques were used for XRF analysis: fused disk and pressed pellets. PC, fly ash, and natural pozzolans were prepared using the fused disk technique. The fused disk technique consisted of combining a fixed amount of sample with lithium tetraborate and fusing the flux-sample mixture into a glass disk. Other SCMs such as GGBFS and silica fume used the pressed pellet technique due to the reduced amount of sulfur present in the samples. The pressed pellet technique consisted of using a fixed amount of sample with a binder made up of X-ray mix powder and boric acid, and then pressing the sample to construct a "pellet."

SuperQ 3.0j was used for analysis of the data. Fundamental parameter (FP) calculations based on the Sherman equation were used to compensate for interelement effects, such as absorption and enhancement in the fused disks and pressed pellets, which are included in the Super Q software.

Air Void Analyzer (AVA) Testing Method

The AVA testing method followed is similar to the procedure recommended by the AASHTO AVA Technical Implementation Group (TIG) (2003) except for the sampling method. In lieu of a vibrating cage sampler, the research team hand-packed the syringes with prepared mortar.

The AVA testing procedure involves placing water into the riser column. The bottom of the column is then filled with glycerol using a special funnel. The mortar sample is injected into the glycerol and a magnetic stir bar mixes the glycerol and mortar for 30 seconds. The air voids released during and after mixing are recorded on an inverted glass dish as a change in mass over time. The test can take up to 30 minutes to complete; and the software displays the cumulative distribution of air voids, a histogram of the air voids, and calculated values of spacing factor and specific surface.

Heat Generation

For determination of heat generated, the mortar was mixed as above and then transferred to 4 x 8 in. cylinders. A t-wire thermocouple was inserted to the center of the cylinder. The samples, usually eight, were placed into a curing chamber with an air temperature of 70°F ± 2°F and the temperature change was recorded every minute for about 24 hours. The data was then reduced using spreadsheet software.

Laser Particle Size Analysis

Particle size analyses are based on diffraction as particles pass through a laser beam. As the particles interact with the beam, light will scatter at different angles according to the particles' size. For example, as particle size decreases, the scattering light angles will increase. Detectors measure the light pattern over several angles. The particle sizes are then calculated based on an optical model.

The Mie Theory is a common model used which predicts the scattering intensities for small and large, transparent and opaque particles. This theory describes the intensity predicted by the refractive index difference between particles and a dispersion medium (Kippax 2007).

Incompatibility

Incompatibility tests were conducted on 10 mix designs for determination of potential compatibility issues regarding the air void system and set time characteristics. For the set time tests, ASTM C 191 was used. The proportion needed to obtain normal consistency was determined for a mix containing 100% Type I PC. The same proportions (mass of water and cementitious material) were used for the 10 mixtures tested. Each mixture design was investigated using MB VR Standard AEA (1.3 mL/kg) with a normal dose of Pozzolith 200N (2.3 mL/kg) and PS-1466 (2.6 mL/kg). The dosage rates of the water reducer were also doubled.

For the determination of the air void structure, the 10 mixtures were produced using each combination of water reducer and AEA producing six mixes for each one mixture, or 60 total mixtures. Dosage rates for the MB VR Standard, MB AE 90, and Microair were 1.3 mL/kg, 1.3 mL/kg, and 0.49 mL/kg, respectively. Dosage rates for the Pozzolith 200N and PS-1466 were 2.3 and 2.6 mL/kg, respectively. The AVA was then used to determine the air void structure on freshly mixed mortar.

MATERIALS

This section describes the materials used throughout this study and is broken down into the areas of cementitious materials, SCMs, sand, and admixtures.

Cementitious Materials

The PCs used in this study came from varying sources and included both Type I and blended cements. At the onset of the project, it was determined that the research team needed sufficient quantities of each cement for use in Phase I and Phase II. The cements were placed into 50-gallon re-sealable drums. Materials were first shipped to Penn State and then to Iowa State for use in laboratory testing. Table 2 shows the XRF results for the cements included in the study.

Table 2. XRF results for all cements used in Phase I

Chemical (%)	Type I/II	Type ISM	Type I	Type IPM	Type IP	Ternary
CaO	63.00	61.46	61.71	59.15	50.88	53.15
SiO_2	20.70	21.66	19.80	24.91	28.88	26.37
Al_2O_3	4.16	4.55	6.18	4.38	8.19	5.90
Fe_2O_3	3.13	3.08	2.50	3.12	3.70	2.61
MgO	3.02	3.45	2.76	1.36	1.60	4.80
K_2O	0.75	0.69	0.74	0.56	0.90	0.38

Na_2O	0.09	0.10	0.36	0.22	0.35	0.24
SO_3	2.84	2.85	2.63	3.33	2.74	3.03
P_2O_5	0.10	0.10	0.21	0.11	0.22	0.14
TiO_2	0.33	0.36	0.28	0.29	0.44	0.35
SrO	0.05	0.05	0.24	0.10	0.20	0.09
Mn_2O_3	0.56	0.54	0.11	0.18	0.20	0.26
LOI	1.26	1.08	2.37	1.60	1.14	1.54
Total	99.99	99.97	99.91	99.31	99.40	98.80
C_3S	58.70	--	48.10	--	--	--
C_2S	15.10	--	20.40	--	--	--
C_3A	5.70	--	12.20	--	--	--
C_4AF	9.50	--	7.60	--	--	--

Supplementary Cementitious Materials

The SCMs were chosen to provide a wide range of material behavior. Three fly ashes, two GGBFS, along with metakaolin and silica fume were chosen for this project. Table 3, Table 4, Table 5, and Table 6 show the XRF results for the fly ashes, GGBFS, metakaolin and silica fume, respectively.

Table 3. XRF results for all fly ashes with ASTM C 618 requirements

Chemical (%)	Port Neal #4	Coal Creek	Cayuga	Class F	Class C
SiO_2	34.02	51.40	45.05	Sum 70% Min	Sum 50% Min
Al_2O_3	18.20	16.21	23.71		
Fe_2O_3	6.59	6.73	16.43		
CaO	27.18	13.15	3.78		
Na_2O	1.56	2.86	0.80		
MgO	5.06	4.41	0.88		
P_2O_5	1.29	0.15	0.24		
SO_3	2.70	0.80	0.68	5.0% Max	5.0% Max
K_2O	0.35	2.33	1.46		
TiO_2	1.57	0.63	1.15		
SrO	0.50	0.33	0.18		
Mn_2O_3	0.06	0.05	0.03		
BaO	0.82	0.59	0.10		
LOI, %	0.27	0.05	5.39	6.0% Max	6.0% Max
Total	100.17	99.69	99.89		

Table 4. XRF results for Grade 100 and 120 GGBFS with ASTM C 989 requirements

Chemical	Grade	Grade	ASTM C

(%)	120	100	989
SiO_2	36.81	37.40	
Al_2O_3	9.66	8.98	
Fe_2O_3	0.61	0.76	
CaO	36.77	36.86	
MgO	10.03	10.60	
S	1.10	1.03	2.5% Max
Na_2O	0.31	0.29	
K_2O	0.35	0.40	
TiO_2	0.49	0.38	
P_2O_5	0.01	0.02	
Mn_2O_3	0.39	0.73	
SrO	0.05	0.04	

Table 5. XRF results for metakaolin with ASTM C 618 requirements

Chemical (%)	Metakaolin	ASTM C 618
SiO_2	51.95	Sum 70% Min
Al_2O_3	44.27	
Fe_2O_3	0.41	
TiO_2	1.44	
Na_2O	0.16	
MgO	0.05	
P_2O_5	0.08	
SO_3	0.02	4.0% Max
K_2O	0.14	
CaO	0.06	
SrO	<0.01	
Mn_2O_3	<0.01	
BaO	<0.01	
LOI, %	0.31	10.0% Max
Total	98.91	

Table 6. XRF results for silica fume with ASTM C 1240 requirements

Chemical (%)	Silica Fume	ASTM C 1240
SiO_2	97.90	85.0% Min
Na2O	0.12	
MgO	0.21	
Al_2O_3	0.18	
P_2O_5	0.12	
SO_3	0.17	

Cl	0.09
K_2O	0.59
CaO	0.42
MnO	0.03
Fe_2O_3	0.07
ZnO	0.08
SrO	0.01
BaO	0.02

Materials Analysis

Mortar mixtures containing ternary cementitious materials were grouped based on their chemistry: C, S, and A. C consisted of the chemicals CaO, MgO, K_2O, Na_2O, and Mn_2O_3. S comprised SiO_2 combined with P_2O_5. A comprised Al_2O_3 combined with Fe_2O_3. The three principal components were normalized to 100%.

To calculate these components, each ternary mixture was broken down into its separate materials, such as cement and SCMs. The percentage of each material within the mixture was used to calculate the C, S, and A each material contributed to the mixture. The values of each material within a mixture were added together to come up with the C, S, and A chemistry for the ternary mixture. For example, the ternary mixture 60TI/20C/20F contains 60% by mass of Type I cement, 20% by mass of Class C fly ash, and 20% by mass of Class F fly ash. Therefore, 60% of the grouped C, S, and A components of the Type I cement were added with 20% of the grouped C, S, and A components of the Class C and Class F fly ash. The normalized C, S, and A proportions of each mixture are shown in Appendix A.

Ternary diagrams were developed to show the compositional variability for the ternary mixtures using the normalized oxide components in the system C, S, and A. Each ternary and control mixture was plotted on a ternary diagram. For each mixture plotted on the ternary diagram, x-y coordinates of the mixture data point were taken in reference to a specific datum point. The x-y coordinates of each mixture were plotted on a contour map with the z axis of the map being the compressive strength or shrinkage. Specific isopac maps of each separate SCM were developed. The above referenced ternary plots can be found in St. Clair (2007).

Sand

Natural river sand was used for the fine aggregate and had a fineness modulus and absorption of 2.81% and 1.12%, respectively. Figure 1 shows the gradation of the sand used with the ASTM C 33 gradation limits.

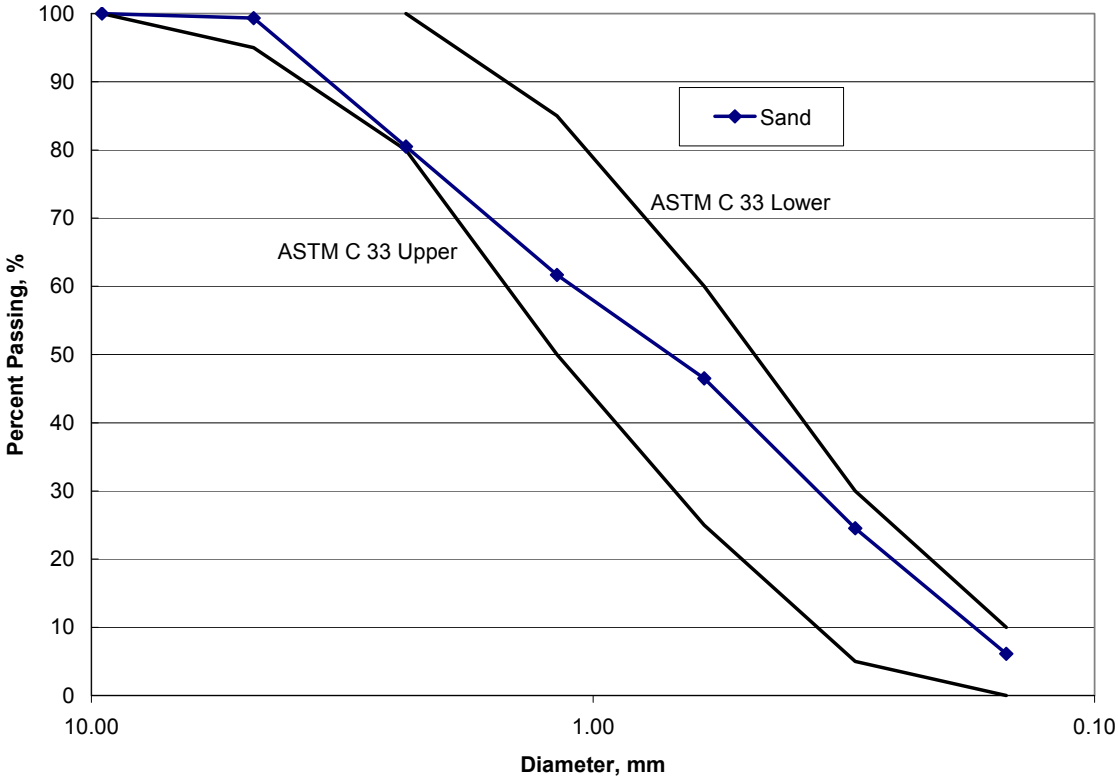

Figure 1. Gradation of natural river sand

Admixtures

This study used one air-entraining agent (AEA) and one water reducer for the major portion of the study: MB VR Standard and Pozzolith 200N, respectively. Two other AEAs and one other water reducer were also included in the incompatibility portion of the study investigating the effects of differing combinations of admixtures and ternary cementitious systems. Other AEAs included MB AE-90 and Microair, and the other water reducer used was PS-1466. The Pozzolith 200N is a sucrose-based Type A water reducer, and PS-1466 is a polycarboxylate ASTM C494 Type F water reducer.

MIXTURE DESIGN

The mixture designs for this project were chosen such that a wide range of engineering behaviors could be observed for many different combinations of cement and SCM. The work plan consisted of 140 mixtures, of which 13 are control mixtures of PC or binary mixtures containing PC and one SCM.

Upon starting the project, several attempts were made to procure a source of grade 80 GGBFS. The research team believes that 80 grade GGBFS would be an excellent solution to hot weather concreting applications to reduce the heat signature. Unable to procure a source of grade 80 GGBFS, the number of mixture designs was reduced to 120 mixtures, of which 12 were control mixtures.

Each mixture was uniquely identified using numbers and symbols. The number before each symbol represents the amount of cementitious material by mass. Each material is separated by a slash. For example, the mixture ID 60TI/20C/20F contains 60% by mass of ASTM C150 Type I cement, 20% by mass of ASTM C618 Class C fly ash, and 20% by mass of ASTM C618 Class F fly ash.

Table 7 shows the materials, specific gravities, and corresponding mixture identification symbols. Table 8 shows the control mixtures for this project. Table 9 shows mixtures containing Type I PC and 20% Class C or F fly ash. Table 10 shows mixtures containing Type I PC and 30% Class C or F fly ash. Table 11 shows mixtures containing Type I PC and GGBFS or Type I PC and metakaolin. Table 12 shows mixtures containing Type I/II PC and Table 13 shows mixtures containing Type IP PC. Table 14 and Table 15 show mixtures containing Type ISM PC and IPM PC, respectively.

Table 7. Material identification

Material	Symbol	Specific gravity
Type I	TI	3.04
Type I/II	TI-II	3.13
Type ISM	TISM	2.95
Type IP	TIP	3.11
Type IPM	TIPM	3.08
Ternary	Ternary	3.05
Class C fly ash	C	2.62
Class F fly ash	F	2.37
Class F fly ash	F2	2.41
GGBFS 100	G100S	2.82
GGBFS 120	G120S	2.96
Silica fume	SF	2.21
Metakaolin	M	2.52

Table 8. Control Mixtures for Phase I

100TI
80TI/20C
80TI/20F
80TI/20F2
65TI/35G100S
65TI/35G120S
100TI-II
80TI-II/20G120S
100TIP
100TISM
100TIPM
100Ternary

Table 9. Mixtures containing Type I PC and 20% Class C or F fly ash

60TI/20C/20F
60TI/20C/20F2
75TI/20C/5SF
77TI/20C/3SF
60TI/20C/20G100S
60TI/20C/20G120S
75TI/20C/5M
60TI/20F/20F2
75TI/20F/5SF
77TI/20F/3SF
60TI/20F/20G100S
60TI/20F/20G120S
75TI/20F/5M
75TI/20F2/5SF
77TI/20F2/3SF
60TI/20F2/20G100S
60TI/20F2/20G120S
75TI/20F2/5M

Table 10. Mixtures containing Type I PC and 30% Class C or F fly ash

60TI/30C/10F
60TI/30C/10F2
65TI/30C/5SF
67TI/30C/3SF
50TI/30C/20G100S
50TI/30C/20G120S
65TI/30C/5M
60TI/30F/10C
60TI/30F2/10C
60TI/30F/10F2
65TI/30F/5SF
67TI/30F/3SF
50TI/30F/20G100S
50TI/30F/20G120S
65TI/30F/5M
65TI/30F2/5SF
67TI/30F2/3SF
50TI/30F2/20G100S
50TI/30F2/20G120S
65TI/30F2/5M

Table 11. Mixtures containing Type I PC and GGBFS or Type I PC and metakaolin

50TI/35G100S/15C
50TI/35G100S/15F
50TI/35G100S/15F2
60TI/35G100S/5SF
62TI/35G100S/3SF
60TI/35G100S/5M
50TI/35G120S/15C
50TI/35G120S/15F
50TI/35G120S/15F2
60TI/35G120S/5SF
62TI/35G120S/3SF
60TI/35G120S/5M
90TI/5M/5SF
92TI/5M/3SF

Table 12. Mixtures containing Type I/II PC

68TI-II/17G120S/15C
68TI-II/17G120S/15F
68TI-II/17G120S/15F2
76TI-II/19G120S/5SF
78TI-II/19G120S/3SF
64TI-II/20G100S/16G120S
76TI-II/19G120S/5M
60TI-II/25C/15G120S
60TI-II/25F/15G120S
60TI-II/25F2/15G120S
52TI-II/35G100S/13G120S

Table 13. Mixtures containing Type IP PC

85TIP/15C
85TIP/15F
85TIP/15F2
95TIP/5SF
97TIP/3SF
80TIP/20G100S
80TIP/20G120S
95TIP/5M
75TIP/25C
75TIP/25F
75TIP/25F2
65TIP/35G100S
65TIP/35G120S
90TIP/5M/5SF
92TIP/5M/3SF

Table 14. Mixtures containing Type ISM PC

85TISM/15C
85TISM/15F
85TISM/15F2
95TISM/5SF
97TISM/3SF
80TISM/20G100S
80TISM/20G120S
95TISM/5M
75TISM/25C
75TISM/25F
75TISM/25F2
65TISM/35G100S
65TISM/35G120S
90TISM/5M/5SF
92TISM/5M/3SF

Table 15. Mixtures containing Type IPM PC

85TIPM/15C
85TIPM/15F
85TIPM/15F2
95TIPM/5SF
97TIPM/3SF
80TIPM/20G100S
80TIPM/20G120S
95TIPM/5M
75TIPM/25C
75TIPM/25F
75TIPM/25F2
65TIPM/35G100S
65TIPM/35G120S
90TIPM/5M/5SF
92TIPM/3SF

RESULTS AND DISCUSSION

X-ray Diffraction

Portland Cement

All XRD results are shown in Appendix B. The XRD results for Type I PC are shown in Figure B-1. Note the large peak for tricalcium aluminate and calcium silicate, as expected for a Type I PC. Figure B-2 shows the results for Type I/II PC. Note the large calcium silicate peaks, but the reduced tricalcium aluminate peak. Also, note the bassanite peak indicating that the cement clinker was ground hot turning the gypsum into bassanite.

Figure B-3 shows the results for Type ISM PC. Note the similarities to the Type I/II are due to the clinker source being the same for each. Figure B-4 shows the results for Type IPM cement. Figure B-5 shows the results for the Type IP cement and Figure B-6 shows the results for the Ternary cement.

Fly Ash

Figure B-7 shows the results for Class C fly ash. Note the quartz peak is reflected strongly due to the high symmetry. Also note the peak for tricalcium aluminate clearly indicating that this sample is a Class C fly ash. Figure B-8 shows the XRD results for the Cayuga Class F fly ash. Note the strong peak for quartz and the spinel mineral magnetite. Hematite is also present in the sample. Figure B-9 shows the XRD results for Coal Creek Class F fly ash. Note the strong reflections for quartz and mullite.

When analyzing X-ray diffractograms for various fly ashes, the background, or glass halo, is an indication of the glass content of the fly ash. Note the Class C fly ash does not have as large a background as either of the Class F fly ashes. This indicates that the Class F fly ashes may have more pozzolanic capabilities.

GGBFS

Figure B-10 and Figure B-11 show the results for grade 100 and grade 120 GGBFS, respectively. Note the slight peaks for quartz and calcite in the grade 100 slag and the small peaks for merwinite in the grade 120 sample. Due to the rapid quenching process used in the formation of slag, nearly 100% of the material is in a glassy phase as evidenced by the background for each sample.

Metakaolin

Figure B-12 shows the XRD results for metakaolin. Metakaolin is a calcined clay mineral with properties that mimic silica fume. The high pozzolanic abilities are shown with the large glass

content noted by the large background halo. Small amounts of anatase are also present in the sample.

Silica Fume

The XRD results for silica fume are shown in Figure B-13. The diffractogram shows the sample is nearly 100% glass, as is expected. Also note the small quantities of quartz, moissanite, and silicon present. The moissanite and silicon are expected due to the manufacturing process. Silicon is heated for production of computer chips, the heating combines some of the carbon present with the silicon forming moissanite.

Pozzolanic Index

The activity index test results for all SCMs are shown in Table 16. All materials met their applicable ASTM standards except the metakaolin at a 20% replacement rate. The water demand was greater than allowed according to ASTM C 311. It is important to note here that although the material has an increased water demand, the material should not be rejected. A larger dosage of water reducer may be required to produce concrete with sufficient workability.

Class C fly ash showed the greatest potential for reduction in water demand followed by the fly ash F2 and F. The order for the two Class F fly ashes is expected due to the increased material fineness.

Table 16. Pozzolanic index test results for all SCMs

	Water requirement %	Strength activity index (%)		Slag activity index (%)		Pozzolanic activity index (%)	
Material		**7 day**	**28 day**	**7 day**	**28 day**	**7 day**	**28 day**
Class C fly ash	86.8	112	108				
Class F fly ash	97.9	85	86				
Class F2 fly ash	90.5	108	107				
Silica fume	--					125	--
Grade 100 slag	--			60	97		
Grade 120 slag	--			80	112		
Metakaolin (20%)	121.9	114	121				
Metakaolin (10%)	104.0	141	144				

Heat Signature

The heat signature of concrete mixtures is important as it defines the hydration process and gives estimates of the time to initial and final set. The heat liberated during hydration is important especially during cold and hot weather concreting applications. A mixture design exhibiting a

large temperature rise during hydration may not be suitable for hot weather concreting applications, but may be ideally suited for cold weather concreting applications.

The results for heat signature are displayed in Appendix C. A reduction in maximum temperature rise when incorporating GGBFS and the expected shift in time to maximum heat generation when incorporating SCMs due to a longer time to initial and final set was observed. One should note with the decrease in heat generated, the general tradeoff is a longer time to initial and final set. Mixtures containing silica fume have a larger heat signature compared to others as is expected. The increased heat liberated is due to the increased pozzolanic action.

The heat of mixtures containing grade 120 GGBFS is significantly larger than mixtures containing grade 100 GGBFS. This is expected due to the fact that the grade 120 GGBFS is ground more finely than the grade 100 GGBFS. The results show the influence of the silica fume replacement (3% or 5%) is negligible when comparing their respective heat signatures. This shows that a 5% replacement rate may be used if needed in high performance concrete applications with no noticeable effect on the heat signature.

Heat Signature Modeling

The heat signature mixtures were characterized using key information from the heat signature including the slope 1 and slope 2 lines, maximum temperature, area under the curve, and time to maximum temperature. Figure 2 shows slope 1, slope 2, maximum temperature, time to maximum temperature, and area under the curve.

Table 17 to Table 24 show the results for slope 1 and slope 2, the maximum temperature and time to maximum temperature, area under the curve, and time to initial and final set for each mixture. Note that slope 1 was calculated using the maximum temperature and the minimum temperature for the data set up to the maximum temperature. Slope 2 was calculated using the maximum temperature and the minimum temperature for the data set after the maximum temperature.

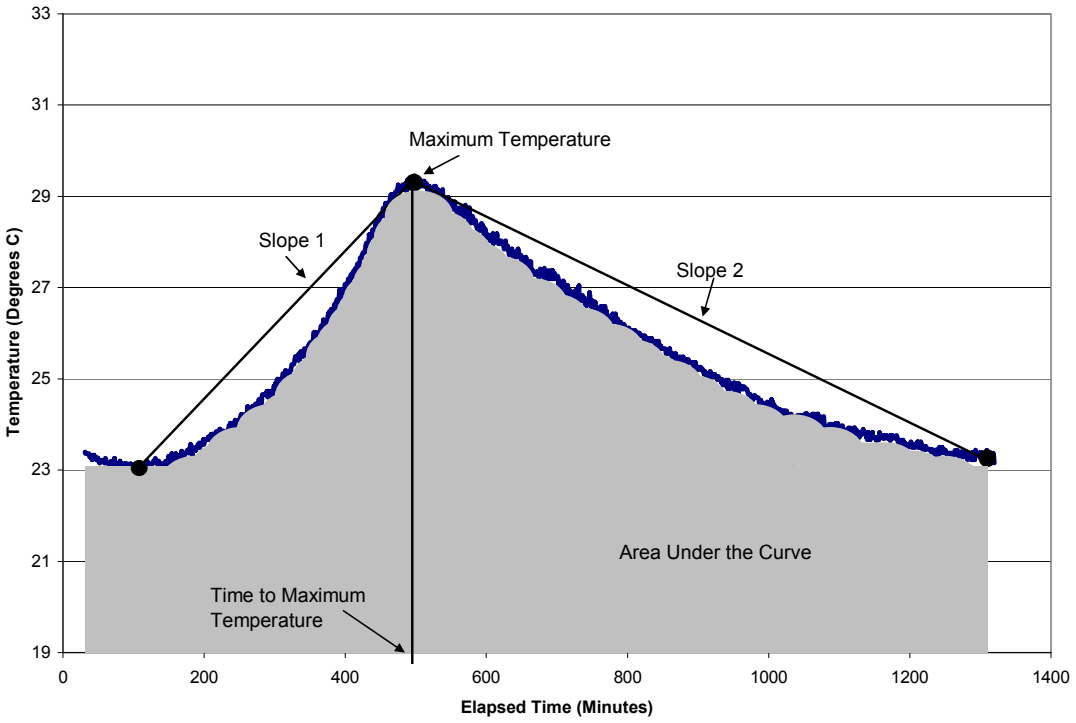

Figure 2. Variables slope 1, slope 2, maximum temperature, time to maximum temperature, and area under the curve

Table 17. Characterization results for the control mixtures

Mixture design	Slope 1	Slope 2	Max. temp. (°C)	Time to max. temp. (min)	Area under the curve (°C*Hour)	Initial set (min)	Final set (min)
100TI	0.0169	-0.0077	29.45	498	545	137	221
80TI/20C	0.0146	-0.0067	28.25	646	534	233	410
80TI/20F	0.0135	-0.0078	28.75	562	533	195	304
80TI/20F2	0.0151	-0.0077	29.13	580	542	232	342
65TI/35G100S	0.0129	-0.0067	26.33	571	488	212	349
65TI/35G120S	0.0160	-0.0060	28.11	503	536	171	274
100TI-II	0.0185	-0.0098	31.01	509	565	134	197
80TI-II/20G120S	0.0152	-0.0077	28.75	534	542	159	230
100TIP	0.0155	-0.0113	30.35	592	548	187	280
100TISM	0.0151	-0.0085	29.36	585	550	169	248
100TIPM	0.0146	-0.0078	29.72	491	569	131	242
100Ternary	0.0115	-0.0075	26.75	598	505	183	283

Table 18. Characterization results for mixtures containing Type I PC and 20% FA

Mixture design	Slope 1	Slope 2	Max. temp. (°C)	Time to max. temp. (min)	Area under the curve (°C*hour)	Initial set (min)	Final set (min)
60TI/20C/20F	0.0074	-0.0057	26.49	747	526	286	525
60TI/20C/20F2	0.0074	-0.0056	26.24	733	520	387	621
75TI/20C/5SF	0.0129	-0.0044	26.50	667	512	226	405
77TI/20C/3SF	0.0115	-0.0044	26.20	686	507	226	392
60TI/20C/20G100S	0.0070	-0.0059	24.72	799	481	384	594
60TI/20C/20G120S	0.0086	-0.0088	25.59	709	488	342	568
75TI/20C/5M	0.0116	-0.0054	26.84	608	517	257	391
60TI/20F/20F2	0.0101	-0.0069	27.76	623	534	249	394
75TI/20F/5SF	0.0140	-0.0067	27.80	556	520	155	274
77TI/20F/3SF	0.0130	-0.0058	27.27	553	515	166	270
60TI/20F/20G100S	0.0098	-0.0055	25.39	585	488	255	419
60TI/20F/20G120S	0.0120	-0.0066	28.39	507	542	205	326
75TI/20F/5M	0.0132	-0.0070	28.19	518	528	189	282
75TI/20F2/5SF	0.0123	-0.0066	27.80	594	520	188	310
77TI/20F2/3SF	0.0126	-0.0072	28.04	577	518	208	309
60TI/20F2/20G100S	0.0081	-0.0061	25.62	660	492	303	457
60TI/20F2/20G120S	0.0100	-0.0063	27.32	587	530	212	338
75TI/20F2/5M	0.0128	-0.0067	27.92	532	525	211	325

Table 19. Characterization results for mixtures containing Type I PC and 30% FA

Mixture design	Slope 1	Slope 2	Max. temp. (°C)	Time to max. temp. (min)	Area under the curve (°C*Hour)	Initial set (min)	Final set (min)
60TI/30F/10C	0.0099	-0.0054	25.94	695	497	270	407
60TI/30F2/10C	0.0061	-0.0059	25.56	768	493	327	475
60TI/30C/10F	0.0072	-0.0051	26.36	707	526	389	623
60TI/30C/10F2	0.0075	-0.0040	25.53	745	513	339	584
65TI/30C/5SF	0.0119	-0.0046	26.83	639	533	224	491
67TI/30C/3SF	0.0102	-0.0037	26.07	624	523	253	496
50TI/30C/20G100S	0.0056	-0.0049	23.67	862	473	445	811
50TI/30C/20G120S	0.0107	-0.0056	25.47	693	502	341	611
65TI/30C/5M	0.0069	-0.0043	25.15	682	500	317	510
60TI/30F/10F2	0.0108	-0.0072	27.82	605	528	234	360
65TI/30F/5SF	0.0149	-0.0082	28.75	556	537	164	270
67TI/30F/3SF	0.0149	-0.0073	28.55	538	536	173	293
50TI/30F/20G100S	0.0070	-0.0056	25.01	614	479	294	493
50TI/30F/20G120S	0.0107	-0.0063	27.12	578	519	250	383
65TI/30F/5M	0.0154	-0.0067	27.77	506	519	193	322
65TI/30F2/5SF	0.0164	-0.0083	28.99	564	538	244	353
67TI/30F2/3SF	0.0149	-0.0080	29.06	585	540	235	356
50TI/30F2/20G100S	0.0067	-0.0061	24.86	726	480	356	559
50TI/30F2/20G120S	0.0091	-0.0056	26.93	624	521	216	355
65TI/30F2/5M	0.0103	-0.0065	27.05	586	511	249	362

Table 20. Characterization results for mixtures containing Type I PC and 35% GGBFS or Type I PC and metakaolin

Mixture Design	Slope 1	Slope 2	Max. temp. (°C)	Time to max. temp. (min)	Area under the curve (°C*Hour)	Initial set (min)	Final set (min)
50TI/35G100S/15C	0.0055	-0.0051	24.31	704	476	423	688
50TI/35G100S/15F	0.0080	-0.0050	25.34	554	488	292	475
50TI/35G100S/15F2	0.0099	-0.0056	25.61	594	485	262	458
60TI/35G100S/5SF	0.0133	-0.0057	26.54	501	498	211	365
62TI/35G100S/3SF	0.0131	-0.0061	26.66	517	498	203	368
60TI/35G100S/5M	0.0119	-0.0050	25.81	494	492	175	351
50TI/35G120S/15C	0.0075	-0.0037	25.18	685	504	302	493
50TI/35G120S/15F	0.0112	-0.0051	26.96	519	521	190	327
50TI/35G120S/15F2	0.0105	-0.0048	26.65	527	519	138	246
60TI/35G120S/5SF	0.0160	-0.0063	28.30	463	534	187	313
62TI/35G120S/3SF	0.0146	-0.0060	28.30	474	539	215	335
60TI/35G120S/5M	0.0115	-0.0054	27.36	451	522	182	287
90TI/5M/5SF	0.0250	-0.0100	31.96	455	579	133	222
92TI/5M/3SF	0.0216	-0.0096	31.51	460	574	137	231

Table 21. Characterization results for mixtures containing Type I/II PC

Mixture Design	Slope 1	Slope 2	Max. temp. (°C)	Time to max. temp. (min)	Area under the curve (°C*Hour)	Initial set (min)	Final set (min)
68TI-II/17G120S/15C	0.0112	-0.0088	28.19	699	534	193	293
68TI-II/17G120S/15F	0.0102	-0.0070	27.79	615	542	150	225
68TI-II/17G120S/15F2	0.0105	-0.0065	27.39	586	534	159	272
76TI-II/19G120S/5SF	0.0176	-0.0103	31.09	551	570	176	247
78TI-II/19G120S/3SF	0.0168	-0.0100	30.38	570	562	163	226
64TI-II/20G100S/16G120S	0.0113	-0.0070	26.38	617	505	212	320
76TI-II/19G120S/5M	0.0174	-0.0104	30.90	538	568	144	218
60TI-II/25C/15G120S	0.0126	-0.0093	28.19	754	532	238	349
60TI-II/25F/15G120S	0.0104	-0.0063	27.22	592	535	144	237
60TI-II/25F2/15G120S	0.0103	-0.0074	27.71	637	539	191	276
52TI-II/35G100S/13G120S	0.0094	-0.0055	25.16	623	491	213	337

Table 22. Characterization results for mixtures containing Type IP PC

Mixture Design	Slope 1	Slope 2	Max. temp. (°C)	Time to max. temp. (min)	Area under the curve (°C*Hour)	Initial set (min)	Final set (min)
85TIP/15C	0.0157	-0.0126	30.80	685	554	246	355
85TIP/15F	0.0127	-0.0108	30.04	652	559	187	271
85TIP/15F2	0.0120	-0.0099	28.69	673	541	216	309
95TIP/5SF	0.0167	-0.0116	31.23	585	562	173	247
97TIP/3SF	0.0178	-0.0118	31.16	584	563	169	244
80TIP/20G100S	0.0101	-0.0083	26.12	670	496	215	345
80TIP/20G120S	0.0120	-0.0098	29.39	626	549	190	288
95TIP/5M	0.0198	-0.0121	32.25	542	571	169	246
75TIP/25C	0.0146	-0.0119	30.17	721	550	307	408
75TIP/25F	0.0120	-0.0106	29.19	675	544	194	286
75TIP/25F2	0.0128	-0.0089	28.51	640	539	254	360
65TIP/35G100S	0.0096	-0.0075	25.83	660	492	252	385
65TIP/35G120S	0.0093	-0.0074	27.51	604	523	194	304
90TIP/5M/5SF	0.0210	-0.0118	32.05	525	565	199	300
92TIP/5M/3SF	0.0221	-0.0121	32.39	514	570	163	246

Table 23. Characterization results for mixtures containing Type ISM PC

Mixture Design	Slope 1	Slope 2	Max. temp. (°C)	Time to max. temp. (min)	Area under the curve (°C*Hour)	Initial set (min)	Final set (min)
85TISM/15C	0.0126	-0.0090	28.30	707	536	217	323
85TISM/15F	0.0129	-0.0071	27.93	579	539	151	236
85TISM/15F2	0.0106	-0.0063	25.83	691	502	201	307
95TISM/5SF	0.0174	-0.0105	31.12	576	567	201	289
97TISM/3SF	0.0160	-0.0107	30.79	599	564	186	271
80TISM/20G100S	0.0108	-0.0060	25.58	632	497	196	298
80TISM/20G120S	0.0106	-0.0059	26.05	621	506	170	268
95TISM/5M	0.0171	-0.0119	31.58	539	572	161	249
75TISM/25C	0.0101	-0.0100	26.77	864	504	250	386
75TISM/25F	0.0096	-0.0070	26.39	668	509	165	276
75TISM/25F2	0.0104	-0.0063	26.20	666	506	226	339
65TISM/35G100S	0.0077	-0.0058	24.72	711	485	210	346
65TISM/35G120S	0.0084	-0.0057	25.22	691	495	175	283
90TISM/5M/5SF	0.0217	-0.0113	32.15	515	576	172	276
92TISM/5M/3SF	0.0139	-0.0083	27.14	544	507	174	251

Table 24. Characterization results for mixtures containing Type IPM PC

Mixture design	Slope 1	Slope 2	Max. temp. (°C)	Time to max. temp. (min)	Area under the curve (°C*Hour)	Initial set (min)	Final set (min)
85TIPM/15C	0.0135	-0.0083	27.47	641	520	181	275
85TIPM/15F	0.0110	-0.0070	26.82	591	518	123	198
85TIPM/15F2	0.0117	-0.0062	26.71	539	517	149	227
95TIPM/5SF	0.0181	-0.0103	30.90	546	567	125	184
97TIPM/3SF	0.0200	-0.0117	32.02	582	581	129	189
80TIPM/20G100S	0.0106	-0.0070	26.34	636	508	177	251
80TIPM/20G120S	0.0119	-0.0057	26.18	528	510	141	216
95TIPM/5M	0.0132	-0.0080	27.23	516	513	114	171
75TIPM/25C	0.0120	-0.0112	28.12	750	522	202	300
75TIPM/25F	0.0094	-0.0058	26.04	573	512	132	203
75TIPM/25F2	0.0105	-0.0064	26.63	622	516	182	262
65TIPM/35G100S	0.0081	-0.0052	24.62	641	487	186	259
65TIPM/35G120S	0.0085	-0.0057	25.51	626	503	144	228
90TIPM/5M/5SF	0.0168	-0.0086	27.48	517	510	109	166
92TIPM/5M/3SF	0.0139	-0.0086	27.35	535	512	111	168

Least Squares Regression Analysis

A least squares fit analysis was completed using JMP (2005) on the data set to determine if the heat signature characterizations fit a linear model. The response variables included slope 1 and slope 2, maximum temperature, time to maximum temperature, maturity, and initial and final set. Parameters used in the analysis included C_3S, C_2S, C_3A, and C_4AF to model the effects of different cement chemistries. The percentage of C_3S, C_2S, C_3A, and C_4AF was multiplied by the percent of Type I PC present in the mixture design to obtain a value for modeling purposes. These input parameters for the cement were chosen due to the ease in which they can be obtained from mill reports.

A weighted average of the fly ash calcium oxide (FACaO) was used to model the effect of the FA on the heat signature and a weighted average of the fineness (S) of the GGBFS was used to model the effect of slag on the heat signature. The fly ash calcium oxide content was used as a model parameter because it is readily available on ASTM C 618 reports required by most state agencies. The percent of silica fume (SF) and metakaolin (M) in the mixture design were used to model their respective effects. Table 25 shows the variables used in modeling and their units.

Equations 1–7 (see Table 26) show the least squares fit regression equations for slope 1, slope 2, maximum temperature, time to maximum temperature, area under the curve, and initial and final set, respectively. The R-Squared values ranging from 0.651 to 0.756 show that the data sets are

modeled well as linear approximations. Note that this regression analysis included no interaction variables and included all variables regardless of significance.

Table 25. Variable and units used in models

Variable name	Symbol	Mass units
Tricalcium silicate	C_3S	%
Dicalcium silicate	C_2S	%
Tricalcium aluminate	C_3A	%
Tetracalcium aluminoferrite	C_4AF	%
Fly ash calcium oxide	FACaO	%
GGBFS fineness	S	%Retained 325 Sieve
Silica fume	SF	%
Metakaolin	M	%

Table 26. Least squares regression analysis results

Equation #	Equation	R^2
1	Slope 1 = $3.6E^{-4}C_3S + 1.0E^{-3}C_2S - 7.6E^{-4}C_3A + 2.9E^{-3}C_4AF - 7.21E^{-5}FACaO + 7.2E^{-4}SF - 4.5E^{-4}S + 3.6E^{-4}M + 1.0E^{-3}$	0.756
2	Slope 2= $4.89E^{-4}C_3S + 8.9E^{-4}C_2S - 8.7E^{-4}C_3A + 4.7E^{-3}C_4AF - 3.8E^{-7}FACaO + 1.9E^{-4}SF + 3.3E^{-4}S - 1.1E^{-4}M - 2.8E^{-3}$	0.667
3	Maximum temperature = $-3.0E^{-1}C_3S + 1.4E^{-1}C_2S - 7.4E^{-2}C_3A + 2.6C_4AF - 3.4E^{-2}FACaO + 2.4E^{-1}SF - S + 7.8E^{-2}M + 22.8$	0.719
4	Time to maximum temperature = $2.4C_3S - 7.2C_2S - 4.6C_3A - 12.7C_4AF + 5.4FACaO - 6.4SF + 6.8S - 10M + 672$	0.687
5	Area under the curve = $-1.8C_3S + 6.4C_2S - 7.4C_3A + 15.6C_4AF - 3.9E^{-1}FACaO + 2.3SF - 21S + 1.3E^{-1}M + 477$	0.651
6	Initial set = $-1.8C_3S - 3.1E^{-1}C_2S + 3.7C_3A - 9.4C_4AF + 3.3FACaO - 3.3SF - 24.1S - 1.3M + 276$	0.675
7	Final set = $4.7E^{-1}C_3S + 15.7C_2S - 9.4C_3A - 56.4C_4AF + 5.9FACaO - 2.4SF + 48.4S - 1.9M + 443$	0.728

Stepwise Regression Analysis

Upon noting the linear approximations from the linear least squares regression analyses, a stepwise regression analysis was conducted using JMP (2005) to identify the insignificant input variables. The analyses used all possible models to identify potential models with large R-Squared values for further refinement. Once the model input parameters were identified, a least squares fit analysis was conducted to obtain a residual plot. Using the residual plot, the best equation for each response variable was determined.

Equations 8–14 (see Table 27) show the results of the stepwise regression analysis. The resulting R-Squared values, ranging from 0.651 to 0.756, show that the linear models are fair. By removing the insignificant input parameters, the linear models were simplified. Note that the stepwise regression analysis removed from one to four insignificant input variables depending upon the equation.

Table 27. Stepwise regression analysis results

Equation #	Equation	R^2
8	Slope 1 = $4.8E^{-4}C_3S + 4.2E^{-4}C_2S + 4.3E^{-3}C_4AF - 6.9E^{-5}$ FACaO + $6.8E^{-4}$SF + $3.6E^{-4}$S – $1.9E^{-4}$	0.756
9	Slope 2 = $5.1E^{-4}C_3S + 9.6E^{-4}C_2S - 9.9E^{-4}C_3A - 5E^{-3}C_4AF$ – $1.9E^{-4}$SF – $1.2E^{-4}$M – $2.1E^{-3}$	0.663
10	Maximum temperature = $–3.1E^{-1}C_3S + 7.9E^{-2}C_2S + 2.7C_4AF$ – $3.4E^{-2}$FACaO + $2.4E^{-1}$SF – S + $7.7E^{-2}$M + 22.8	0.719
11	Time to maximum temperature = $–11.2C_2S$ + 5.2FACaO – 5.3SF – 9.9M + 705	0.658
12	Area under the curve = $–3.0C_3S + 28.4C_4AF - 4.0E^{-1}$FACaO + 1.7SF – 20.8S + 478	0.651
13	Initial set = $–3.2C_3S + 3.7C_3A$ + 3.4FACaO – 2.2SF + 27.3S +264	0.655
14	Final set = $8.0C_2S – 46.5C_4AF$ + 6.0FACaO – 4.0SF + 50.3S + 436	0.726

The equation for slope 1 is as expected. An increase in C_3S, C_2S, GGBFS fineness, and silica fume content will increase the slope. Note the influence of C_4AF in nearly all the equations. The influence of C_4AF is usually small due to the smaller quantities of C_4AF in the PC, but the heat liberated is moderate leading to significance in the heat signature curve.

Note that the C_3A content is not significant in all equations except the initial set prediction model. This is due to the rapid C_3A hydration not significantly contributing to the later portion of the heat generation curve. Note that C_3S or C_2S are included in nearly every equation. This is due to the high amount of heat liberated for the C_3S and the moderate reaction rate for

determination of initial and final setting times. The C_2S input is notably less due to its decreased heat liberation contribution and slower rate of hydration (Lea 1998).

The maximum temperature is dependent upon C_3S, C_2S, C_4AF, FACaO content, silica fume, GGBFS fineness and metakaolin content. This equation is as expected, since an increase in the silica fume and metakaolin content will increase the maximum temperature; and addition of fly ash generally decreased the maximum temperature.

The time to maximum temperature equation shows that an increase in the fly ash calcium oxide content will increase the time to maximum temperature; and an increase in metakaolin and silica fume will decrease the time to maximum temperature. This is expected, since silica fume and metakaolin tend to reduce the time to initial and final set when used without a water reducer.

The area under the curve shows that C_4AF is important in determining the area even though it is a small fraction of the cement chemistry. This is most likely due to the moderate amount of heat liberated during hydration. The influence of the GGBFS fineness is also clearly shown. As the amount of GGBFS retained on the #325 sieve is increased, the area under the curve becomes smaller due to decrease in the reactivity of the GGBFS compared to that of PC.

The equations for initial set and final set are as expected with the C_3S and fly ash calcium oxide content and the GGBFS fineness playing large roles in determination of the set times. The C_3S contributes to early-age strength development and the fly ash calcium oxide (free lime) also contributes to set.

The stepwise regression analysis results allow a producer or engineer to predict key engineering properties such as the area under the curve, time to initial and final set, the maximum temperature, and time to maximum temperature. This is important due to the wide range of mixture combinations available. By using a prediction model, one can narrow the list of possible mix designs in the preconstruction verification stage using set response criteria, saving money and time.

The linear least squares regression analysis showed good R^2 values and adequately models the heat signature characterizations. The stepwise regression analysis allowed simplification of the least squares analysis by removing the variables not significantly affecting the model. Interaction effects may further refine the regression models. Interaction effects were not analyzed due to the good R^2 values obtained without interaction effects.

It should be noted that the models described above are valid for the ranges of PC, FA, SF, GGBFS, and metakaolin used, and care should be exercised if extrapolating these models beyond the aforementioned ranges and for materials other than what was used for this study. It is important to note that this study was conducted in a laboratory setting, and field results may differ depending upon climatic conditions.

Set Time and Mortar Flow

The time to initial set, final set, and mortar flow values are shown in Appendix D. The y-axis for all figures was set at 900 minutes for easy comparison between figures and mixtures. The results for the control mixtures are shown in Figure 3. Note that the blended cements increased the time to initial and final set and the introduction of SCMs to replace Type I PC increased the time to initial and final set as well as increased the workability, as expected. Note the Class C fly ash mixtures initial set time compared to those mixtures containing Class F fly ash. The decrease in set time for those mixtures containing Class F fly ash was unexpected and is most likely due to the increased fineness of the Class F fly ashes.

Note that the increase in FA, (20% to 30%,) significantly increases the time to initial and final set. Mortar flow values were also increased for mixes containing Class C fly ash, but the flow values remained the same or decreased with the increase in fly ash replacement for mixes containing Class F fly ash. This is most likely due to the finer Class F fly ash. The grade 120 GGBFS tended to decrease the flow and time to initial and final set as is expected due to the finer grind. A weak relationship exists between the flow value and time to initial set.

The times to initial set and final set for mixtures containing Type I/II PC are reduced compared to the Type I PC. This is most likely due to a finer product with increased surface area. Times to initial and final set ranged from 140 to 225 minutes for initial set and 225 to 350 minutes for final set.

For mixtures containing Type IP PC, the times to initial and final set ranged from 180 to 300 minutes for initial set and 250 to 400 minutes for final set. The set times for the Type IP are significantly larger than those for the Type I/II PC as is expected due to the 20% Class F fly ash incorporated in the Type IP cement.

For mixtures containing Type ISM PC, the times to initial and final set ranged from 150 to 250 minutes for initial set and 225 to 380 minutes for final set. The times to initial set are slightly lower than the Type IP results and the times to final set are also lower when compared to the Type IP results. This is expected due to the nature of SCM replacement.

Note the low flow values due to the increased fineness of the Type IPM PC with silica fume as the SCM. The times to initial and final set range from 110 to 200 minutes for initial set and 160 to 300 minutes for and final set.

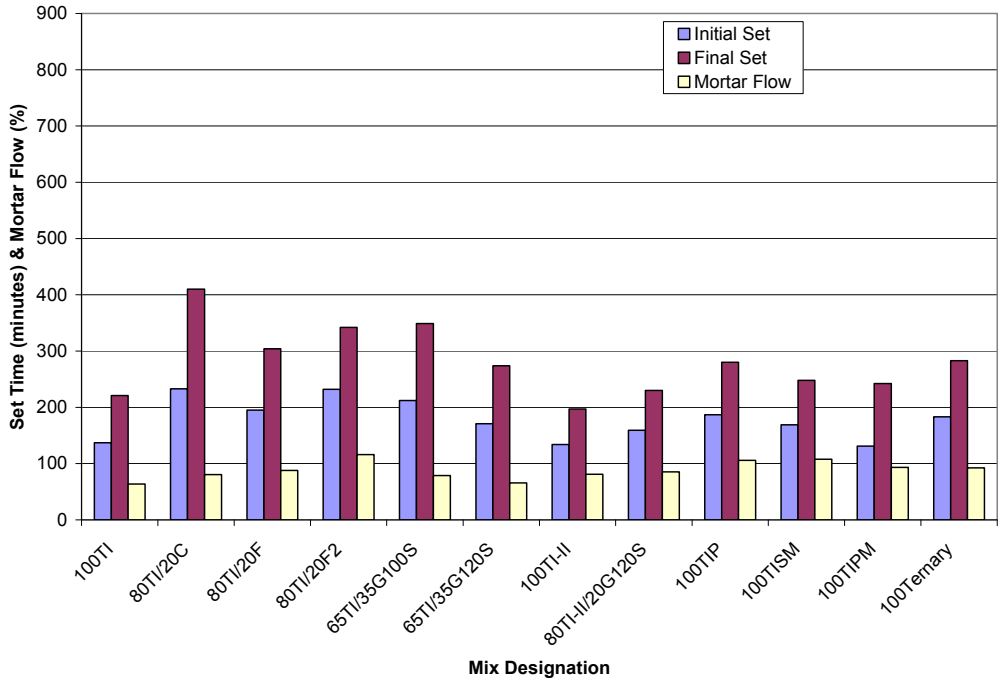

Figure 3. Set time and mortar flow for all control mixtures

Incompatibility

Set Time

Table 28 shows the set time results for all 10 mixtures. Note that the Pozzolith 200N water reducer showed significant reduction in time to initial and final set when used at a doubled dosage rate. Mixtures containing Class C fly ash generally set quicker and show the incompatibility of some Class C fly ashes with water reducers. Note the set time incompatibility is eliminated when using the high range water reducer (HRWR) PS-1466. The results also show that when the dose of HRWR is increased, the time to initial set is affected to a greater degree than the time to final set.

Upon analyzing the results, the research team decided to further investigate the incompatibility with the low range water reducer (Pozzolith 200N). To eliminate the Class C fly ash as the source of the incompatibility, i.e., false set with tricalcium aluminate, Mixture 60TI/30C/10F was completed with no water reducer. The results showed the time to initial set was 219 minutes and the time to final set was 450 minutes. This showed that the incompatibility was related to the specific combination of Type I PC, Class C fly ash, and water reducer.

Table 28. Incompatibility set time results

Mixture ID	Pozzolith 200N		Pozzolith 200N (2X)		PS-1466		PS-1466 (2X)	
	Initial set (min)	Final set (min)	Initial set (min)	Final set (min)	Initial set (min)	Final set (min)	Initial set (min)	Final set (min)
60TI/30C/10F	53	100	14	35	211	345	284	360
60TI/30C/10F2	45	90	18	27	271	315	542	590
50TI/30C/20G120S	47	110	18	60	271	495	400	495
75TIP/25C	114	240	47	165	443	585	464	570
75TISM/25C	73	180	51	150	319	585	151	345
75TIPM/25C	217	350	67	120	402	541	584	664
60TI/30F/10C	59	225	16	40	337	480	398	555
60TI/30F/10F2	153	360	27	120	348	450	538	615
65TI/30F/5M	32	210	13	105	239	375	444	555
75TIP/25F	300	420	96	450	329	435	541	645

These results show that careful planning and engineering judgment must be exercised when designing field concrete mixes. Using the Vicat test may flag a potential incompatibility issues before field construction begins.

Air Void Structure

Table 29 shows the water reducers and AEA used for the air void structure incompatibility study and their corresponding dosage rates. Each combination of water reducer and AEA was studied with two AVA samples for an average.

Figure 4 shows the relationship between spacing factor and specific surface. Figure 5 shows the relationship between spacing factor and % D < 300 μm. Figure 6 shows the relationship between specific surface and % D < 300 μm. Note that the correlation between all variables is good.

The relationship shown in Figure 4 is as expected, with a decrease in spacing factor as the specific surface is increased. This shows an increasingly finer air void system leading to shorter distances between air voids. Increasing the % D < 300 μm in the mortar increases the specific surface as shown in Figure 6. This is expected and is an indication of a finer air void system that may be more resistant to freeze-thaw. Note the very good correlation in Figure 5 between the spacing factor and the % D < 300 μm. The results show that decreasing the spacing factor increases the amount of air voids less than 300 μm in diameter.

Table 29. AEA and water reducer dosage rates

Admixture	Symbol	Dosage rate ml/kg (oz/cwt)
MB-VR Standard	AEA1	1.3 (2.0)
MB AE 90	AEA2	1.3 (2.0)
Micro Air	AEA3	0.49 (0.75)
Pozzolith 200N	WR1	2.3 (3.5)
PS-1466	WR2	2.6 (4.0)

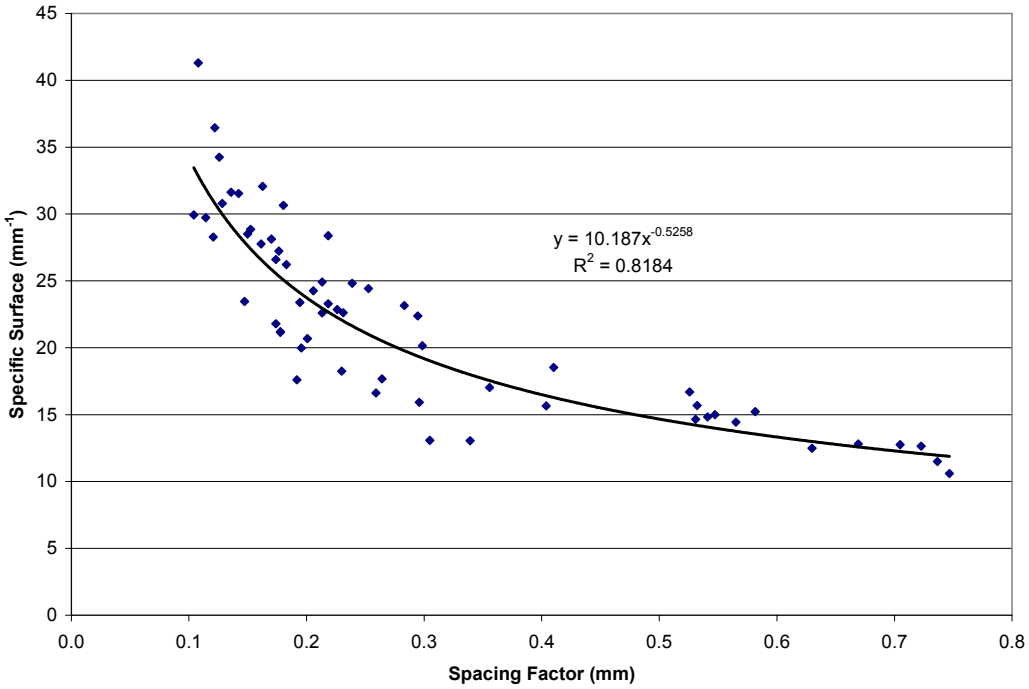

Figure 4. Relationship between specific surface and spacing factor for all mixtures

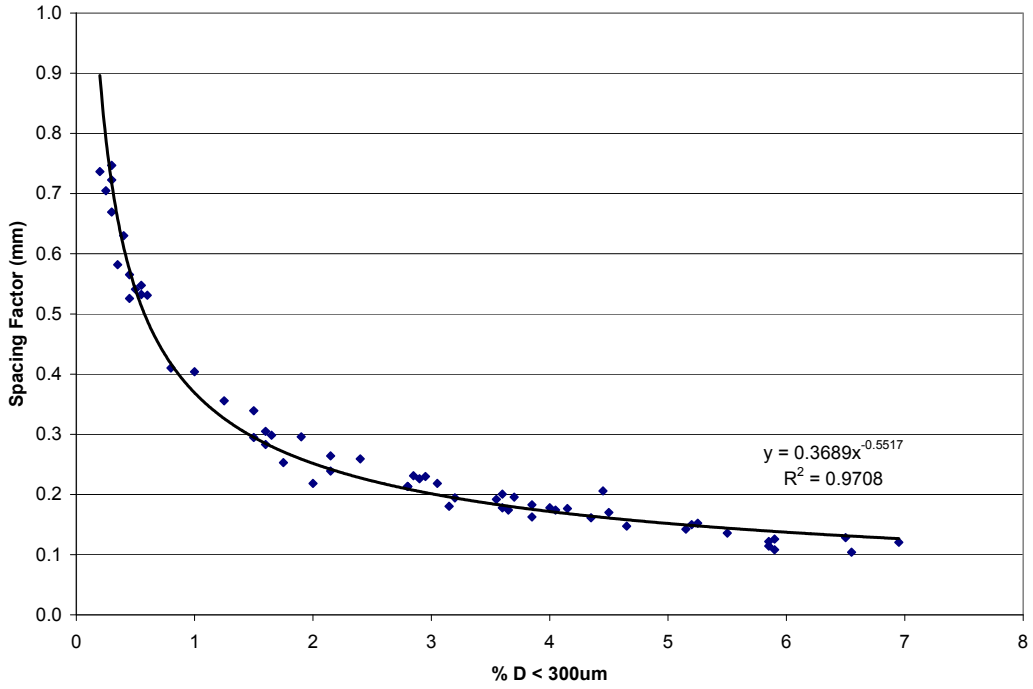

Figure 5. Relationship between spacing factor and % D < 300 µm for all mixtures

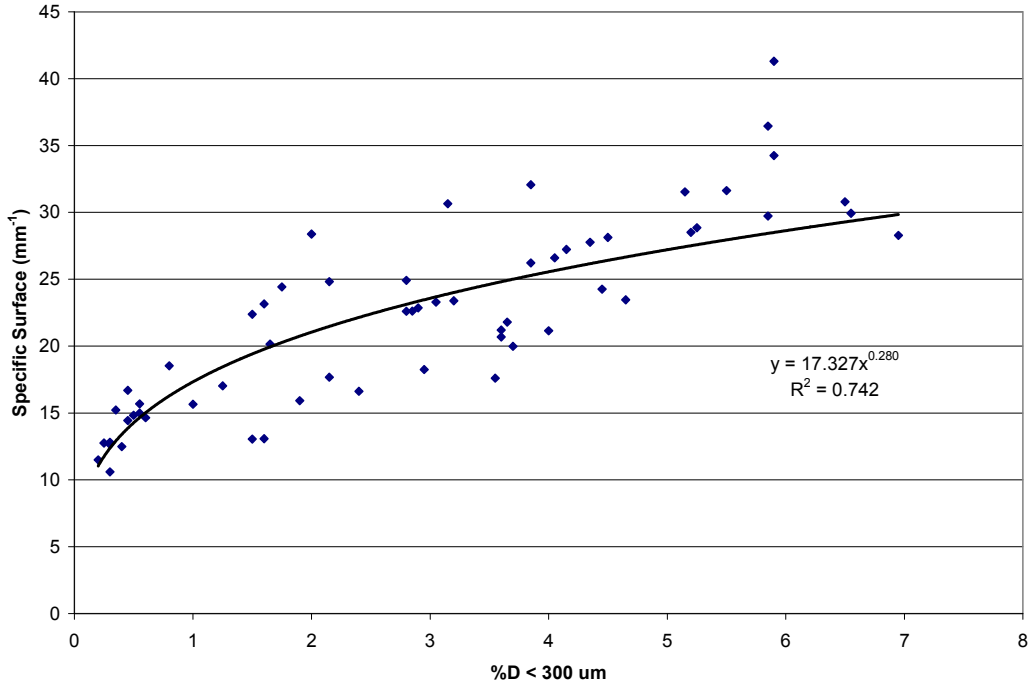

Figure 6. Relationship between specific surface and % D < 300 µm for all mixtures

Figure 7 shows the relationship between spacing factor and the seven-day compressive strength for all mixtures. Note the general trend showing an increase in spacing factor is associated with an increase in compressive strength. Note the trend continues until an upper limit of about 31,000 kPa. Also notice the outliers with low strength, indicating an incompatibility.

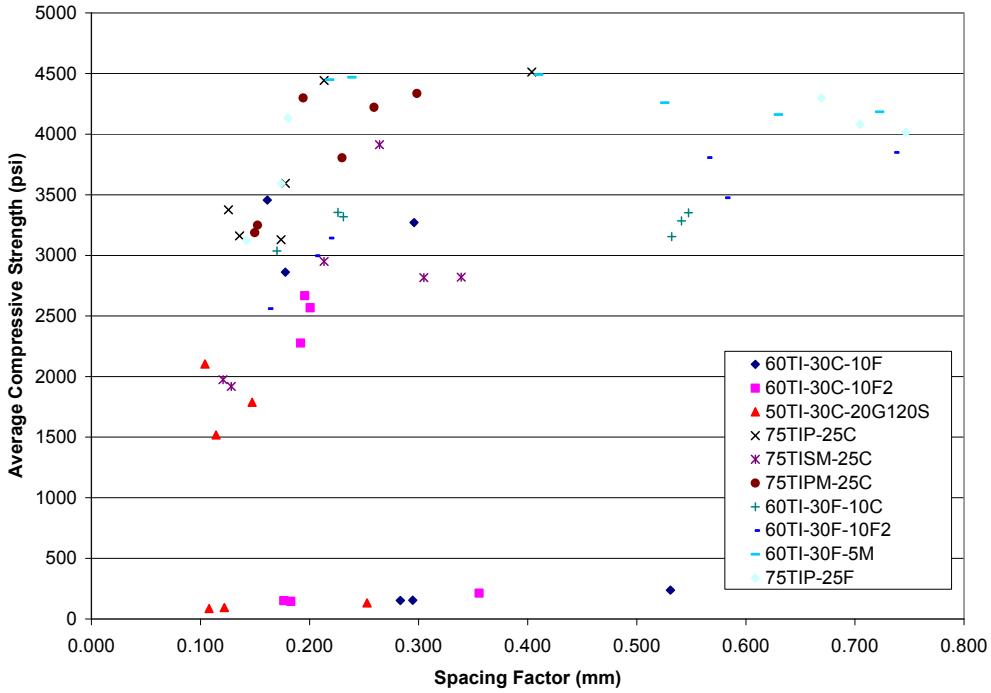

Figure 7. Effect of spacing factor on the average compressive strength for all mixtures

Figure 8 shows the relationship between specific surface and seven-day compressive strength for all mixes. Note the weak relationship showing a decrease in specific surface indicating an increase in the compressive strength. A decrease in specific surface is an indication of lower air content or larger air voids in general which would lead to higher strengths.

Figure 9 shows the relationship between percent of air voids less than 300 µm and the average seven-day compressive strength for all mixes. The general trend shows an increase in compressive strength with a decrease in the percent of air voids less than 300 µm. A decrease in the finer fraction of air voids indicates lower air content or larger air voids within the mix. Lower air contents will lead to increased strengths.

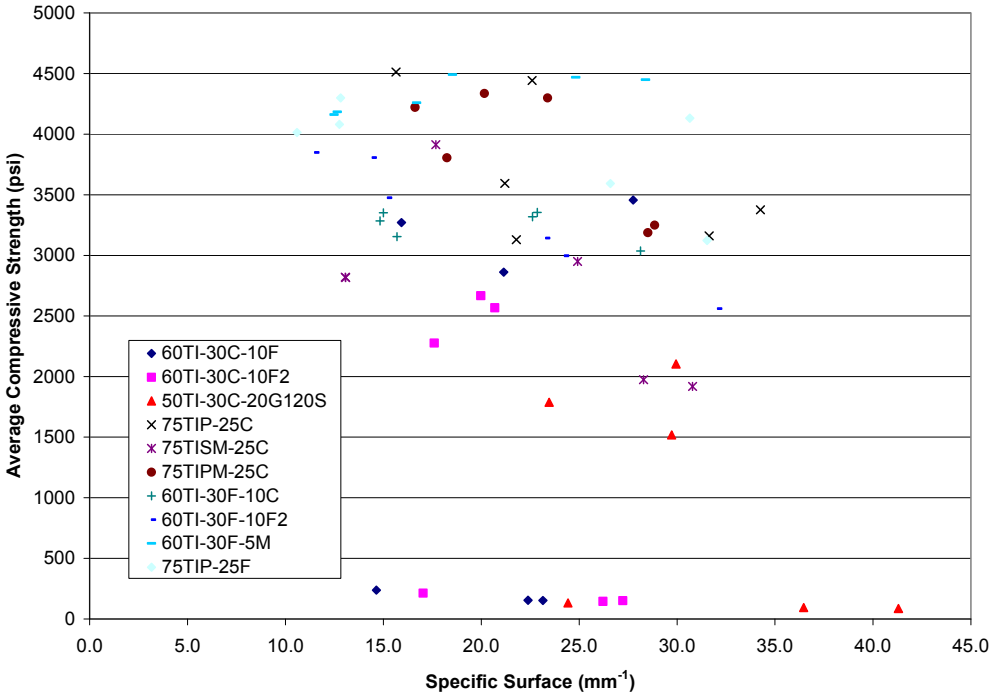

Figure 8. Effect of specific surface on the average compressive strength for all mixtures

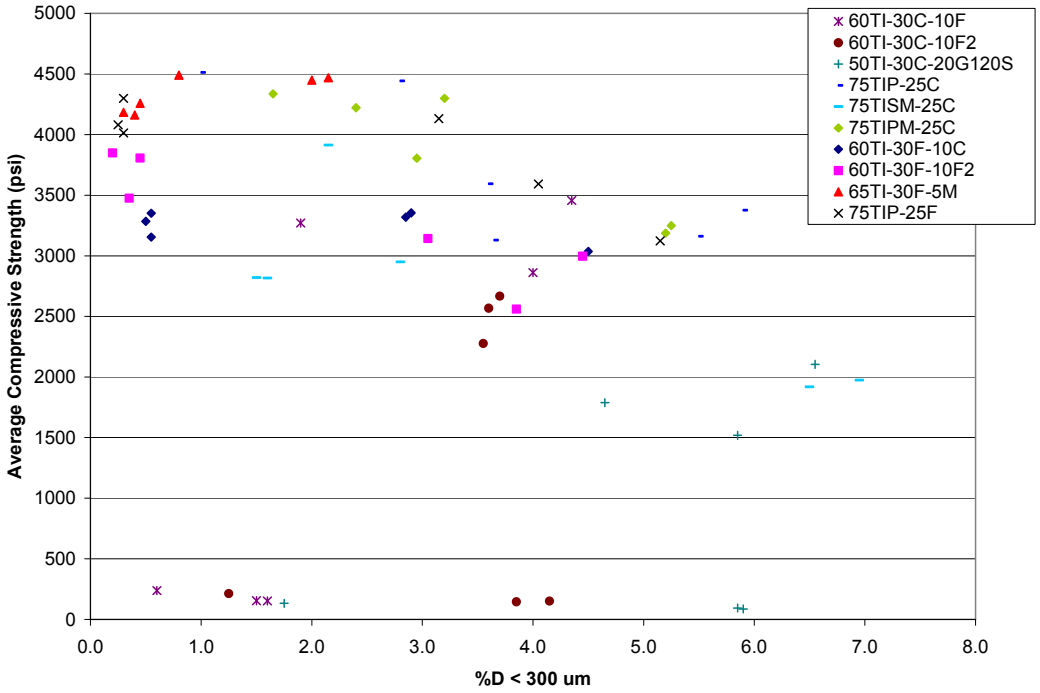

Figure 9. Effect of % D < 300 µm on the average compressive strength for all mixtures

Figure 10 and Figure 11 show the relationship between spacing factor and combinations of AEA and water reducer for the mixtures containing high amounts of Class C and Class F fly ash respectively. As shown in Figure 7, the blended cements (TIP, TISM, TIPM) generally produced better air void structure, and the reverse is true for mixtures containing large amounts of Class F fly ash as shown in Figure 8. Note that all three AEAs used in the study seem to produce similar spacing factors when comparing results with the same water reducer.

Note in Figure 11 the significant difference between the spacing factor results for the two water reducers. The results show for high loss on ignition (LOI) Class F fly ash, a polycarboxylate high range water reducer may be better suited for aiding in generation of an adequate air void system for freeze-thaw durability. This is as expected because polycarboxylates are known to entrain air. When comparing the results for spacing factor between Figure 10 and Figure 11, the increased spacing factors for mixes containing the high LOI Class F fly ash are expected due to the inherent difficulty in entraining air into those mixtures.

When comparing the results in Figure 10 and Figure 11, it is important to note that the majority of mixtures in Figure 10 meet the limit of a 0.2 mm (0.008 in.) spacing factor, but the mixtures shown in Figure 11 do not meet the limit unless WR2 (PS-1466) is used. These results show that a greater dosage of AEA is needed when incorporating a high LOI Class F fly ash.

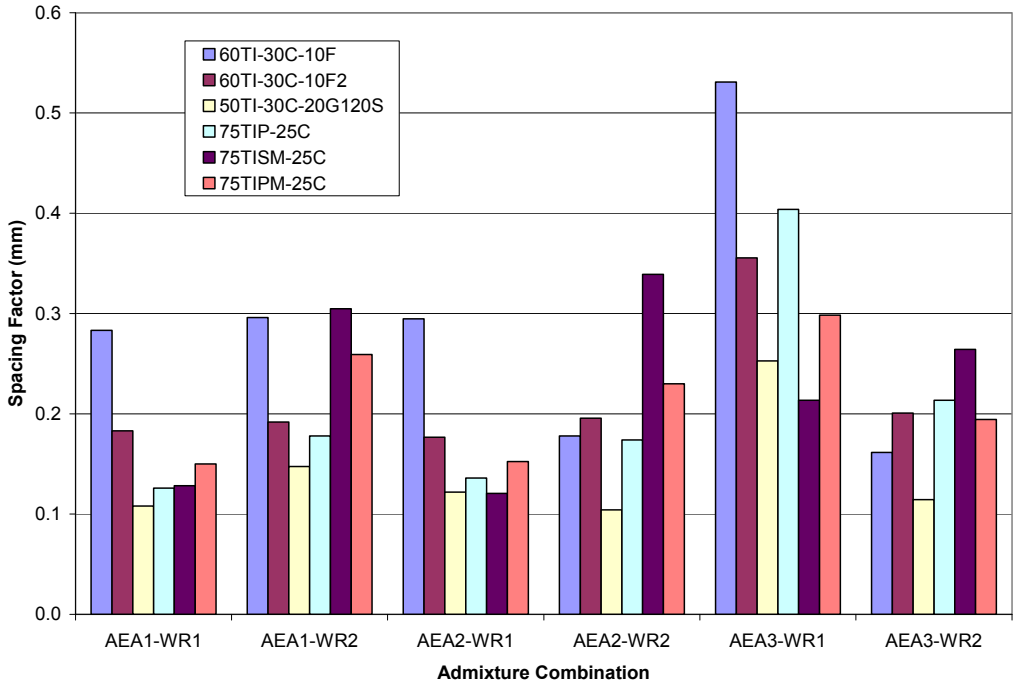

Figure 10. Effect of admixture combination on the spacing factor for mixtures containing large amounts of Class C fly ash

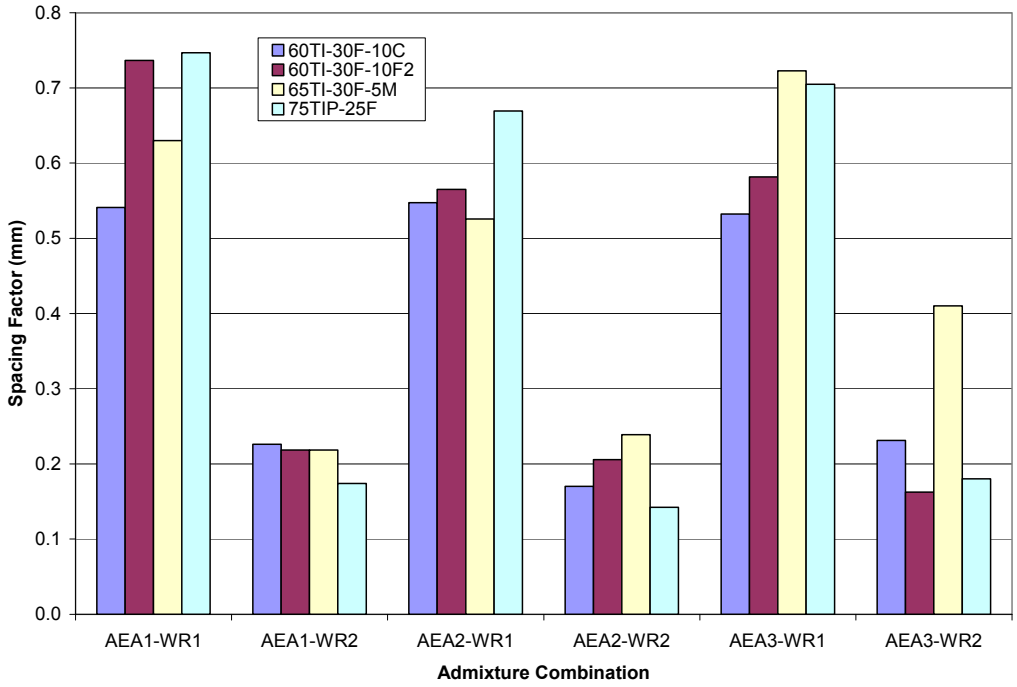

Figure 11. Effect of admixture combination on the spacing factor for mixtures containing large amounts of Class F fly ash

Figure 12 shows the effect of admixture combination on the specific surface for mixtures containing large amounts of Class C fly ash. Note that the AEA3 (Micro Air) combinations produced mixtures with lower specific surface values compared to combinations with AEA2 (MB AE 90) and AEA1 (MB-VR Standard). This seems counterintuitive because Micro Air is noted for producing a finer air void system.

Figure 13 shows the effect of admixture combinations on the specific surface for mixtures containing large amounts of Class F fly ash. Note that the results for specific surface are generally the same for combinations containing WR1 (Pozzolith 200N). When comparing the results shown in Figure 12 to those in Figure 13, the mixtures containing Class F fly ash significantly reduced the specific surface of the air void structure. These results show that a greater dosage of AEA is required when incorporating a high LOI class F fly ash, which is consistent with the literature.

Although most mixtures meet the limit of 0.2 mm (0.008 in) spacing factor (see Figure 10 and Figure 11), the majority of mixtures do not meet the minimum criteria of 23–43 mm^{-1} (600–1000 in^{-1}) for specific surface. This does not necessarily mean the corresponding concrete would fail in freeze-thaw, but steps should be taken to increase the specific surface and create a finer air void system.

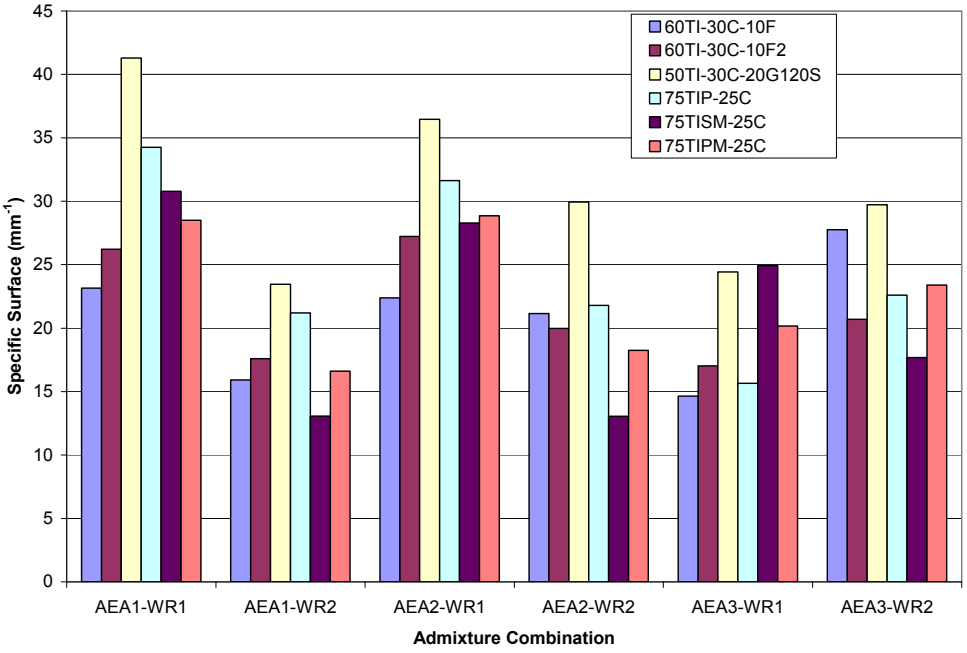

Figure 12. Effect of admixture combination on the specific surface for mixtures containing large amounts of Class C fly ash

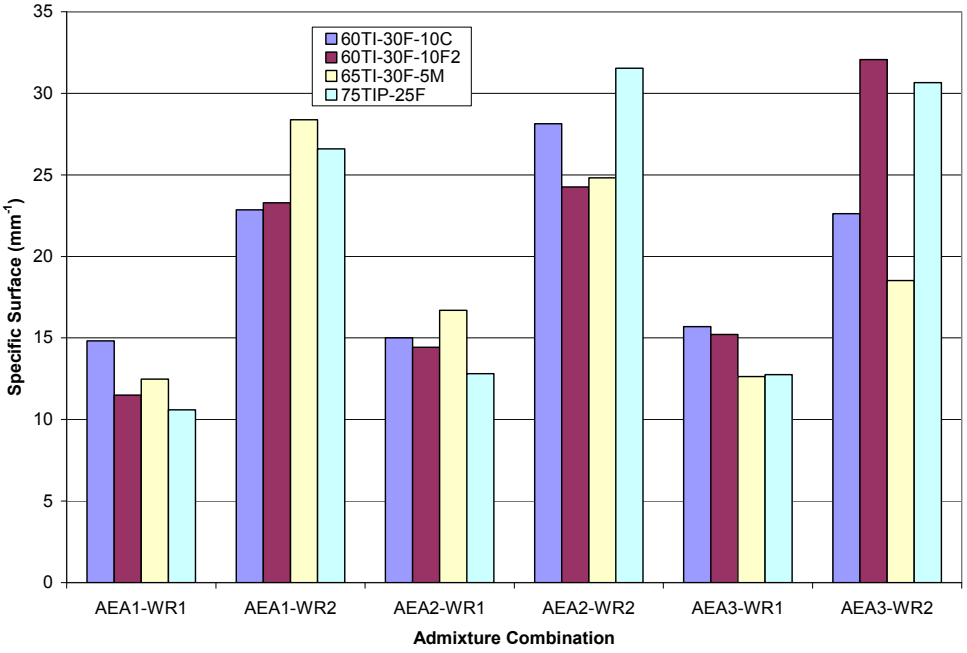

Figure 13. Effect of admixture combination on the specific surface for mixtures containing large amounts of Class F fly ash

Figure 14 and Figure 15 show the effect of admixture combinations on the percent of air voids less than 300 µm for mixtures containing Class C and Class F fly ashes, respectively. The percentage of air voids less than 300 µm is important as this is the effective size required for prevention of freeze-thaw damage (Dansk Beton Teknik 2004).

For mixtures containing large amounts of Class C fly ash (Figure 14), note that WR2 (PS-1466) tended to decrease the percentage of air voids less than 300 µm in diameter except for mixtures containing AEA3 (Micro Air).

Figure 15 shows significantly different results compared to Figure 14 for percentage of air voids with a diameter less than 300 µm. Note that WR2 (PS-1466) produced an increase in percent of air voids less than 300 µm in diameter on the order of eight times greater when compared to mixtures containing WR1 (Pozzolith 200N).

Although the mixtures containing Class F fly ash showed a reduction in the effective air void size, it is important to note that an increase in the AEA dosage will most likely prove an acceptable solution.

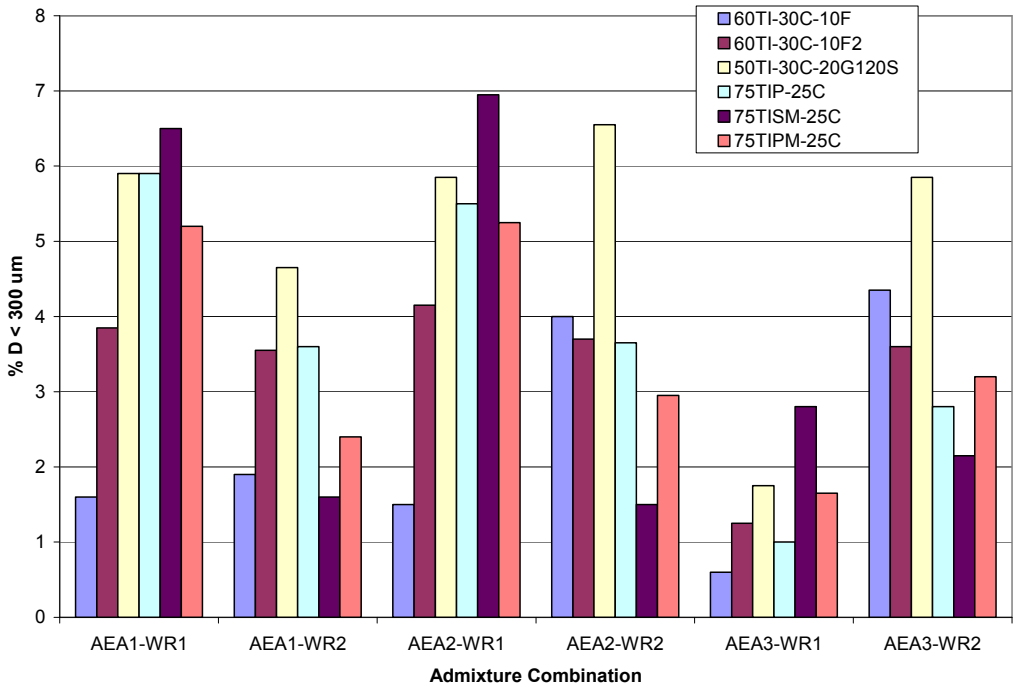

Figure 14. Effect of admixture combination on the percent of air voids less than 300 µm for mixtures containing large amounts of Class C fly ash

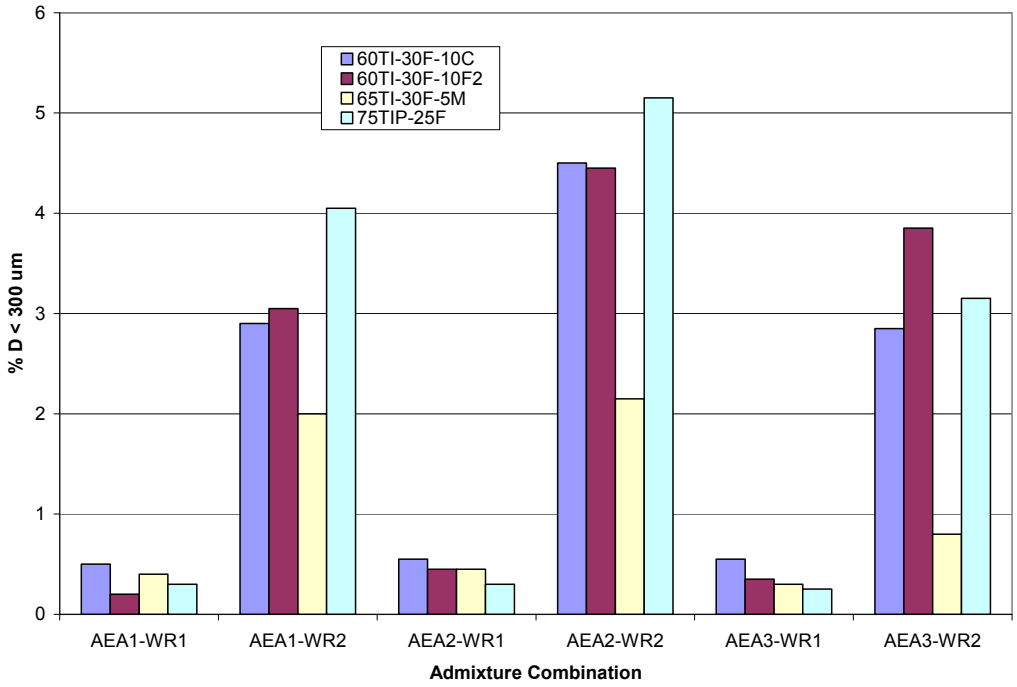

Figure 15. Effect of admixture combination on the percent of air voids less than 300 µm for mixtures containing large amounts of Class F fly ash

Figure 16 and Figure 17 show the effect of admixture combination on the average seven-day compressive strength for mixtures containing Class C and Class F fly ash, respectively. Figure 16 immediately indicates an admixture incompatibility issue resulting in retarded compressive strengths for the mixtures containing 30 % Class C fly ash and Type I PC. These results are most likely due to a sulfate imbalance combined with a sucrose-based water reducer.

Although there existed an incompatibility with WR1 (Pozzolith 200N) in terms of strength gain, the incompatibility is not evident when using WR2 (PS-1466). This is important to note for field applications. Also important is that the incompatibility was eliminated when a blended cement was used in place of Type I PC. In the event this occurs in the field, a simple substitution of water reducers or blended cement may solve the problem.

The results shown in Figure 17 indicate that there are no incompatibility issues such as those found when using Class C fly ash. Note that the results are generally the same when comparing between admixture combinations.

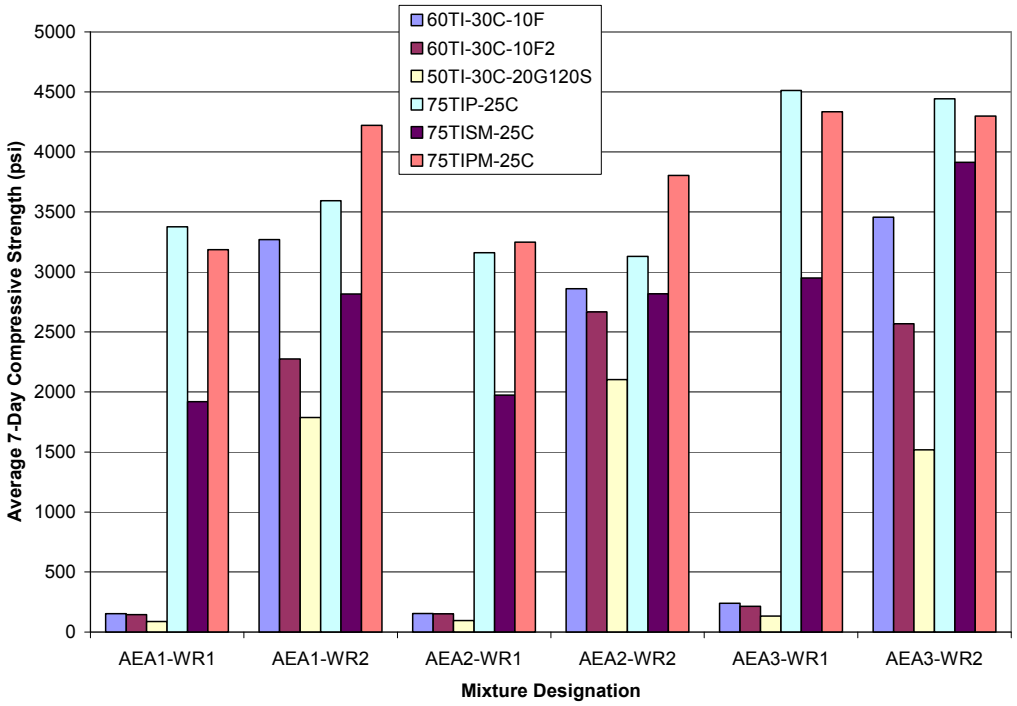

Figure 16. Effect of admixture combination on the average compressive strength for mixtures containing large amounts of Class C fly ash

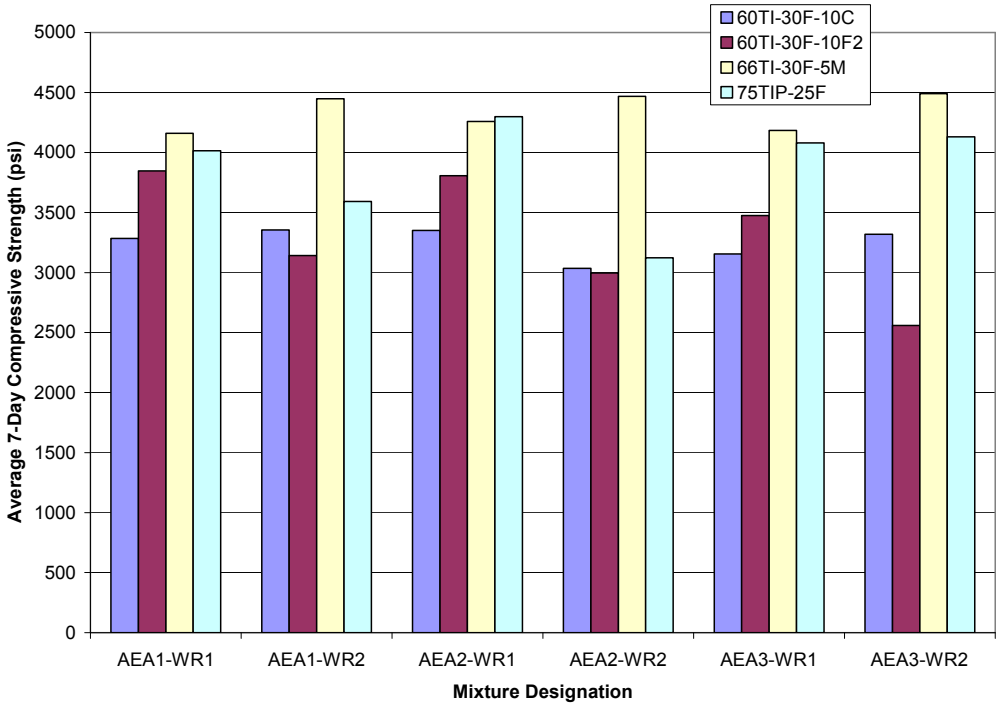

Figure 17. Effect of admixture combination on the average compressive strength for mixtures containing large amounts of Class F fly ash

Compressive Strength

Results for the control mixtures can be found in Table 30. The remaining compressive strength results are broken down by specific SCM and are shown in Tables 31–37.

Graphs of compressive strength versus time were plotted to compare the strength development of various mixtures. The compressive strength of all mortar mixtures with ternary cementitious combinations were separated into individual SCMs and are presented in Appendix E.

Table 30. Compressive strength results for the control mixtures

	Compressive strength (psi)		
Mixture ID	**3 day**	**7 day**	**28 day**
100TI	4,700	6,260	6,170
80TI/20C	2,430	3,820	4,710
80TI/20F	3,420	4,050	5,500
80TI/20F2	3,430	3,770	5,630
65TI/35G100S	2,770	4,310	6,720
65TI/35G120S	3,110	5,000	7,110
100TI-II	3,880	4,650	6,410
80TI-II/20G120S	3,700	4,370	6,780
100TIP	3,610	4,310	6,680
100TISM	3,220	4,700	6,040
100TIPM	4,320	4,970	7,150
100Ternary	4,310	6,050	7,490

Table 31. Compressive strength results for mixtures containing Class C fly ash

	Compressive strength (psi)		
Mixture ID	**3 day**	**7 day**	**28 day**
60TI/20C/20F	2,270	3,150	4,400
60TI/20C/20F2	2,160	3,660	4,640
75TI/20C/5SF	2,840	4,380	5,610
77TI/20C/3SF	1,230	4,460	6,700
60TI/20C/20G100S	1,260	2,790	4,940
60TI/20C/20G120S	1,590	3,520	6,350
75TI/20C/5M	1,920	3,460	5,460
60TI/30C/10F	2,560	4,150	5,480
60TI/30C/10F2	2,050	2,380	4,350
60TI/30F2/10C	2,190	3,500	4,450
68TI-II/17G120S/15C	3,040	3,700	6,330
60TI-II/25C/15G120S	2,240	3,000	5,540
85TIP/15C	3,590	4,230	5,690
75TIP/25C	2,180	2,790	3,970
85TISM/15C	2,630	3,990	5,260
75TISM/25C	2,370	4,080	6,740
85TIPM/15C	4,240	4,630	7,520
75TIPM/25C	3,050	3,700	5,670

Table 32. Compressive strength results for mixtures containing Class F fly ash

	Compressive strength (psi)		
Mixture ID	**3 day**	**7 day**	**28 day**
60TI/20C/20F	2,270	3,150	4,400
60TI/20F/20F2	2,490	3,290	4,120
75TI/20F/5SF	3,230	4,150	6,400
77TI/20F/3SF	3,420	4,100	5,640
60TI/20F/20G100S	2,550	3,100	6,210
60TI/20F/20G120S	3,090	4,340	6,810
75TI/20F/5M	3,490	4,260	6,720
60TI/30C/10F	2,560	4,150	5,480
60TI/30F/10F2	2,340	3,060	4,170
65TI/30F/5SF	2,670	4,310	7,020
67TI/30F/3SF	2,520	3,870	5,530
50TI/30F/20G100S	2,030	2,770	5,070
50TI/30F/20G120S	2,660	4,150	5,970
65TI/30F/5M	2,940	4,050	5,390
50TI/35G100S/15F	1,990	3,390	5,900
50TI/35G120S/15F	2,060	3,330	5,370
68TI-II/17G120S/15F	3,050	3,920	5,880
60TI-II/25F/15G120S	2,730	3,390	6,390
85TIP/15F	3,190	3,910	5,220
75TIP/25F	2,920	3,190	4,780
85TISM/15F	2,700	2,970	6,090
75TISM/25F	2,880	4,070	5,940
85TIPM/15F	4,290	4,580	8,340
75TIPM/25F	3,220	3,910	6,530

Table 33. Compressive strength results for mixtures containing Class F2 fly ash

	Compressive strength (psi)		
Mixture ID	**3 day**	**7 day**	**28 day**
60TI/20C/20F2	2,160	3,660	4,640
60TI/20F/20F2	2,490	3,290	4,120
75TI/20F2/5SF	3,670	5,090	6,570
77TI/20F2/3SF	3,680	4,780	5,640
60TI/20F2/20G100S	2,280	3,480	5,320
60TI/20F2/20G120S	2,440	4,060	5,520
75TI/20F2/5M	2,980	4,310	5,260
60TI/30C/10F2	2,050	2,380	4,350
60TI/30F2/10C	2,190	3,500	4,450
60TI/30F/10F2	2,340	3,060	4,170
65TI/30F2/5SF	2,690	3,560	5,210
67TI/30F2/3SF	2,620	3,690	4,660
50TI/30F2/20G100S	1,510	2,640	5,020
50TI/30F2/20G120S	1,870	2,950	5,130
65TI/30F2/5M	2,820	4,160	6,030
50TI/35G100S/15F2	1,880	3,040	5,890
50TI/35G120S/15F2	2,290	3,580	6,070
68TI-II/17G120S/15F2	2,600	3,310	5,580
60TI-II/25F2/15G120S	2,180	2,990	5,470
85TIP/15F2	2,810	3,510	4,950
75TIP/25F2	2,490	2,990	4,060
85TISM/15F2	2,980	4,120	6,830
75TISM/25F2	2,500	3,290	4,840
85TIPM/15F2	3,580	3,980	6,080
75TIPM/25F2	2,910	3,700	5,960

Table 34. Compressive strength results for mixtures containing Grade 100 GGBFS

	Compressive strength (psi)		
Mixture ID	**3 day**	**7 day**	**28 day**
60TI/20C/20G100S	1,260	2,790	4,940
60TI/20F/20G100S	2,550	3,100	6,210
60TI/20F2/20G100S	2,280	3,480	5,320
50TI/30F/20G100S	2,030	2,770	5,070
50TI/30F2/20G100S	1,510	2,640	5,020
50TI/35G100S/15F	1,990	3,390	5,900
50TI/35G100S/15F2	1,880	3,040	5,890
60TI/35G100S/5SF	2,670	4,110	6,580
62TI/35G100S/3SF	2,970	4,220	7,130
60TI/35G100S/5M	2,780	4,820	6,610
64TI-II/20G100S/16G120S	2,860	3,490	7,030
52TI-II/35G100S/13G120S	2,180	3,290	6,910
80TIP/20G100S	2,950	3,560	5,530
65TIP/35G100S	2,360	3,220	6,410
80TISM/20G100S	3,130	3,640	6,210
65TISM/35G100S	2,460	3,300	6,030
80TIPM/20G100S	3,450	3,920	6,870
65TIPM/35G100S	2,480	4,010	6,780

Table 35. Compressive strength results for mixtures containing Grade 120 GGBFS

	Compressive strength (psi)		
Mixture ID	**3 day**	**7 day**	**28 day**
60TI/20C/20G120S	1,590	3,520	6,350
60TI/20F/20G120S	3,090	4,340	6,810
60TI/20F2/20G120S	2,440	4,060	5,520
50TI/30F/20G120S	2,660	4,150	5,970
50TI/30F2/20G120S	1,870	2,950	5,130
50TI/35G120S/15F	2,060	3,330	5,370
50TI/35G120S/15F2	2,290	3,580	6,070
60TI/35G120S/5SF	2,960	4,890	7,320
62TI/35G120S/3SF	3,060	5,100	6,450
60TI/35G120S/5M	3,200	5,750	7,260
68TI-II/17G120S/15C	3,040	3,700	6,330
68TI-II/17G120S/15F	3,050	3,920	5,880
68TI-II/17G120S/15F2	2,600	3,310	5,580
76TI-II/19G120S/5SF	3,830	4,920	6,380
78TI-II/19G120S/3SF	3,600	4,790	7,720
64TI-II/20G100S/16G120S	2,860	3,490	7,030
76TI-II/19G120S/5M	3,550	4,520	7,520
60TI-II/25C/15G120S	2,240	3,000	5,540
60TI-II/25F/15G120S	2,730	3,390	6,390
60TI-II/25F2/15G120S	2,180	2,990	5,470
52TI-II/35G100S/13G120S	2,180	3,290	6,910
80TIP/20G120S	3,490	4,190	6,710
65TIP/35G120S	2,890	3,960	7,660
80TISM/20G120S	3,110	3,750	7,540
65TISM/35G120S	2,800	4,170	7,240
80TIPM/20G120S	3,580	5,260	6,950
65TIPM/35G120S	3,170	4,680	7,190

Table 36. Compressive strength results for mixtures containing silica fume

	Compressive strength (psi)		
Mixture ID	**3 day**	**7 day**	**28 day**
75TI/20C/5SF	2,840	4,380	5,610
77TI/20C/3SF	1,230	4,460	6,700
75TI/20F/5SF	3,230	4,150	6,400
77TI/20F/3SF	3,420	4,100	5,640
75TI/20F2/5SF	3,670	5,090	6,570
77TI/20F2/3SF	3,680	4,780	5,640
65TI/30F/5SF	2,670	4,310	7,020
67TI/30F/3SF	2,520	3,870	5,530
65TI/30F2/5SF	2,690	3,560	5,210
67TI/30F2/3SF	2,620	3,690	4,660
60TI/35G100S/5SF	2,670	4,110	6,580
62TI/35G100S/3SF	2,970	4,220	7,130
60TI/35G120S/5SF	2,960	4,890	7,320
62TI/35G120S/3SF	3,060	5,100	6,450
90TI/5M/5SF	4,350	5,390	6,430
92TI/5M/3SF	4,470	5,390	7,210
76TI-II/19G120S/5SF	3,830	4,920	6,380
78TI-II/19G120S/3SF	3,600	4,790	7,720
95TIP/5SF	3,890	4,570	6,020
97TIP/3SF	4,120	5,060	6,420
95TISM/5SF	4,120	5,060	6,820
97TISM/3SF	3,850	5,800	7,040
95TIPM/5SF	4,380	6,270	6,560
97TIPM/3SF	4,770	5,330	5,640

Table 37. Compressive strength results for mixtures containing metakaolin

	Compressive strength (psi)		
Mixture ID	**3 day**	**7 day**	**28 day**
75TI/20C/5M	1,920	3,460	5,460
75TI/20F/5M	3,490	4,260	6,720
75TI/20F2/5M	2,980	4,310	5,260
65TI/30F/5M	2,940	4,050	5,390
65TI/30F2/5M	2,820	4,160	6,030
60TI/35G100S/5M	2,780	4,820	6,610
60TI/35G120S/5M	3,200	5,750	7,260
90TI/5M/5SF	4,350	5,390	6,430
92TI/5M/3SF	4,470	5,390	7,210
76TI-II/19G120S/5M	3,550	4,520	7,520
95TIP/5M	3,690	5,200	6,650
95TISM/5M	3,470	5,260	7,530
95TIPM/5M	4,460	6,550	8,150

Class C Fly Ash

Three and seven-day compressive strengths of ternary mixtures with Class C fly ash resulted in strengths ranging from 1,230 psi to 4,240 psi and 2,380 to 4,630 psi, respectively, compared to the binary mixture of PC and 20% Class C fly ash, which had a three-day compressive strength of 2,430 psi and a seven-day compressive strength of 3,820 psi.

Ternary mixtures containing Class C fly ash had 28-day compressive strengths ranging from 3,970 psi to 7,520 psi. The strengths correlated well with the bulk chemistry of the mixture, especially the chemical percentages of CaO and Al_2O_3. Twenty-eight day strengths with mixtures having Class C fly ash were generally greater than 5,000 psi for CaO contents greater than 58 percent and for Al_2O_3 contents less than 14%. Mixtures with CaO contents less than 58% ranged from 3,970 psi to 4,640 psi, with two mixtures having 28-day strengths in the mid 5,000 psi. The binary mixture containing PC and 20% Class C fly ash had a 28-day compressive strength of 4,710 psi.

Class F Fly Ash

Three- and seven-day compressive strengths for ternary mixtures containing Class F fly ash had strengths ranging from 1,990 psi to 4,290 psi and 2,770 to 4,580 psi, respectively, compared to the binary mixture of PC and 20% Class F fly ash, which had a three-day compressive strength of 3,240 psi and a seven-day compressive strength of 4,050 psi.

Ternary mixtures containing Class F fly ash had 28-day compressive strengths ranging from 4,120 psi to 8,340 psi. The strengths correlated well with the bulk chemistry of the mixture, especially the chemical percentage of Al_2O_3. Twenty-eight day strengths ranged from 5,880 psi to 8,340 psi for Al_2O_3 percentages lower than 14%; and strengths ranged from 5,480 psi to 6,810 psi for Al_2O_3 percentages varying from 16% to 18%. The ternary mixtures with Al_2O_3 percentages of 14% to 16% had 28-day strengths ranging from 5,370 psi to 5,900 psi. Twenty-eight day compressive strengths ranged from 4,120 psi to 5,970 psi for Al_2O_3 percentages greater than 18%, with two mixtures, 75TIPM/25F and 65TI/30F/5SF having strengths of 6,530 psi to 7,020 psi. The binary mixture containing PC and 20% Class F fly ash had a seven-day compressive strength of 5,500 psi.

Class F2 Fly Ash

Ternary mixtures containing Class F2 fly ash had three-day compressive strengths ranging from 1,510 psi to 3,680 psi. The strengths correlated well with the bulk chemistry of the mixture, especially the chemical percentage of CaO. Three-day strengths for mixtures having Class F2 fly ash ranged from 2,980 psi to 3,680 psi for CaO contents greater than 57%. Mixtures with CaO contents lower than 57% had three-day compressive strengths ranging from 1,510 psi to 2,910 psi. The binary mixture containing PC and 20% Class F2 fly ash had a three-day compressive strength of 3,430 psi.

Seven-day compressive strengths for ternary mixtures containing Class F2 fly ash had strengths ranging from 2,380 psi to 5,090 psi. The strengths correlated well with the bulk chemistry of the mixture, especially the chemical percentages of CaO and SiO_2. Seven-day strengths with mixtures having Class F2 fly ash ranged from 3,310 psi to 5,090 psi for CaO contents greater than 57% and for SiO_2 contents less than 32%. Other mixtures falling out of this range had seven-day compressive strengths between 2,640 psi to 3,660 psi with one mixture, 65TI/30F2/5M, having a strength of 4,160 psi. The binary mixture containing PC and 20% Class F2 fly ash had a seven-day compressive strength of 3,770 psi.

Ternary mixtures containing Class F2 fly ash had 28-day compressive strengths ranging from 4,120 psi to 6,830 psi. The strengths correlated well with the bulk chemistry of the mixture, especially the chemical percentages of CaO and Al_2O_3. Twenty-eight day strengths with mixtures having Class F2 fly ash ranged from 4,840 psi to 6,830 psi for CaO contents greater than 55%, and ranged from 5,530 psi to 6,830 psi for Al_2O_3 contents less than 12%. Other ternary strengths ranged from 4,000 psi to the low 5,000 psi. The binary mixture containing PC and 20% Class F2 fly ash had a 28-day compressive strength of 5,630 psi.

Grade 100 GGBFS

Three-day compressive strengths for ternary mixtures containing GGBFS Grade 100 slag had strengths ranging from 1,260 psi to 3,450 psi. The binary mixture containing PC and 35% GGBFS Grade 100 slag had a three-day compressive strength of 2,770 psi.

Ternary mixtures containing GGBFS Grade 100 slag had seven-day compressive strengths ranging from 2,640 psi to 4,820 psi. The strengths correlated well with the bulk chemistry of the mixture, especially the chemical percentage of CaO. Strengths ranged from 3,290 psi to 4,820 psi for CaO percentages greater than 60%, 3,040 psi to 3,560 psi for CaO percentages between 53% and 60%, and 2,640 psi to 2,770 psi for CaO percentages less than 53%. The binary mixture containing PC and 35% GGBFS Grade 100 slag had a seven-day compressive strength of 4,310 psi.

Twenty eight-day compressive strengths for ternary mixtures containing GGBFS Grade 100 slag had strengths ranging from 4,940 psi to 7,130 psi. Strengths of mixtures containing GGBFS Grade 100 slag were dependant on the CaO content: the higher the CaO percentage the higher the strengths. CaO percentages equal to and greater than 59% had the highest strengths ranging from 6,030 psi to 7,130 psi. Strengths ranging from 4,940 psi to 6,410 psi were correlated with CaO percentages less than 59%. The binary mixture containing PC and 35% GGBFS Grade 100 slag had a 28-day compressive strength of 6,720 psi.

Grade 120 GGBFS

Three-day compressive strengths for ternary mixtures containing GGBFS Grade 120 slag had strengths ranging from 1,590 psi to 3,830 psi. The binary mixtures containing Type I PC with 35% GGBFS Grade 120 slag and Type I/II cement with 20% GGBFS Grade 120 slag had a three-day compressive strengths of 3,110 psi and 3,700 psi, respectively.

Seven-day compressive strengths for ternary mixtures containing GGBFS Grade 120 slag had strengths ranging from 2,950 psi to 5,750 psi. The binary mixtures containing Type I/II cement with 20% GGBFS Grade 120 slag and Type I PC with 35% GGBFS Grade 120 slag had a seven-day compressive strengths of 4,370 psi and 5,000 psi, respectively.

Ternary mixtures containing GGBFS Grade 120 slag had 28-day compressive strengths ranging from 5,130 psi to 7,720 psi. The strengths correlated well with the bulk chemistry of the mixture, especially the chemical percentages of CaO and Al_2O_3. Strengths were consistently greater than 6,000 psi and ranged from 5,580 psi to 7,720 psi for CaO percentages greater than 60% and Al_2O_3 smaller than 14%. Other mixtures falling out of the range had strengths varying from 5,130 psi to 6,810 psi with eight of the 12 mixtures consisting of strength of 5,000 psi. The binary mixtures containing Type I/II cement with 20% GGBFS grade 120 slag and Type I PC with 35% GGBFS Grade 120 slag had 28-day compressive strengths of 6,780 psi and 7,110 psi, respectively.

Silica Fume

Three-day compressive strengths for ternary mixtures containing silica fume had strengths ranging from 1,230 psi to 4,770 psi. The strengths were dependent upon the bulk chemistry of the mixture, especially the chemical percentages of CaO and Al_2O_3. Strengths consistently ranged from 3,000 psi to 4,500 psi correlating with CaO contents generally greater than 55% and Al_2O_3 contents less than 12%. Other mixtures falling out of the range were mostly less than

3,000 psi; however, there were several mixtures not falling within the range which had compressive strengths greater than 3,000 psi.

Seven-day compressive strengths for ternary mixtures containing silica fume had strengths ranging from 3,560 psi to 6,270 psi. The strengths correlated well with the bulk chemistry of the mixture, especially the chemical percentages of Al_2O_3. Strengths ranged from 4,110 psi to 6,270 psi with Al_2O_3 levels less than 12%, while the mixtures having Al_2O_3 greater than 12% had strengths ranging from 160 psi to 4,310 psi.

Ternary mixtures containing silica fume had 28-day compressive strengths ranging from 3,670 psi to 7,720 psi. Compressive strengths of mixtures containing silica fume correlated well with the Al_2O_3 content. Al_2O_3 contents less than 11% showed compressive strengths ranging from 6,380 to 7,720 psi. Mixtures with Al_2O_3 contents greater than 11% ranged from 4,660 psi to 6,700 psi.

Metakaolin

Three-day compressive strengths for ternary mixtures containing metakaolin had strengths ranging from 1,920 psi to 4,470 psi. The strengths correlated well with the bulk chemistry of the mixture, especially the chemical percentages of CaO and Al_2O_3. Strengths ranged from 3,470 psi to 4,470 psi with CaO contents greater than 60% and Al_2O_3 contents less than 11%. Mixtures falling out of the CaO and Al_2O_3 range had strengths between 130 psi to 3,490 psi with the exception of the ternary mixture 95TIP/5M which had a strength of 3,690 psi.

Seven-day compressive strengths for ternary mixtures containing metakaolin had strengths ranging from 3,460 psi to 6,550 psi. The strengths correlated well with the bulk chemistry of the mixture, especially the chemical percentages of CaO and Al_2O_3. Strengths ranged from 4,520 psi to 6,550 psi with CaO percentages greater than 60% and Al_2O_3 percentages less than 12%. Mixtures falling out of the CaO and Al_2O_3 range had strengths of 310 psi to 4,310 psi.

Ternary mixtures containing metakaolin had 28-day compressive strengths ranging from 5,260 psi to 8,150 psi. Mixtures containing the metakaolin correlated well with the bulk chemistry with specific chemicals CaO and Al_2O_3. Strengths ranging from 6,430 psi to 8,150 psi had CaO contents greater than 60% and Al_2O_3 contents less than 12%. Mixtures not within the range had strengths of 5,260 psi to 6,030 psi with the exception of the ternary mixture 75TI/20F/5M which had a strength of 6,720 psi.

Discussion of Severe Retardation and Early Compressive Strengths

Several early age compressive strength results were affected by the water reducer added to the mixtures. When the recommended dosage amount was exceeded in order to acquire a sufficient flow, severely retarded early strengths were exhibited and are shown in Table 38. Table 39 represents the same mixtures as shown in Table 38 with the three- and seven-day strengths when the 200 N recommended dosage rates were followed.

Table 38. Mortar mixtures over the recommended water reducer dosage rate

Mixture	Cement (g)	200N (mL)	Flow	Compressive strength (psi) 3 day	7 day
80TI/20C	1363.6	5.0	102	90	2070
80TI/20F	1363.6	8.0	82	130	3960
80TI/20F2	1363.6	5.0	90	2470	3930

Table 39. Mortar mixtures following the recommended water reducer dosage rate

Mixture	Cement (g)	200N (mL)	Flow	Compressive strength (psi) 3 day	7 day
80TI/20C	1110.0	1.7	108	1950	3950
80TI/20F	1110.0	2.1	89	3340	3920
80TI/20F2	1110.0	1.5	117	3230	3640

For the particular mixtures presented above, results show that following the recommended water reducer dosage rates led to 31% to 2,500% greater three-day compressive strengths. The particular mixtures that exceeded the recommended water reducer dosage rates with the Class F fly ash recovered from their slow strength gain within seven days to comparable strengths to the same mixtures that followed the recommended water reducer dosage rate; however, the mixture over the recommended water reducer dosage rate with the Class C fly ash had only half the seven-day compressive strength as the same mixture following the recommended water reducer dosage rate.

Early strengths were retarded when using the Class C fly ash, even when recommended dosage rates of the water reducer were followed. All mixtures with three-day compressive strengths less than 1,000 psi are presented in Table 40.

All ternary mixtures within this table have Type I cement and Class C fly ash in common. The lowest three-day compressive strengths, below 100 psi, were ternary mixtures 65TI/30C/5SF, 67TI/30C/3SF, and 50TI/35G120S/15C. By seven days, half of these mixtures had recovered from the slow rate gain while 65TI/30C/5SF, 67TI/30C/3SF, 65TI/30C/5M, and 50TI/35G120S/15C still had strengths below 1,000 psi. All ternary mixtures recovered from their slow strength gain by 28 days, which suggests the retardation effect of the water reducer (200N) had no long term effects.

Table 40. Mortar mixtures containing ternary cementitious materials with early retarded strengths following the recommended water reducer dosage rate

Mixture	Cement (g)	200N (mL)	Flow	Compressive strength (psi) 3 day	7 day	28 day
65TI/30C/5SF	1110.0	2.5	105	90	160	4660
67TI/30C/3SF	1110.0	2.2	112	80	830	3670
50TI/30C/20G100S	1110.0	1.0	106	710	1930	4300
50TI/30C/20G120S	1110.0	1.0	118	150	2150	4640
65TI/30C/5M	1110.0	2.4	101	130	310	5550
60TI/30F/10C	1110.0	2.9	92	510	2770	4220
50TI/35G100S/15C	1110.0	1.8	92	950	2510	5610
50TI/35G120S/15C	1110.0	2.8	112	80	890	6090

A statistical analysis was completed using the previously mentioned methods of least squares and stepwise regression. The results for the linear least squares analysis for the three- seven- and 28- day compressive strength results (in psi) are shown in Table 41. Note that the correlation coefficients range from 0.79 to 0.45 as the age of testing is increased from three days to 28 days.

Table 42 shows the results of the stepwise regression analysis. Note the correlation coefficients ranged from 0.78 to 0.45, as is expected, due to the removing of some variables.

Table 41. Linear least squares regression analysis results for three- seven- and 28-day compressive strengths

Equation #	Equation	R^2
1	3 Day = $-62.6C_3S - 295.6C_2S + 391C_3A + 1020.7C_4AF - 29.3FACaO + 57.4SF - 150.9S + 35.8M + 668.1$	0.792
2	7 Day= $-11.5C_3S - 4.6C_2S + 86.6C_3A + 361.5C_4AF - 25.2FACaO + 124.2SF + 16.2S + 120.8M + 1900.4$	0.624
3	28 Day = $60.1C_3S + 129.3C_2S - 218.5C_3A - 270.2C_4AF - 25.5FACaO + 103.1SF + 541.8S + 139.7M + 5022.5$	0.447

Table 42. Stepwise regression analysis results for three- seven- and 28-day compressive strengths

Equation #	Equation	R^2

1	3 Day = $-69.7C_3S - 331.8C_2S + 456.6C_3A + 1132.1C_4AF - 28.4FACaO + 50.9SF + 272.4$	0.780
2	7 Day= $-10.3C_3S + 79.9C_2S + 347.8C_4AF - 25.4FACaO + 124.1SF + 120.6M + 1933.1$	0.624
3	28 Day = $33.4C_3S + 22.5C_2S - 84.7C_3A - 25.9FACaO + 97.7SF + 568S + 139.1M + 4907$	0.445

Shrinkage

Each mixture consists of a 28-day shrinkage value or length change of hardened hydraulic-cement mortar. The results for individual mixtures are shown in Appendix F by SCM replacement type.

Control mixtures containing 100% portland or blended cement had 28-day shrinkage values ranging from -0.0667% to -0.1178%. The lowest shrinkage value of the control mixtures consisted of the 100% Type I/II cement while the highest shrinkage value was the 100% Type I PC mixture. This is consistent with the chemistry of the cements.

Mixtures containing Class C fly ash had 28-day shrinkage values ranging from -0.0630% to -0.0978%. The lowest shrinkage value was the ternary mixture 85TIPM/15C and the highest shrinkage value was the 60TI/20C/20G120S mixture. Shrinkage did not correlate well with the bulk chemistry of the mixture. The binary mixture consisting of PC and 20% Class C fly ash had a shrinkage value of -0.1109%. All mixtures with Class C fly ash had a shrinkage mean of -.0810% with a standard deviation of 0.0088.

Mixtures containing Class F fly ash had 28-day shrinkage values ranging from -0.0653% to -0.1193%. The lowest shrinkage value was the ternary mixture 75TISM/25F and the highest shrinkage value was the 50TI/30F/20G100S mixture. Shrinkage did not correlate well with the bulk chemistry of the mixture. The binary mixture consisting of PC and 20% Class F fly ash had a shrinkage value of -0.1006%. The mean of all shrinkage specimens containing Class F fly ash was -0.0870% with a standard deviation of 0.0122.

Mixtures containing Class F2 fly ash had 28-day shrinkage values ranging from -0.0660% to -0.1030%. The lowest shrinkage value was the ternary mixture 85TIPM/15F2 and the highest shrinkage value was the 50TI/30F2/20G120S mixture. Shrinkage did not correlate well with the bulk chemistry of the mixture. The binary mixture consisting of PC and 20% Class F2 fly ash had a shrinkage value of -0.1077%. The mean of all shrinkage specimens containing Class F2 fly ash was -0.0865% with a standard deviation of 0.0106.

Mixtures containing Grade 100 GGBFS had 28-day shrinkage values ranging from -0.0735% to -0.1193%. The lowest shrinkage value was the ternary mixture 65TISM/35G100S and the highest shrinkage value was the 50TI/30F/20G100S mixture. Strengths were dependent upon the bulk chemistry of the mixture. Shrinkage values ranged from -0.0735% to -0.0888% with CaO

percentages greater than 59%. Mixtures with CaO percentages less than 59% had shrinkage values from -0.0903% to -0.1193%. The binary mixture consisting of PC and 35% grade 100 GGBFS had a shrinkage value of -0.0866%. All mixtures containing grade 100 GGBFS had a mean of -0.0889% with a standard deviation of 0.0111.

Mixtures containing grade 120 GGBFS had 28-day shrinkage values ranging from -0.0723% to -0.1030%. The lowest shrinkage value was the ternary mixture 76TI-II/19G120S/5M and the highest shrinkage value was the 50TI/30F2/20G120S mixture. Shrinkage did not correlate well with the bulk chemistry of the mixture. The binary mixture consisting of Type I/II cement with 20% Grade 120 GGBFS had a shrinkage value of -0.0893%, while the mixture containing PC with 35% Grade 120 GGBFS had a shrinkage value of -0.0938%. All shrinkage specimens with the Grade 120 GGBFS had a mean of -0.0854% with a standard deviation of 0.0073.

Mixtures containing silica fume had 28-day shrinkage values ranging from -0.0705% to -0.1005%. The lowest shrinkage value was the ternary mixture 95TISM/5SF and the highest shrinkage value was the 92TI/5M/3SF mixture. Shrinkage did not correlate well with the bulk chemistry of the mixture. All shrinkage specimens with silica fume had a mean of -0.0883% and a standard deviation of 0.0078.

Mixtures containing metakaolin had 28-day shrinkage values ranging from -0.0707% to -0.1005%. The lowest shrinkage value was the ternary mixture 65TI/30C/5M and the highest shrinkage value was the 92TI/5M/3SF mixture. Shrinkage did not correlate well with the bulk chemistry of the mixture. The mean of all shrinkage specimens containing metakaolin was -0.0835% with a standard deviation of 0.0106.

Each ternary mixture was compared to its respective control mixture (i.e., cement type) by comparing the paste content and shrinkage as a percent of the control mixture. The results are presented by cement type in Table 43–Table 48.

Table 43. Paste content and shrinkage (as a percent of the control) for mortar mixtures containing Type I PC

Mixtures	Paste content (%)	Shrinkage (%)
60TI/20C/20F	2.1	-34.0
60TI/20C/20F2	2.0	-28.7
75TI/20C/5SF	1.2	-31.9
77TI/20C/3SF	1.0	-30.4
60TI/20C/20G100S	1.1	-31.5
60TI/20C/20G120S	0.9	-17.0
75TI/20C/5M	1.0	-39.5
60TI/20F/20F2	2.6	-35.1
75TI/20F/5SF	1.8	-25.5
77TI/20F/3SF	1.6	-30.8
60TI/20F/20G100S	1.7	-16.2
60TI/20F/20G120S	1.5	-21.9
75TI/20F/5M	1.6	-21.7
75TI/20F2/5SF	1.7	-19.1
77TI/20F2/3SF	1.5	-15.1
60TI/20F2/20G100S	1.6	-21.9
60TI/20F2/20G120S	1.4	-23.8
75TI/20F2/5M	1.5	-27.7
60TI/30C/10F	1.8	-31.7
60TI/30C/10F2	1.8	-26.2
65TI/30C/5SF	1.6	-27.4
67TI/30C/3SF	1.4	-19.1
50TI/30C/20G100S	1.5	-23.4
50TI/30C/20G120S	1.3	-34.7
65TI/30C/5M	1.4	-40.0
60TI/30F/10C	2.4	-26.0

Table 44. Paste content and shrinkage (as a percent of the control) for mortar mixtures containing Type I PC (cont.)

Mixtures	Paste content (%)	Shrinkage difference from control (%)
60TI/30F2/10C	2.2	-28.7
60TI/30F/10F2	2.6	-13.4
65TI/30F/5SF	2.5	-21.5
67TI/30F/3SF	2.3	-23.4
50TI/30F/20G100S	2.4	1.2
50TI/30F/20G120S	2.1	-16.0
65TI/30F/5M	2.3	-16.2
65TI/30F2/5SF	2.3	-20.0
67TI/30F2/3SF	2.1	-18.1
50TI/30F2/20G100S	2.2	-17.7
50TI/30F2/20G120S	2.0	-12.6
65TI/30F2/5M	2.1	-33.2
50TI/35G100S/15C	1.2	-21.1
50TI/35G100S/15F	1.7	-20.9
50TI/35G100S/15F2	1.6	-18.8
60TI/35G100S/5SF	1.1	-32.3
62TI/35G100S/3SF	0.9	-31.0
60TI/35G100S/5M	0.9	-33.0
50TI/35G120S/15C	0.8	-26.4
50TI/35G120S/15F	1.2	-37.0
50TI/35G120S/15F2	1.2	-32.3
60TI/35G120S/5SF	0.7	-25.3
62TI/35G120S/3SF	0.5	-26.6
60TI/35G120S/5M	0.5	-37.4
90TI/5M/5SF	0.7	-16.8
92TI/5M/3SF	0.5	-14.7

Table 45. Paste content and shrinkage (as a percent of the control) for mortar mixtures containing Type I/II PC

Mixtures	Paste content (%)	Shrinkage difference from control (%)
68TI-II/17G120S/15C	0.9	31.5
68TI-II/17G120S/15F	1.4	34.9
68TI-II/17G120S/15F2	1.3	34.2
76TI-II/19G120S/5SF	0.8	23.3
78TI-II/19G120S/3SF	0.6	39.8
64TI-II/20G100S/16G120S	0.7	31.2
76TI-II/19G120S/5M	0.5	8.3
60TI-II/25C/15G120S	1.4	21.8
60TI-II/25F/15G120S	2.1	28.2
60TI-II/25F2/15G120S	2.0	36.4
52TI-II/35G100S/13G120S	1.1	33.0

Table 46. Paste content and shrinkage (as a percent of the control) for mortar mixtures containing Type ISM PC

Mixtures	Paste content (%)	Shrinkage difference from control (%)
85TISM/15C	0.7	1.4
85TISM/15F	1.1	-7.7
85TISM/15F2	1.0	-4.2
95TISM/5SF	0.5	-10.9
97TISM/3SF	0.3	4.0
80TISM/20G100S	0.5	-4.9
80TISM/20G120S	0.2	-5.2
95TISM/5M	0.3	-6.8
75TISM/25C	1.1	-11.5
75TISM/25F	1.8	-17.5
75TISM/25F2	1.7	-9.0
65TISM/35G100S	0.9	-7.1
65TISM/35G120S	0.4	-0.1

Table 47. Paste content and shrinkage (as a percent of the control) for mortar mixtures containing Type IP PC

Mixtures	Paste content (%)	Shrinkage difference from control (%)
85TIP/15C	0.5	-11.5
85TIP/15F	0.9	-9.7
85TIP/15F2	0.8	-11.5
95TIP/5SF	0.4	14.6
97TIP/3SF	0.2	8.3
80TIP/20G100S	0.2	12.5
80TIP/20G120S	0.0	2.3
95TIP/5M	0.2	-1.3
75TIP/25C	0.8	-19.6
75TIP/25F	1.5	-18.7
75TIP/25F2	1.4	-12.4
65TIP/35G100S	0.4	16.1
65TIP/35G120S	0.0	0.8

Table 48. Paste content and shrinkage (as a percent of the control) for mortar mixtures containing Type IPM PC

Mixtures	Paste content (%)	Shrinkage difference from control (%)
85TIPM/15C	0.6	-17.7
85TIPM/15F	1.1	6.1
85TIPM/15F2	1.0	-13.8
95TIPM/5SF	0.5	2.2
97TIPM/3SF	0.3	4.5
80TIPM/20G100S	0.4	0.2
80TIPM/20G120S	0.2	8.1
95TIPM/5M	0.3	4.1
75TIPM/25C	1.0	-7.9
75TIPM/25F	1.8	9.0
75TIPM/25F2	1.6	0.5
65TIPM/35G100S	0.8	-0.4
65TIPM/35G120S	0.3	11.4

Type I Cement

All ternary mixtures containing Type I cement had paste contents 0.5% to 2.6% greater than the control mixture of plain cement. The shrinkage of all mortar bars was less than the control mixtures of plain cement except for one ternary mixture (50TI/30F/20G100S), which had a 1.2% greater shrinkage value than 100% Type I cement. The mean shrinkage of all mixtures was 24.9% with a standard deviation of 8.2.

Ternary mixtures containing Type I cement, Class C fly ash, and another cementitious material had paste contents ranging from 0.8% to 2.4% greater than the plain Type I cement and shrinkage values ranging from 17% to 40% less than the control cement. The average shrinkage percentage of these ternary mixtures was 20% with a standard deviation of 17.0.

Mixtures containing Type I cement, Class F fly ash, and another cementitious material had paste contents ranging from 1.2% to 2.6% greater than the control cement and shrinkage values ranging from 13.4% to 37% less than the plain cement. One mixture (50TI/30F/20G100S) had a 1.2% greater shrinkage in comparison to the 100% Type I cement. The mean shrinkage was 15% with a standard deviation of 18.2.

Paste contents for mixtures containing Type I cement, Class F2 fly ash, plus another SCM ranged from 1.2% to 2.6% greater than the control Type I cement with shrinkage values ranging 12.6% to 35.1% less than the plain cement. The average shrinkage percentage of ternary mixtures containing Type I cement, Class F2 fly ash, and another cementitious material was 15% with a standard deviation of 17.5.

All ternary mixtures with Type I cement, GGBFS grade 100 slag, and another cementitious material had paste contents 0.9% to 2.4% greater than the control Type I cement and shrinkage values 16.2% to 33.0% less than the plain cement. One mixture, 50TI/30F/20G100S, did have a 1.2% higher shrinkage value in comparison to the control cement. The mean shrinkage percentage of these mixtures was 12% with a standard deviation of 18.

Mixtures containing Type I cement, GGBFS Grade 120 slag, plus another constituent had paste contents ranging from 0.5% to 2.1% greater than the control Type I cement and shrinkage values 12.6% to 37.4% less than plain cement. All mixtures with Type I cement and GGBFS grade 120 slag had a mean shrinkage percentage of 1.0% with a standard deviation of 26.2.

Paste contents of mixtures containing Type I cement, silica fume, plus another SCM ranged from 0.5% to 2.5% greater than a mixture of 100% Type I cement, and shrinkage values 14.7% to 32.3% less than the control cement. The mean shrinkage percentage of these ternary mixtures was 13% with a standard deviation of 18.8.

Ternary mixtures with Type I cement, metakaolin, and another cementitious material had past contents 0.5% to 2.3% greater than the mixture 100% Type I cement and shrinkage values 14.7% to 40% less than the control cement. The mean shrinkage percentage was 20% with a standard deviation of 16.3%.

Type I/II Cement

All ternary mixtures containing Type I/II cement had paste contents 0.5% to 2.1% greater than the control mixture of plain Type I/II cement. The shrinkage of all mortar bars was 8.3% to 39.8% greater than the control mixtures of plain Type I/II cement. The mean shrinkage percentage of all mixtures was 29.3% with a standard deviation of 8.8.

Type ISM Cement

Mixtures containing Type ISM cement had paste contents ranging from 0.2% to 1.8% greater than the plain Type ISM cement mixture. Shrinkage of mortar bars ranged from 0.1% to 17.5% less than the control cement with the exception of two mixtures, 85TISM/15C and 97TISM/3SF, which had a 1.4% and 4.0% increase in shrinkage. The statistical average for the shrinkage percentage was 6.1% with a standard deviation of 5.7%.

Type IP Cement

Paste contents of ternary mixtures containing Type IP cement ranged from 0% to 1.5% greater than the control Type IP cement. All mixtures containing the Type IP cement with fly ash or metakaolin had shrinkage values of 9.7% to 19.6% and 1.3% less than the control Type IP cement. Mixtures with Type IP cement and GGBFS or silica fume had shrinkage values 0.8% to 16.1% greater than Type IP control mixture. The statistical average was 2.3% with a standard deviation of 12.5.

Type IPM Cement

All ternary mixtures containing the Type IPM cement had paste contents 0.2% to 1.8% greater than the control mixture of plain Type IPM cement. Mixtures had shrinkage values 0.2% to 11.4% greater than the Type IPM cement control. Four mixtures, 85TIPM/15C, 85TIPM/15F2, 75TIPM/25C, and 65TIPM/35G100S, had shrinkage values 0.4% to 17.7% less than the Type IPM cement control. The mean value of all mixtures containing the Type IPM cement was 0.5% greater than the control with a standard deviation of 8.8.

A statistical analysis was conducted to determine the effect of paste content as well as chemistry on the shrinkage results. The paste content analysis showed inconclusive results most likely due to the very narrow range of paste contents from 42.1% to 43.4%. Linear least squares regression analysis including cement chemistry, fly ash calcium oxide content, GGBFS fineness, metakaolin, and silica fume contents showed a poor correlation coefficient of about 0.38. The authors note that the shrinkage results may be more conclusive when investigating the concrete mixtures in Phase II.

Sulfate Resistance

The sulfate resistance of each of the cementitious material combinations was measured according to ASTM C1012. The mortar bars will be under exposure for 12–18 months. At this point in the project, the three-month results are completed, but do not reveal any meaningful data that can be used to draw results of recommendations. The minimum evaluation time for C1012 is six months.

Alkali Silica Reaction

The resistance to alkali silica reaction of each of the cementitious material combinations was measured according to ASTM C1567. The accelerated mortar bar testing is under exposure at this time and will be completed by the December panel meeting. At this point in the project, 95% of all the mixtures are either under exposure or completed.

SUMMARY

Phase I of the study created the baseline for a broad array of ternary cementitious material combinations for concrete. The work shows that ternary cementitious combinations have no as-yet-identified technical barriers to their wider use in pavements, bridges and other structures. The results presented herein show that compressive strength potential at all ages for ternary combinations is excellent. Clearly this work has shown that nearly all combinations of materials were able to meet general transportation use and concrete strength requirements. The heat of hydration and setting time of all mixtures were acceptable. The lower heat of hydration of some of the mixtures may be especially valuable in hot weather applications. Setting time was delayed by the use of a sucrose-based water reducing admixture. The compatibility of admixtures with more complex cementitious systems was expected and was one of the potential tasks in Phase I. The work presented in this report shows that use of polycarboxylate-based water reducers was effective in reducing compatibility issues.

Shrinkage generally increased for ternary combinations incorporating Type I/II cement when compared to the Type I/II cement control, but decreased for many combinations with Type I cement and blended cements. This would indicate that the cement plays a major role in shrinkage reduction. Sulfate resistance testing is ongoing. The key component of this testing is the effect of a third pozzolan to cementitious combinations containing Class C fly ash. It will take some months before it can be determined if sulfate attack exacerbated by Class C fly ash can be mitigated by the combination of other pozzolans. The effectiveness of ternary combinations in mitigating ASR is also a result that will be known in the coming weeks.

The major result of Phase I is that we did not identify any combinations of materials that would prohibit them from use in concrete for pavements, bridges, or other structures. Depending on the technical requirements of the application, some have preferential properties, but all performed well in the screening tests in this phase. Some compatibility issues were identified, but solutions were also identified.

RECOMMENDATIONS

The study is progressing into the laboratory testing of Phase II. This will use 564 lbs/yd^3, or "6-sack" mixtures containing 48 different cementitious combinations. The combinations include

- Type I cement with binary combination controls and 26 ternary combinations (31 total combinations with TI cement),
- Type IP with six SCM combinations (seven total),
- Type IPM with four SCM combinations (five total),
- and Type ISM with four SCM combinations (five total).

Each of these combinations is technically advantageous for highway applications, economical, and represents potential combinations that the project could use in Phase III. At least 11 of these ternary mixtures have the potential to have maturity in cold weather concrete operations (measured as greater than 3,500 psi at three days), and at least 11 of these mixtures have the maturity characteristics for hot weather concrete (measured as less than 2,500 psi at three days).

Control	Compressive Strength (psi)		
Mixture ID	**3 Day**	**7 Day**	**28 Day**
100TI	4,700	6,260	6,170
80TI/20C	2,430	3,820	4,710
80TI/20F	3,420	4,050	5,500
80TI/20F2	3,430	3,770	5,630
65TI/35G120S	3,110	5,000	7,110
100TIP	3,610	4,310	6,680
100TISM	3,220	4,700	6,040
Mixture ID	**3 Day**	**7 Day**	**28 Day**
60TI/20C/20F	2,270	3,150	4,400
60TI/20C/20F2	2,160	3,660	4,640
60TI/30C/10F	2,560	4,150	5,480
60TI/30F2/10C	2,190	3,500	4,450
60TI/20F/20F2	2,490	3,290	4,120
75TI/20F/5SF	3,230	4,150	6,400
77TI/20F/3SF	3,420	4,100	5,640
60TI/20F/20G120S	3,090	4,340	6,810
75TI/20F/5M	3,490	4,260	6,720
60TI/30F/10F2	2,340	3,060	4,170
65TI/30F/5SF	2,670	4,310	7,020
67TI/30F/3SF	2,520	3,870	5,530
50TI/30F/20G120S	2,660	4,150	5,970
65TI/30F/5M	2,940	4,050	5,390

50TI/35G120S/15F	2,060	3,330	5,370
75TI/20F2/5SF	3,670	5,090	6,570
77TI/20F2/3SF	3,680	4,780	5,640
60TI/20F2/20G120S	2,440	4,060	5,520
75TI/20F2/5M	2,980	4,310	5,260
60TI/30C/10F2	2,050	2,380	4,350
65TI/30F2/5SF	2,690	3,560	5,210
67TI/30F2/3SF	2,620	3,690	4,660
65TI/30F2/5M	2,820	4,160	6,030
50TI/35G120S/15F2	2,290	3,580	6,070
62TI/35G120S/3SF	3,060	5,100	6,450
60TI/35G120S/5M	3,200	5,750	7,260
85TIP/15C	3,590	4,230	5,690
85TIP/15F	3,190	3,910	5,220
85TIP/15F2	2,810	3,510	4,950
65TIP/35G120S	2,890	3,960	7,660
97TIP/3SF	4,120	5,060	6,420
95TIP/5M	3,690	5,200	6,650
75TIP/25C	2,180	2,790	3,970
75TIP/25F	2,920	3,190	4,780
75TIP/25F2	2,910	3,700	5,960
50TIP/50G120S	na	,na	na
75TISM/25C	2,370	4,080	6,740
75TISM/25F2	2,500	3,290	4,840
65TISM/35G120S	2,800	4,170	7,240
97TISM/3SF	3,850	5,800	7,040

REFERENCES

AASHTO AVA Technology Implementation Group. (2003). Standard Test Method for Air-Void Characteristics of Freshly Mixed Concrete by Buoyancy Change. Draft Provisional Standard.

Abdun-Nur, E.A. "Fly Ash in Concrete, An Evaluation." *Highway Research Board Bulletin 284*, 1961.

American Coal Ash Association. "Who we are." http://www.acaa-usa.org/who.htm. Accessed August 29, 2003.

American Concrete Institute; "Ground Granulated Blast-Furnace Slag as a Cementitious Constituent in Concrete." *Manual of Concrete Practice, Part 1—Materials and General Properties of Concrete,* ACI 233R-03. Farmington Hills, MI: ACI, 2007.

American Concrete Institute. "Use of Fly Ash in Concrete." *Manual of Concrete Practice, Part 1—Materials and General Properties of Concrete,* ACI 232.2R-96, Committee 226, Admixtures for Concrete. Farmington Hills, MI: American Concrete Institute, 2007.

American Concrete Institute. "Use of Silica Fume in Concrete." *Manual of Concrete Practice, Part 1—Materials and General Properties of Concrete,* ACI 234R-96, Committee 226, Admixtures for Concrete, ACI, Farmington Hills, MI, 2002.

ASTM C 109/C 109M-05. Standard Test Method for Compressive Strength of Hydraulic Cement Mortars (Using 2-in. or (50-mm) Cube Specimens). *Annual Book of ASTM Standards*, Vol. 4.01. West Conshohocken, PA: American Society for Testing and Materials, 2005.

ASTM C 128-01. Standard Test Method for Density, Relative Density (Specific Gravity), and Absorption of Fine Aggregate. *Annual Book of ASTM Standards,* Vol. 4.02. West Conshohocken, PA: American Society for Testing and Materials, 2003.

ASTM C 150-02a. Standard Specification for Portland Cement. *Annual Book of ASTM Standards,* Vol. 4.01. West Conshohocken, PA: American Society for Testing and Materials, 2003.

ASTM C 157/C 157M-06. Standard Test Method for Length Change of Hardened Hydraulic-Cement Mortar and Concrete. *Annual Book of ASTM Standards*, Vol. 4.02. West Conshohocken, PA: American Society for Testing and Materials, 2006.

ASTM 185-02. Standard Specification for Air Content of Hydraulic Cement Mortar. *Annual Book of ASTM Standards*, Vol. 4.01. West Conshohocken, PA: American Society for Testing and Materials, 2003.

ASTM C 187-98. Standard Test Method for Normal Consistency of Hydraulic Cement. *Annual Book of ASTM Standards*, Vol. 4.01. West Conshohocken, PA: American Society for Testing and Materials, 2003.

ASTM C 188-95. Standard Test Method for Density of Hydraulic Cement. *Annual Book of ASTM Standards*, Vol. 4.01. West Conshohocken, PA: American Society for Testing and Materials, 2003.

ASTM C 191-01a. Standard Test Method for Time of Setting of Hydraulic by Vicat Needle. *Annual Book of ASTM Standards*, Vol. 4.01. West Conshohocken, PA: American Society for Testing and Materials, 2003.

ASTM C 204-00. Standard Test Method for Fineness of Hydraulic Cement by Air-Permeability Apparatus. *Annual Book of ASTM Standards*, Vol. 4.01. West Conshohocken, PA: American Society for Testing and Materials, 2003.

ASTM C 260-06. Standard Specification for Air-Entraining Admixtures for Concrete. *Annual Book of ASTM Standards*, Vol. 4.02. West Conshohocken, PA: American Society for Testing and Materials, 2006.

ASTM 305-06. Standard Practice for Mechanical Mixing of Hydraulic Cement Pastes and Mortars of Plastic Consistency. *Annual Book of ASTM Standards*, Vol. 4.02. West Conshohocken, PA: American Society for Testing and Materials, 2006.

ASTM C 311-02. Standard Test Methods for Sampling and Testing Fly Ash or Natural Pozzolans for Use as a Mineral Admixture in Portland-Cement Concrete. *Annual Book of ASTM Standards*, Vol. 4.02. West Conshohocken, PA: American Society for Testing and Materials, 2003.

ASTM C 403/C 403M-99. Standard Test Method for Time of Setting of Concrete Mixtures by Penetration Resistance. *Annual Book of ASTM Standards*, Vol. 4.02. West Conshohocken, PA: American Society for Testing and Materials, 2003.

ASTM C 494/C 494M-05. Standard Specification for Chemical Admixtures for Concrete. *Annual Book of ASTM Standards*, Vol. 4.02. West Conshohocken, PA: American Society for Testing and Materials, 2005.

ASTM C 441-02a. Standard Test Method for Effectiveness of Pozzolans or Ground Granulated Blast-Furnace Slag in Preventing Excessive Expansion on Concrete Due to Alkali-Silica Reaction. *Annual Book of ASTM Standards*, Vol. 4.02. West Conshohocken, PA: American Society for Testing and Materials, 2003.

ASTM C 595-03. Standard Specification for Blended Hydraulic Cements. *Annual Book of ASTM Standards*, Vol. 4.01. West Conshohocken, PA: American Society for Testing and Materials, 2003.

ASTM C 618-03. Standard Specification for Coal Fly Ash and Raw or Calcined Natural Pozzolan for Use in Concrete. *Annual Book of ASTM Standards*, Volume 4.02. West Conshohocken, PA: American Society for Testing and Materials, 2003.

ASTM C 989-99. Standard Specification for Ground Granulated Blast-Furnace Slag for Use in Concrete and Mortars. *Annual Book of ASTM Standards*, Volume 4.02. West Conshohocken, PA: American Society for Testing and Materials, 2003.

ASTM C 1012-02. Standard Test Method for Length Change of Hydraulic-Cement Mortars Exposed to a Sulfate Solution. *Annual Book of ASTM Standards*, Vol. 4.01. West Conshohocken, PA: American Society for Testing and Materials, 2003.

ASTM C 1240-03. Standard Specification for Silica Fume Used in Cementitious Mixtures. *Annual Book of ASTM Standards*, Vol. 4.02. West Conshohocken, PA: American Society for Testing and Materials, 2003.

ASTM C 1437-01. Standard Test Method for Flow of Hydraulic Cement Mortar. *Annual Book of ASTM Standards*, Vol. 4.01. West Conshohocken, PA: American Society for Testing and Materials, 2003.

Baoyu, L., Anqi, L., and Pengfei, X. "Application of Concrete Incorporating Both Condensed Silica Fume and Fly Ash at Fancuo Hydropower Station." *Fly Ash, Silica Fume, Slag, & Natural Pozzolans in Concrete, Proceedings* 3rd CANMET/ACI International Conference; Trondheim, Norway, Vol. 1, 1989, 593-606.

Barnes, A. "Pavement thickness design using reclaimed hydrated Iowa Class C fly ash as a base material." MSci thesis, Iowa State University, Ames, IA, 1997.

Bhanumathidas, N. and Kumar Mehta, P. "Concrete Mixtures Made with Ternary Blended Cements Containing Fly Ash and Rice-Husk Ash." *Fly Ash, Silica Fume, Slag, & Natural Pozzolans in Concrete, Proceedings* 7th CANMET/ACI International Conference; Chennai (Madras), India, Vol. 1, 2001, 379-391.

Bijen, J., van der Wegen, G., and van Selst, R. "Carbonation of Portland Blast Furnace Slag Cement Concrete with Fly Ash." *Fly Ash, Silica Fume, Slag, & Natural Pozzolans in Concrete, Proceedings* 3rd CANMET/ACI International Conference; Trondheim, Norway, Vol. 1, 1989, 645-668.

Borsoi, A., Collepardi, S., Coppola, L., Troli, R., and Collepardi, M. "Sulfate Attack on blended Portland Cements." *Durability of Concrete, Proceedings* Fifth International Conference; Barcelona, Spain, Vol. 1, 2000, 417-432.

Cain, C.J. "Effects of Various Types of fly Ash on Behavior and Properties of Concrete." *Effects of Fly Ash Incorporation in Cement and Concrete, Proceedings,* Materials Research Society Symposium, 1981, 260-268.

Canadian Standards Association. "Supplementary Cementing Materials," Canadian Specification CAN/CSA-A23.5-98. Etobicoke, Ontario, Canada: Canadian Standards Association, 1998.

Carrasquillo, P.M., Tikalsky, P.J., and Carrasquillo, R.L.; "Mix Proportioning of Concrete Containing Fly Ash for Highway Applications," Texas State Department of Highways and Public Transportation, Report No. FHWA-TX-1987-4-364-4F, May 1986.

Collepardi, S., Corinaldesi, V., Moriconi, G., Bonora, G., and Collepardi, M. "Durability of High-Performance Concretes with Pozzolanic and Composite Cements." Durability of Concrete, Proceedings Fifth International Conference; Barcelona, Spain, Vol. 1, 2000, 161-172.

Curcio, F., DeAngelis, B.A., and Pagliolico, S. "Metakaolin as a Microfiller for High-Performance Mortars." *Cement and Concrete Research*, Vol. 28, No. 6, 1998, 803-809.

Dansk Beton Teknik. "The DBT Air Void Analyzer for Assessment of Quality of Air Void Structures in the Fresh Still Plastic Concrete." Denmark: Dansk Beton Teknik, 2004.

Diamond, S. "The Characterization of Fly Ashes." *Effects of Fly Ash Incorporation in Cement and Concrete, Proceedings, Symposium N.* Materials Research Society, 1981 12-23.

Dikeou, J.T. *Fly Ash Increases Resistance to Concrete Sulfate Attack.* Research Report 23. Water Resources Technical Publication. Denver: Bureau of Reclamation, 1975.

Dunstan, E.R., Jr. "A Possible Method for Identifying Fly Ashes That Will Improve the Sulfate Resistance of Concretes." *ASTM, Cement, Concrete, and Aggregates,* Vol. 2, No. 1, 20-30, 1980.

FHWA. *Fly Ash Facts for Highway Engineers*. Report No. FHWA-SA-94-081, 1995.

Fidjestol, P. and R. Lewis. "Microsilica as an Addition." Chapter 12 in *Lea's Chemistry of Cement and Concrete*. 4th Edition. London: Arnold Publishing Company, P. Hewlett editor. 1998. 675-708.

Frias, M., Sanchez de Rojas, M.I., and Cabrera, J. "The Effect that the Pozzolanic Reaction of Metakaolin has on the Heat Evolution in Metakaolin-Cement Mortars." *Cement and Concrete Research*, Vol. 30, 2000, 209-216.

Ganesh Babu, K. and Sree Rama Kumar, V. "Chloride Diffusivity of GGBFS Concretes." *Fly Ash, Silica Fume, Slag, & Natural Pozzolans in Concrete, Proceedings* 7th CANMET/ACI International Conference; Chennai (Madras), India, Vol. 2, 2001, 611-621.

Giergiczny, Z. "The Properties of Cements Containing Fly Ash Together with Other Admixtures." *Fly Ash, Silica Fume, Slag, & Natural Pozzolans in Concrete, Proceedings* 4th CANMET/ACI International Conference; Istanbul, Turkey, Vol. 1, 1992, 439-456.

Hanson, Todd. Personal Communication. Iowa Department of Transportation, May 2003.

Helmuth, R. *Fly Ash in Cement and Concrete.* Skokie, IL: Portland Cement Association, 1987.

JMP 6.0.0. Statistical Discovery. From SAS. SAS Institute Inc. 2005.

Kashima, S., Furuya, N., and Yamaoka, R. "High-Strength Concrete for Wall Foundation Using Ternary Blended Cement with Intermixture of Blast-Furnace Slag and Fly Ash." *Fly Ash, Silica Fume, Slag, & Natural Pozzolans in Concrete, Proceedings* 4th CANMET/ACI International Conference; Istanbul, Turkey, Vol. 2, 1992, 1451-1469.

Kashima, S., Sakamoto, M., Okada, S., Iho, T., and Nakagawa, Y. "Application of High Slag and Fly Ash, Low-Heat Cement to Antiwashout Underwater Concrete." *Fly Ash, Silica Fume, Slag, & Natural Pozzolans in Concrete, Proceedings*, 4th CANMET/ACI International Conference; Istanbul, Turkey, Vol. 2, 1992, 1601-1619.

Kelham, S., Damtoft, J.S., and Talling, B.L.O. "The Influence of High Early-Strength (HES) Mineralized Clinker on the Strength Development of Blended Cements Containing Fly Ash, Slag, or Ground Limestone*." Fly Ash, Silica Fume, Slag, & Natural Pozzolans in Concrete, Proceedings* 5th CANMET/ACI International Conference; Milwaukee, United States, 1995, 229-247.

Khatri, R.P. and Sirivivatnanon, V. "Optimum Fly Ash Content for Lower Cost and Superior Durability." *Fly Ash, Silica Fume, Slag, & Natural Pozzolans in Concrete, Proceedings* 7th CANMET/ACI International Conference; Chennai (Madras), India, Vol. 1, 2001, 205-219.

Kippax, P. Measuring Particle Size Using Modern Laser Diffraction Techniques. Chemie.De: Information Service, UK. 12 February 2007 <http://www.chemie.de/articles>.

Kosmatka, S.H., Kerkhoff, B., and Panarese, W.C. *Design and Control of Concrete Mixtures*. 14th Edition. Engineering Bulletin 001. Skokie, IL; Portland Cement Association, 2002.

Lea, F.M. *The Chemistry of Cement and Concrete, Fourth Edition, Arnold Publishing,* London, 1998.

Luther, Mark. Personal Communication. Holcim Inc., February 2000.

Lynsdale, C.J. and Khan, M.I. "Chloride and Oxygen Permeability of Concrete Incorporating Fly Ash and Silica Fume in Ternary Systems." *Durability of Concrete, Proceedings* Fifth International Conference; Barcelona, Spain, Vol. 2, 2000, 739-753.

Majko, R.M. "Status of ASTM and Other National Standards for the Use of Fly Ash Pozzolans in Concrete." *Proceedings.* Material Research Symposium, Vol. 86, 1987, 293-306.

Malhotra, V.M. et al. *Condensed Silica Fume in Concrete*. Boca Raton, Florida: CRC Press. 1987.

Manz, O.E. "Coal Fly Ash: A Retrospective and Future Look." *Energeia,* Vol. 9, No. 2, 1-5. University of Kentucky, Center for Applied Energy Research, 1998.

Massazza, F. "Pozzolana and Pozzolanic Cements" Chapter 10 in *Lea's Chemistry of Cement and Concrete.* 4th Edition. London: Arnold Publishing Company, P. Hewlett editor. 1998, 471-631.

McCarthy, G.J., et al. "Mineralogy of Western Fly Ash." *Cement and Concrete Research*, Vol. 14, No. 4, 471-478, 1984.

McCarthy, G.J., et al. "Use of a Database of Chemical, Minerological and Physical Properties of North American Fly Ash to Study the Nature of Fly Ash and its Utilization as a Mineral Admixture in Concrete." *Proceedings*, Materials Research Society Symposium, Vol. 178, 3-33, 1990.

Mehta, P.K. "Role of Pozzolanic and Cementitious Material in Sustainable Development of the Concrete Industry." *Fly Ash, Silica Fume, Slag, & Natural Pozzolans in Concrete, Proceedings* 6th CANMET/ACI International Conference, Bangkok, Thailand, 1998, 1-20.

Menendez, G., Bonavetti, V.L., Donza, H., Trezza, M., and Irassar, E.F. "Ternary Blended Cements for High-Performance Concrete." *High Performance Concrete: Performance and Quality of Concrete Structures, Proceedings* 3rd International Conference; Recife, PE, Brazil, 2002, 435-448.

Mielenz, R.C. "Mineral Admixtures-History and Background," *Concrete International.* Aug. 1983.

Mindess, S., Young, J.F. and Darwin, D. *Concrete*, Second Edition. Pearson Education, Inc, Upper Saddle River, NJ, 2003.

Misra, A. "Utilization of western coal fly ash in construction of highways in the Midwest." *MATC UMC 96-2 Final Report*, Mid-America Transportation Center, University of Nebraska-Lincoln, Lincoln, NE, 2000.

Papadakis, V.G. "Effeciency Factors (K-Values) for Supplementary Cementing Materials Regarding Carbonation and Chloride Penetration." *Durability of Concrete, Proceedings* Fifth International Conference; Barcelona, Spain, Vol. 1, 2000, 173-187.

Parry, J.M. "Wisconsin Department of Transportation Experience with High Fly Ash Content and Reduction of the Ash Replacement Ratio in Concrete Pavements." Paper No. 01-0109, 80th Annual Meeting, Transportation Research Board, January 7-11, 2001.

Pera, J. "Metakaolin and Calcined Clays." *Cement and Concrete Composites.* Guest Editorial, Vol. 23, 2001.

Portland Cement Association. *Design and Control of Concrete Mixtures*. 14th Edition. PCA: Skokie, IL, 2002.

Portland Cement Association. "Supplementary Cementing Materials for Use in Blended Cements." PCA Research and Development Bulletin RD112T. PCA: Skokie, IL, 1995.

Potgieter-Vermaak, S.S. and J.H. Potgieter. "Metakaolin as an Extender in South African Cement" *Journal of Materials in Civil Engineering*, Vol. 18, No. 4, 2006, 619-623.

Ramezanianpour, A.A., Radfar, Hadikhanloo, Moslehi, and Maghsoodi. "Performance of a Different Pozzolanic Cement Concretes Under Cyclic Wetting and Drying." *Fly Ash, Silica Fume, Slag, & Natural Pozzolans in Concrete, Proceedings* 6th CANMET/ACI International Conference, Bangkok, Thailand, Vol. 2, 1998, 759-777.

Ramlochan, T., Thomas, M., and Gruber, K. "The Effect of Metakaolin on Alkali-Silica Reaction in Concrete." *Cement and Concrete Research*, Vol. 31, 2000, 339-344.

Roberts, L.R. and Taylor, P.C. "Understanding Cement-SCM-Admixture Interaction Issues." *Concrete International*, January 2007, v. 29, n. 1, pp. 33-41.

Sabir, B.B, Wild, S., and Bai, J. "Metakaolin and Calcined Clays as Pozzolans for Concrete: A Review." *Cement and Concrete Composites*, Vol. 23, 2001, 441-454.

Sandberg, P. J. and Roberts, L. R. "Cement-Admixture Interactions Related to Aluminate Control." *Journal of ASTM International*, v. 2, n. 6, June 2005, pp. 1-14.

Shehata, M.H., and Thomas, M.D.A. "Use of Ternary Blends Containing Silica Fume and Fly ash to Suppress Expansion due to Alkali-Silica Reaction in Concrete." *Cement and Concrete Research*, Vol. 32, 2002, 341-349.

Shiathas, C., Muntasser, T.Z., and Nwaubani, S.O. "A Comparative Study of the Properties and Durability of binary and Ternary Cementitious Systems." *Durability of Concrete*, Sixth CANMET/ACI International Conference on Durability of Concrete; Thessaloniki, Greece, 2003, 459-474.

Swamy, R.N. and Darwish, A.A. "Engineering Properties of Concretes with Combinations of Cementitious Materials." *Fly Ash, Silica Fume, Slag, & Natural Pozzolans in Concrete, Proceedings* 6th CANMET/ACI International Conference, Bangkok, Thailand, 1998, 661-684.

Swamy, R.N. and Laiw, J.C. “Effectiveness of Supplementary Cementing Materials in Controlling Chloride Penetration into Concrete.” *Fly Ash, Silica Fume, Slag, & Natural Pozzolans in Concrete, Proceedings* 5th CANMET/ACI International Conference; Milwaukee, United States, 1995, 657-674.

Talbot, C., Pigeon, M., Marchand, J., and Hornain, H. “Properties of Mortar Mixtures Containing High Amounts of Various Supplementary Cementitious Materials.” *Fly Ash, Silica Fume, Slag, & Natural Pozzolans in Concrete, Proceedings* 5th CANMET/ACI International Conference; Milwaukee, United States, 1995, 125-151.

Taylor, P.C., Streicher, P.E., Goch, G, and Fliss, L. “Comparative Testing of Portland Cement, Fly Ash, Ground Granulated Blast Furnace Slag, and Silica Fume Concretes for Potential Durability.” *Fly Ash, Silica Fume, Slag, & Natural Pozzolans in Concrete, Proceedings* 5th CANMET/ACI International Conference; Milwaukee, United States, 1995, 479-495.

Tikalsky, P.J., Carrasquillo, R.L., "Influence of Fly Ash on the Sulfate Resistance of Concrete," Journal of the American Concrete Institute-Materials, Vol. 89, No. 1, Jan.-Feb. 1992.

Tikalsky, P.J., Carrasquillo, R.L., and Carrasquillo, P.M., "Durability and Strength Considerations of Concrete Containing Fly Ash," Journal of the American Concrete Institute-Materials, Vol. 85, No. 6, pp. 505-511, Nov.-Dec. 1988.

Tikalsky, Paul J., Schokker, Andrea J., and Tepke, David G.; Potential Concrete Mixture Designs for the I-99 Corridor, Pennsylvania Department of Transportation, Report No.: FHWA-PA-2002-040-97-04 (81-4), March 2003.

Torii, K. and Kawamura, M. “Pore Structure and Chloride Permeability of Concretes Containing Fly Ash, Blast-Furnace Slag and Silica Fume.” *Fly Ash, Silica Fume, Slag, & Natural Pozzolans in Concrete, Proceedings*, 4th CANMET/ACI International Conference; Istanbul, Turkey, Vol. 1, 1992, 135-150.

Torii, K., Sasatani, T., and Kawamura, M. “Effects of Fly Ash, Blast Furnace Slag, and Silica Fume on Resistance of Mortar to Calcium Chloride Attack.” *Fly Ash, Silica Fume, Slag, & Natural Pozzolans in Concrete, Proceedings* 5th CANMET/ACI International Conference; Milwaukee, United States, 1995, 931-949.

Tuthill, L.H. “Mineral Admixtures.” *Significance of Tests and Properties of Concrete and Concrete-Making Materials, ASTM STP 169B.* West Conshohocken, PA: American Society for Testing and Materials, 1978, 804-822.

Transportation Research Board. “Admixtures and Ground Slag for Concrete.” *Transportation Research Circular* 365, December 1990.

Wang, H., Qi, C., Farzam, H., and Turici, J. “Interaction of Materials Used in Concrete.” *Concrete International*, v. 28, n. 4, April 2006, pp. 47-52.

Wild, S., Khatib, J.M., and Jones, A. “Relative Strength, Pozzolanic Activity and Cement Hydration in Superplasticized Metakaolin Concrete.” *Cement and Concrete Research*, Vol. 26, No. 10, 1996, 1537-1544.

Winkerton, H., and Pamukcu, S. “Soil stabilization and grouting.” *Foundation Engineering Handbook, 2nd Edition*, New York, NY, 1991.

Wolsiefer, John, Sr. Personal Communication. NORCHEM Concrete Products, Inc., Oct. 1999.

Zhang, M.H. and Malhotra, V.M. “Characteristics of a Thermally Activated Alumino-Silicate Pozzolanic Material and Its Use in Concrete.” *Cement and Concrete Research,* Vol. 25, No. 8, 1995, 1713-1725.

APPENDIX A – CHEMICAL PROPERTIES OF EACH MIXTURE

Table A-1. CaO, SiO_2, and Al_2O_3 properties of each mixture

	Chemical (%)		
Mixture ID	**CaO**	**SiO_2**	**Al_2O_3**
60TI/20C/20F	50.5	30.0	19.5
60TI/20C/20F2	53.7	30.8	15.5
75TI/20C/5SF	59.5	28.3	12.2
77TI/20C/3SF	60.9	26.8	12.4
60TI/20C/20G100S	59.2	28.0	12.8
60TI/20C/20G120S	59.1	28.0	12.9
75TI/20C/5M	59.5	26.1	14.5
60TI/20F/20F2	47.9	33.1	18.9
75TI/20F/5SF	53.8	30.6	15.6
77TI/20F/3SF	55.1	29.1	15.8
60TI/20F/20G100S	53.4	30.3	16.2
60TI/20F/20G120S	53.3	30.3	16.4
75TI/20F/5M	53.7	28.4	17.9
75TI/20F2/5SF	57.0	31.4	11.6
77TI/20F2/3SF	58.3	29.9	11.8
60TI/20F2/20G100S	56.6	31.1	12.3
60TI/20F2/20G120S	56.5	31.1	12.4
75TI/20F2/5M	56.9	29.2	13.9
60TI/30C/10F	53.4	28.9	17.8
60TI/30C/10F2	55.0	29.3	15.8
65TI/30C/5SF	56.2	29.9	13.9
67TI/30C/3SF	57.6	28.4	14.1
50TI/30C/20G100S	55.9	29.6	14.5
50TI/30C/20G120S	55.8	29.6	14.7
65TI/30C/5M	56.1	27.7	16.2
60TI/30F/10C	47.6	31.2	21.2
60TI/30F2/10C	52.4	32.4	15.2

Table A-1. CaO, SiO_2, and Al_2O_3 properties of each mixture (cont.)

	Chemical (%)		
Mixture ID	**CaO**	**SiO_2**	**Al_2O_3**
65TI/30F/5SF	47.6	33.4	19.0
67TI/30F/3SF	48.9	31.9	19.2
50TI/30F/20G100S	47.2	33.1	19.7
50TI/30F/20G120S	47.1	33.1	19.8
65TI/30F/5M	47.5	31.2	21.3
65TI/30F2/5SF	52.3	34.6	13.1
67TI/30F2/3SF	53.7	33.1	13.2
50TI/30F2/20G100S	52.0	34.3	13.7
50TI/30F2/20G120S	51.9	34.3	13.8
65TI/30F2/5M	52.3	32.4	15.4
50TI/35G100S/15C	58.1	29.9	12.1
50TI/35G100S/15F	53.7	31.6	14.7
50TI/35G100S/15F2	56.1	32.2	11.7
60TI/35G100S/5SF	59.6	31.3	9.1
62TI/35G100S/3SF	61.0	29.7	9.3
60TI/35G100S/5M	59.6	29.0	11.4
50TI/35G120S/15C	57.9	29.8	12.3
50TI/35G120S/15F	53.6	31.5	14.9
50TI/35G120S/15F2	55.9	32.1	11.9
60TI/35G120S/5SF	59.5	31.2	9.3
62TI/35G120S/3SF	60.8	29.7	9.5
60TI/35G120S/5M	59.4	29.0	11.6
90TI/5M/5SF	62.7	26.7	10.6
92TI/5M/3SF	64.1	25.1	10.8
68TI-II/17G120S/15C	62.0	27.0	11.0
68TI-II/17G120S/15F	57.7	28.8	13.5
68TI-II/17G120S/15F2	60.1	29.4	10.6

Table A-1. CaO, SiO_2, and Al_2O_3 properties of each mixture (cont.)

	Chemical (%)		
Mixture ID	**CaO**	**SiO_2**	**Al_2O_3**
78TI-II/19G120S/3SF	64.7	27.3	8.0
64TI-II/20G100S/16G120S	63.4	27.9	8.6
76TI-II/19G120S/5M	63.2	23.9	7.9
60TI-II/25C/15G120S	59.0	28.2	12.8
60TI-II/25F/15G120S	51.8	31.1	17.1
60TI-II/25F2/15G120S	55.8	32.1	12.1
52TI-II/35G100S/13G120S	61.1	30.0	8.9
85TIP/15C	53.7	31.7	14.6
85TIP/15F	49.4	33.4	17.2
85TIP/15F2	51.8	34.0	14.2
95TIP/5SF	54.0	34.0	11.9
97TIP/3SF	55.2	32.7	12.2
80TIP/20G100S	55.6	32.3	12.0
80TIP/20G120S	55.5	32.3	12.2
95TIP/5M	54.0	31.8	14.2
75TIP/25C	51.7	32.4	16.0
75TIP/25F	44.5	35.2	20.3
75TIP/25F2	48.5	36.2	15.3
65TIP/35G100S	54.7	33.6	11.7
65TIP/35G120S	54.6	33.5	11.9
85TISM/15C	62.1	26.6	11.3
85TISM/15F	57.8	28.4	13.9
85TISM/15F2	60.2	28.9	10.9
95TISM/5SF	63.4	28.4	8.2
97TISM/3SF	64.7	26.9	8.4
80TISM/20G100S	63.5	27.6	8.9
80TISM/20G120S	63.4	27.5	9.1

Table A-1. CaO, SiO_2, and Al_2O_3 properties of each mixture (cont.)

	Chemical (%)		
Mixture ID	**CaO**	**SiO_2**	**Al_2O_3**
75TISM/25C	59.1	27.9	13.1
75TISM/25F	51.9	30.8	17.3
75TISM/25F2	55.8	31.8	12.4
65TISM/35G100S	61.1	29.7	9.2
65TISM/35G120S	61.0	29.6	9.4
85TIPM/15C	61.0	28.2	10.7
85TIPM/15F	56.7	30.0	13.3
85TIPM/15F2	59.1	30.6	10.3
95TIPM/5SF	62.2	30.2	7.6
97TIPM/3SF	63.5	28.8	7.7
80TIPM/20G100S	62.5	29.1	8.4
80TIPM/20G120S	62.4	29.1	8.5
95TIPM/5M	62.2	28.0	9.9
75TIPM/25C	58.1	29.3	12.6
75TIPM/25F	50.9	32.2	16.8
75TIPM/25F2	54.9	33.2	11.9
65TIPM/35G100S	60.3	30.9	8.7
65TIPM/35G120S	60.1	30.9	9.0
100TI	69.6	21.2	9.2
80TI/20C	62.9	24.4	12.6
80TI/20F	57.2	26.8	16.1
80TI/20F2	60.4	27.6	12.1
65TI/35G100S	63.1	27.4	9.5
65TI/35G120S	62.9	27.4	9.8
100TI-II	70.6	21.8	7.6
80TI-II/20G120S	66.5	25.2	8.3
100TIP	56.8	30.7	12.5
100TISM	66.7	24.7	8.6
100TIPM	65.4	26.6	8.0

APPENDIX B – X-RAY DIFFRACTION RESULTS

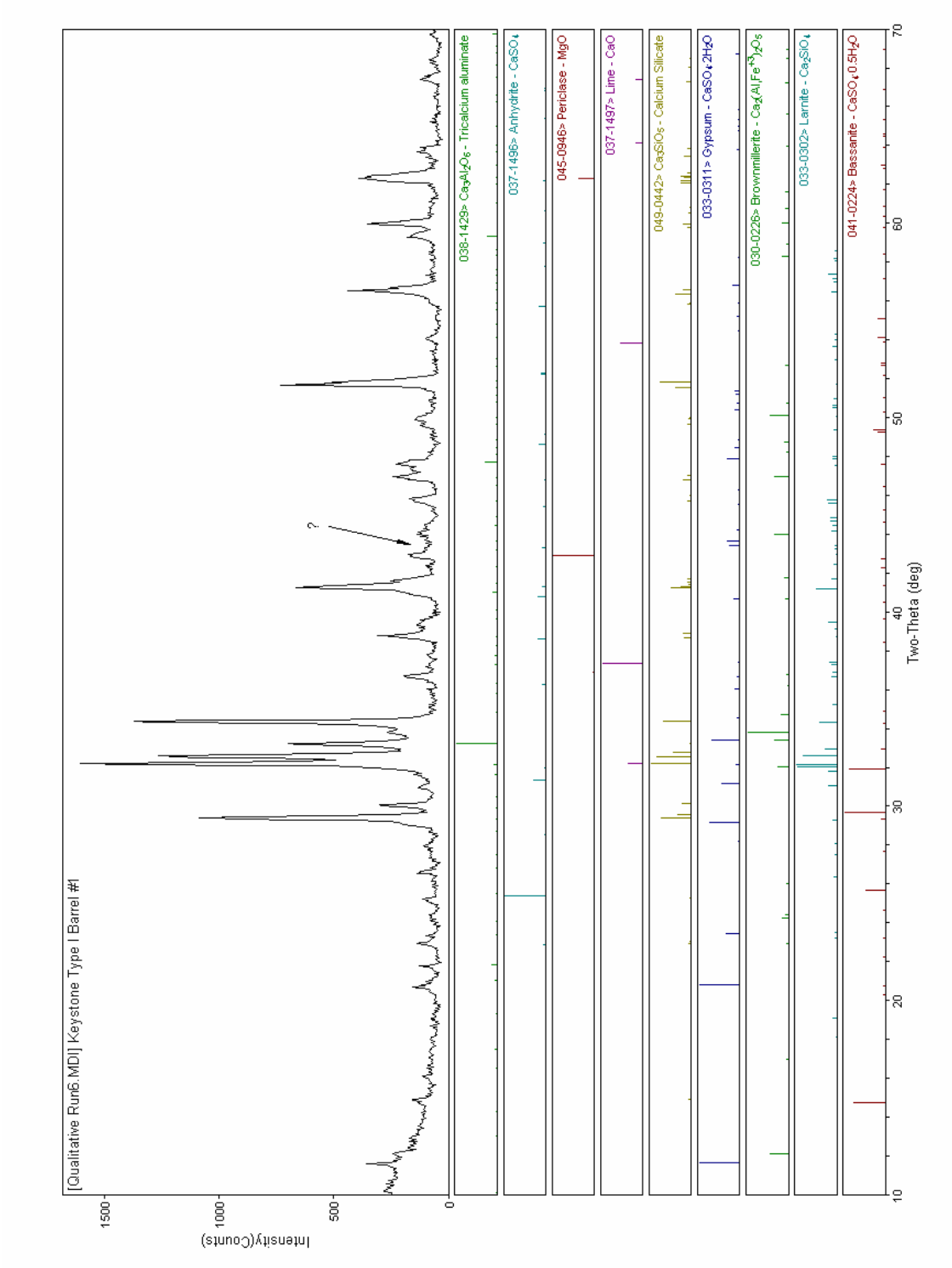

Figure B-1. XRD results for Type I PC

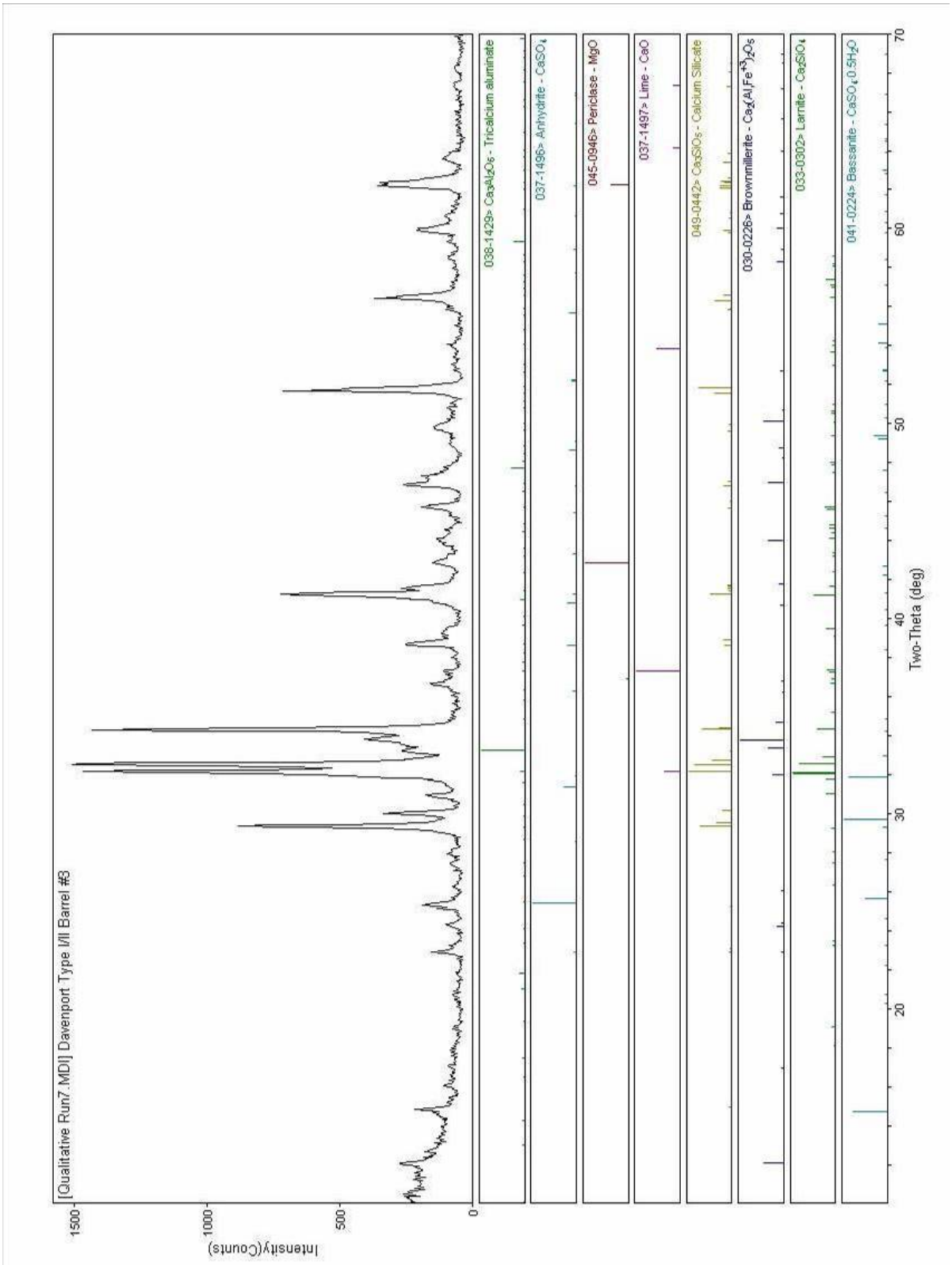

Figure B-2. XRD results for Type I/II PC

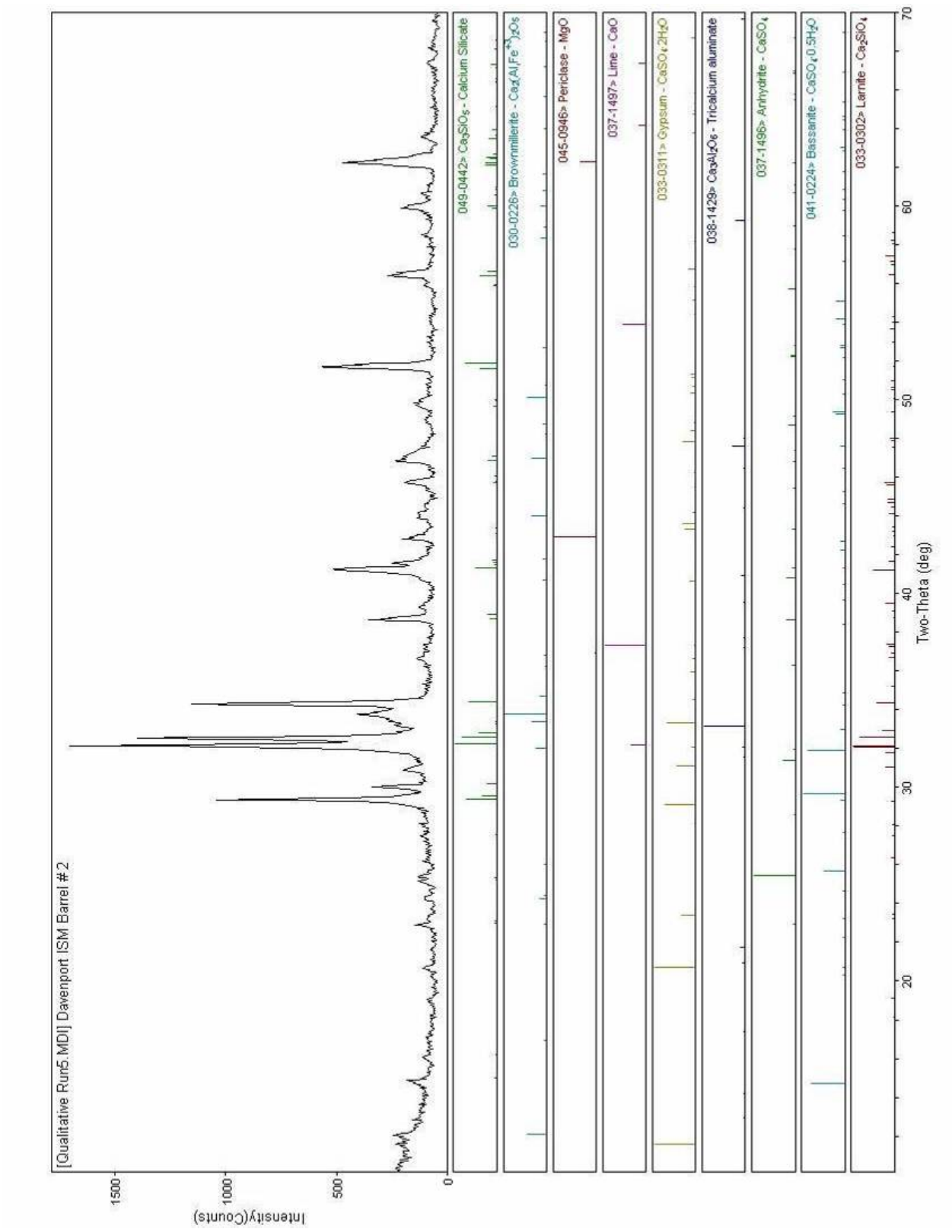

Figure B-3. XRD results for Type ISM PC

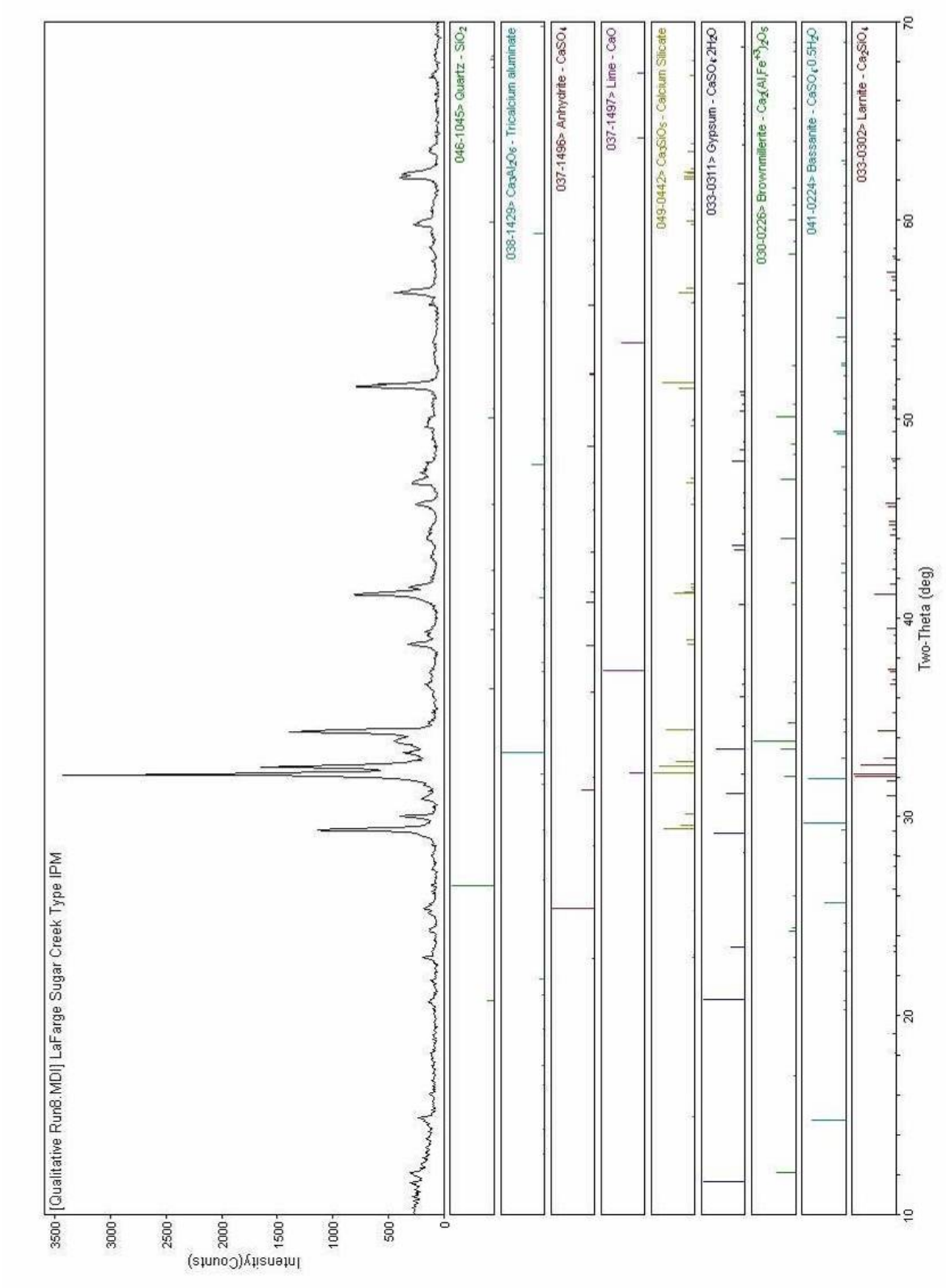

Figure B-4. XRD results for Type IPM PC

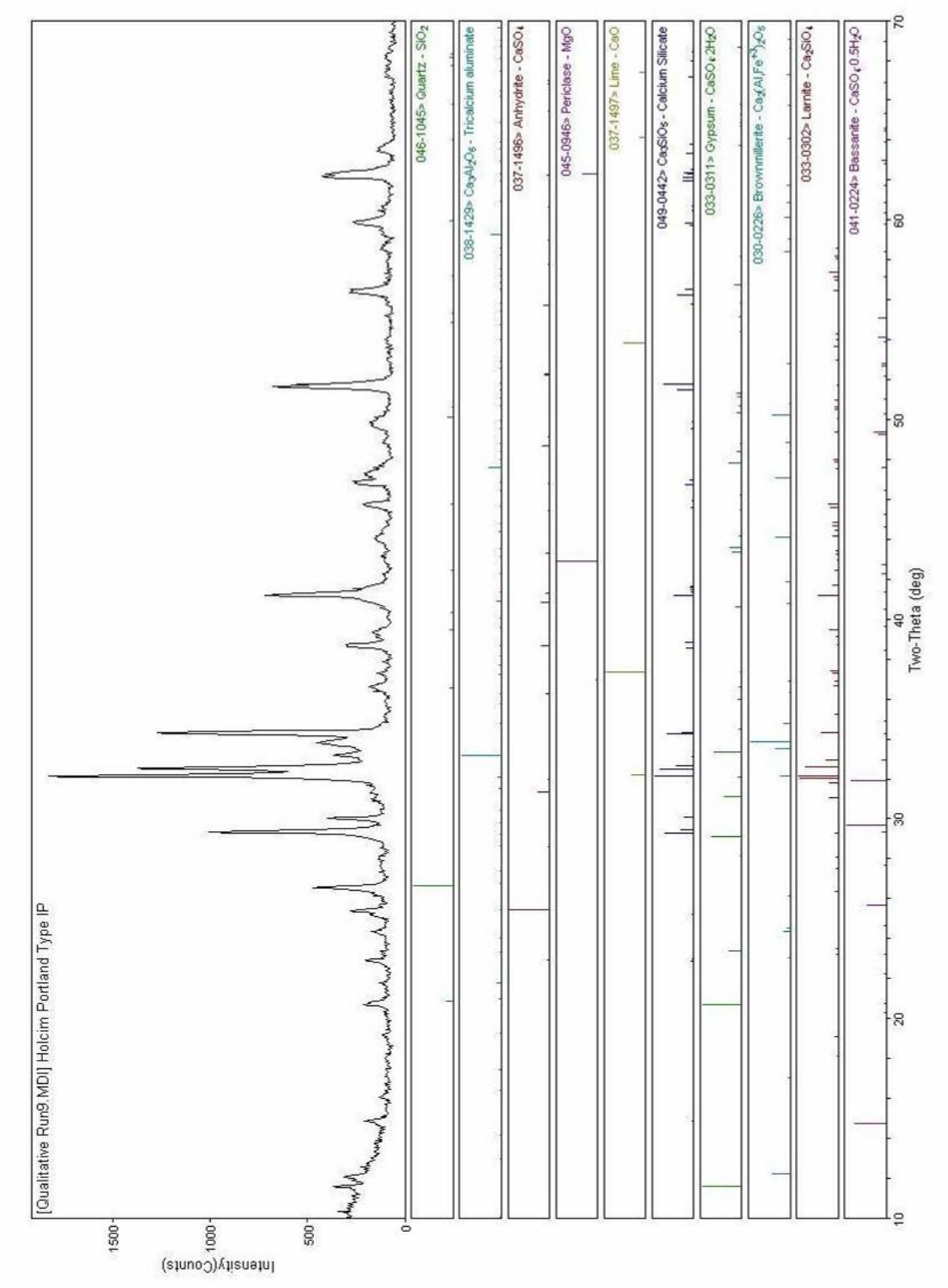

Figure B-5. XRD results for Type IP PC

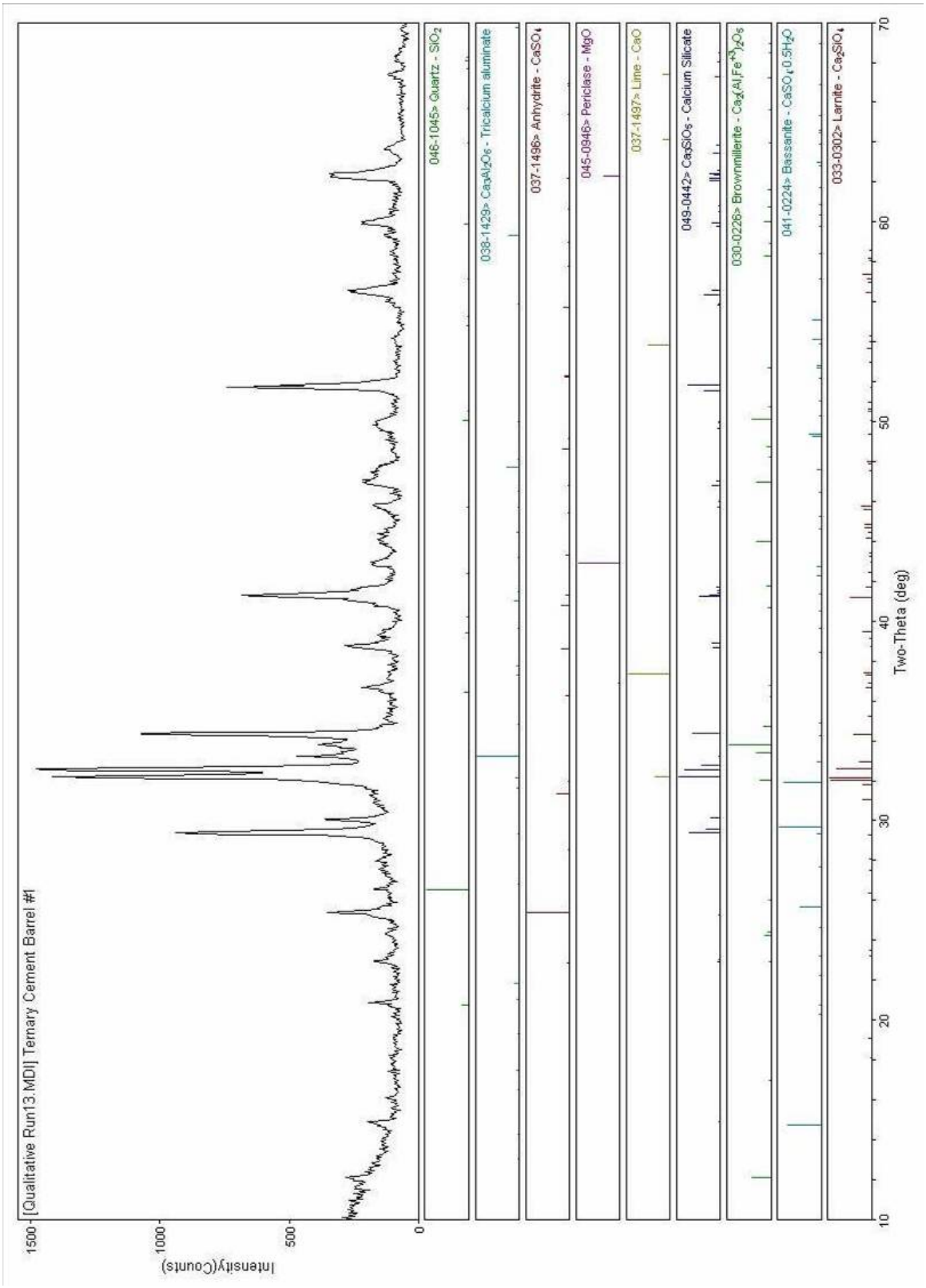

Figure B-6. XRD results for ternary cement

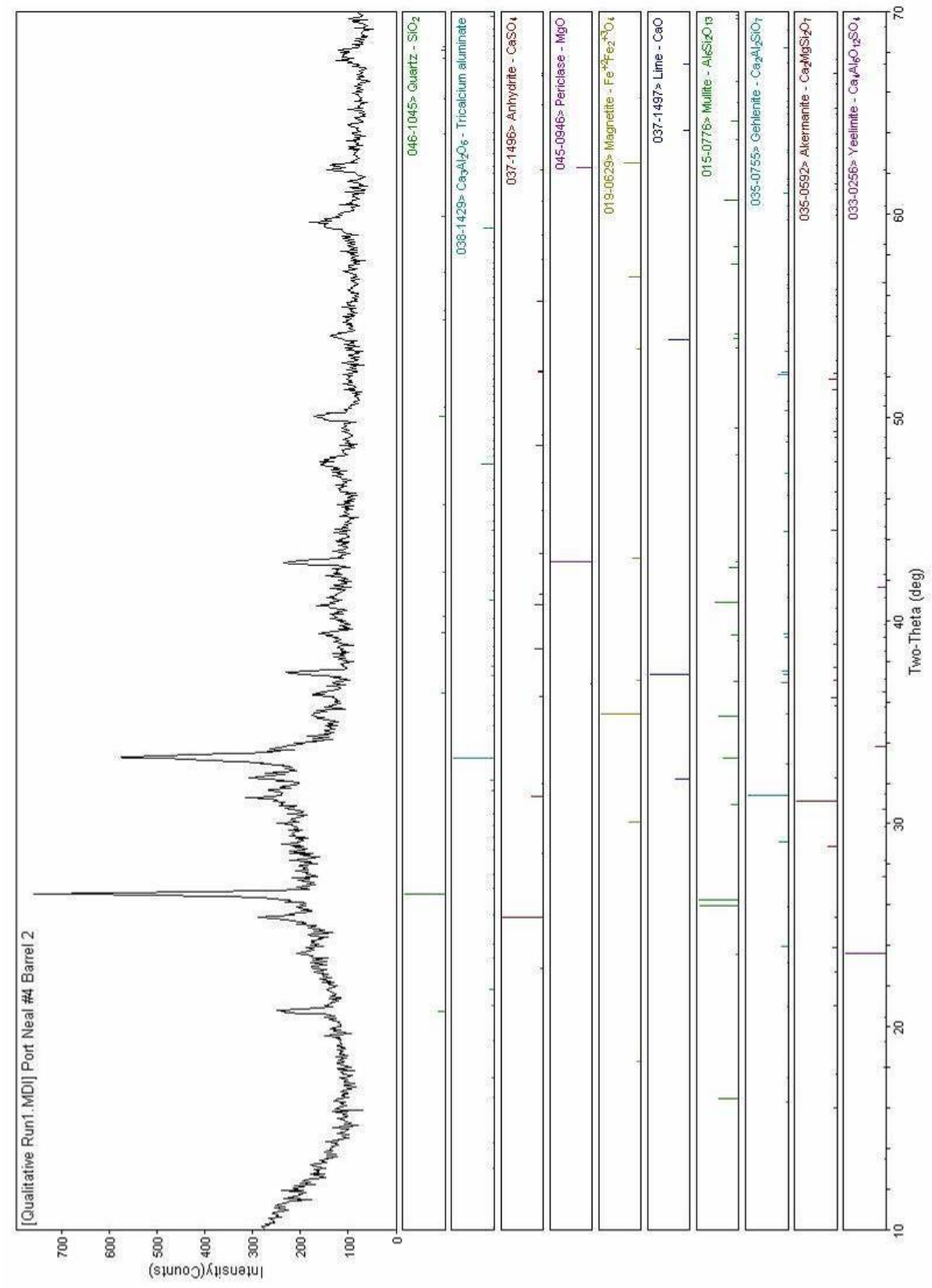

Figure B-7. XRD results for Class C fly ash

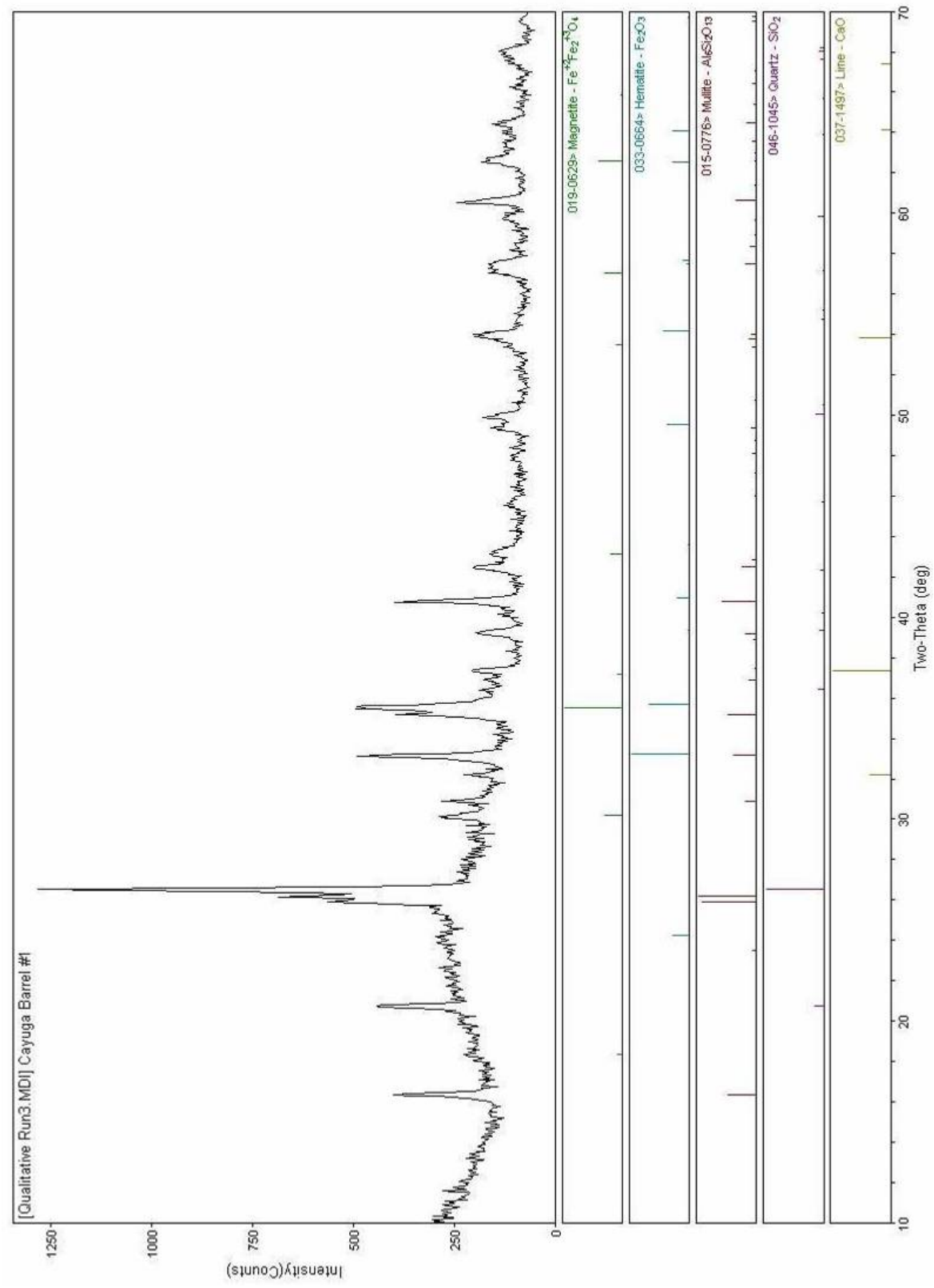

Figure B-8. XRD results for Cayuga Class F fly ash

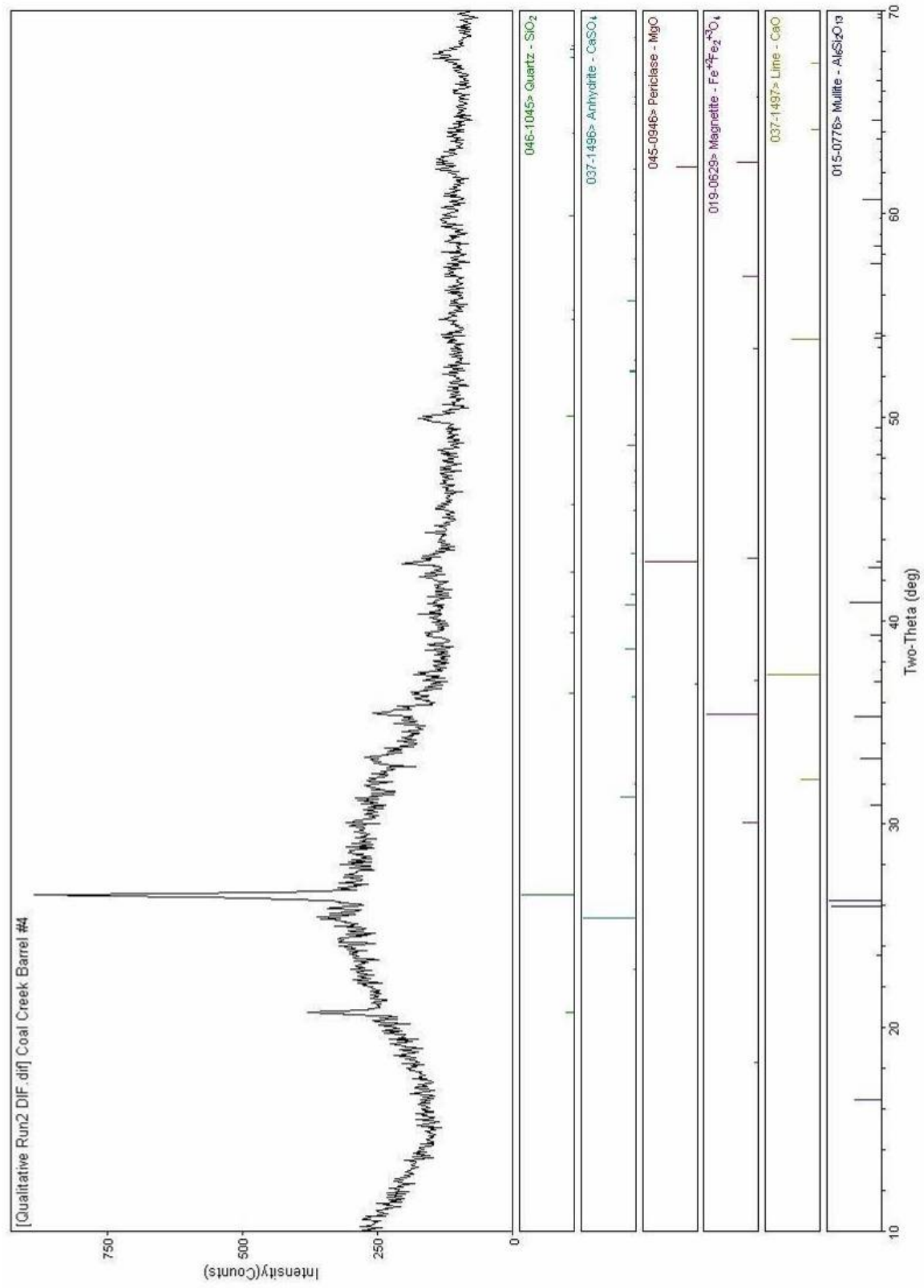

Figure B-9. XRD results for Coal Creek Class F fly ash

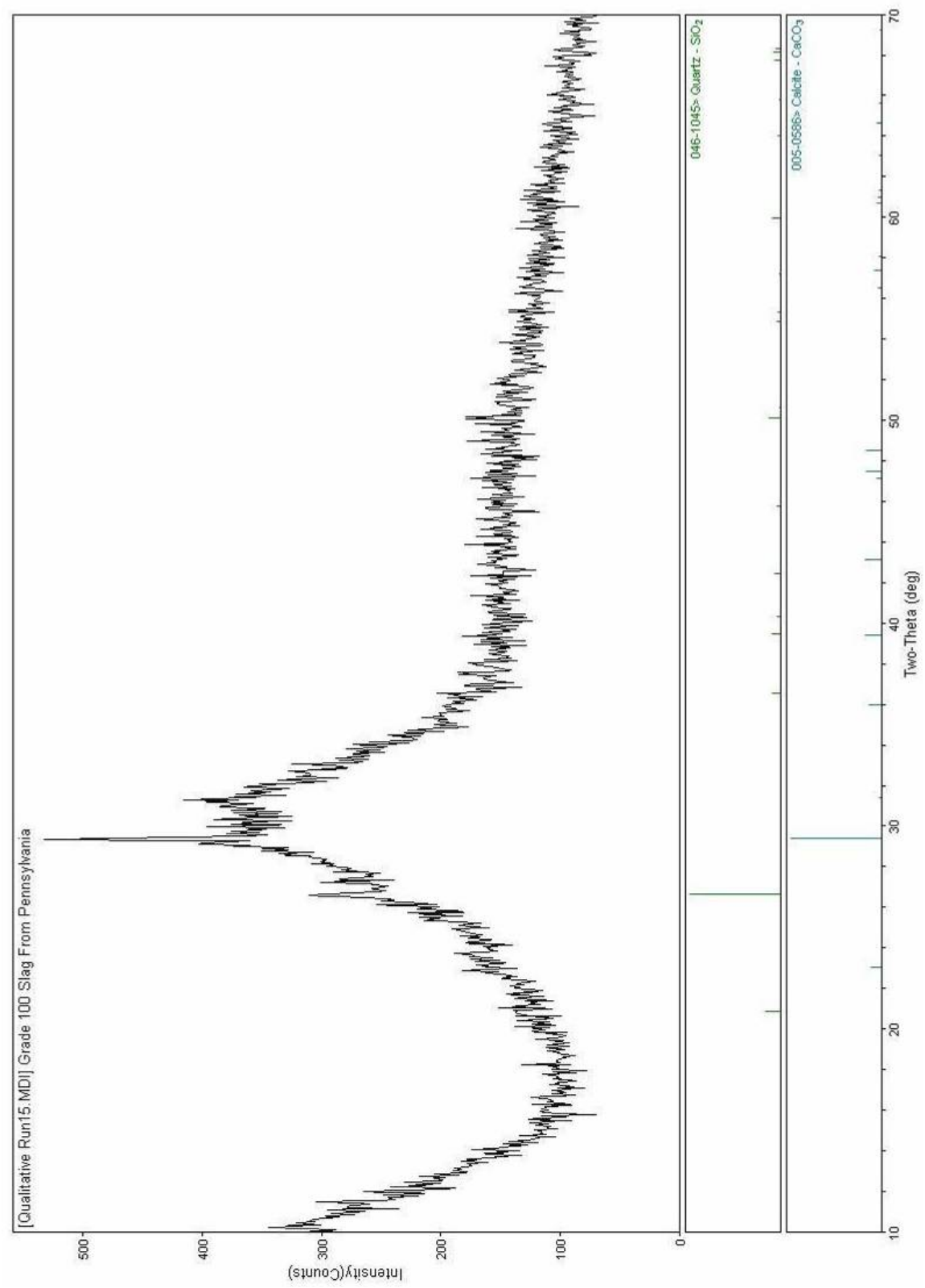

Figure B-10. XRD results for Grade 100 GGBFS

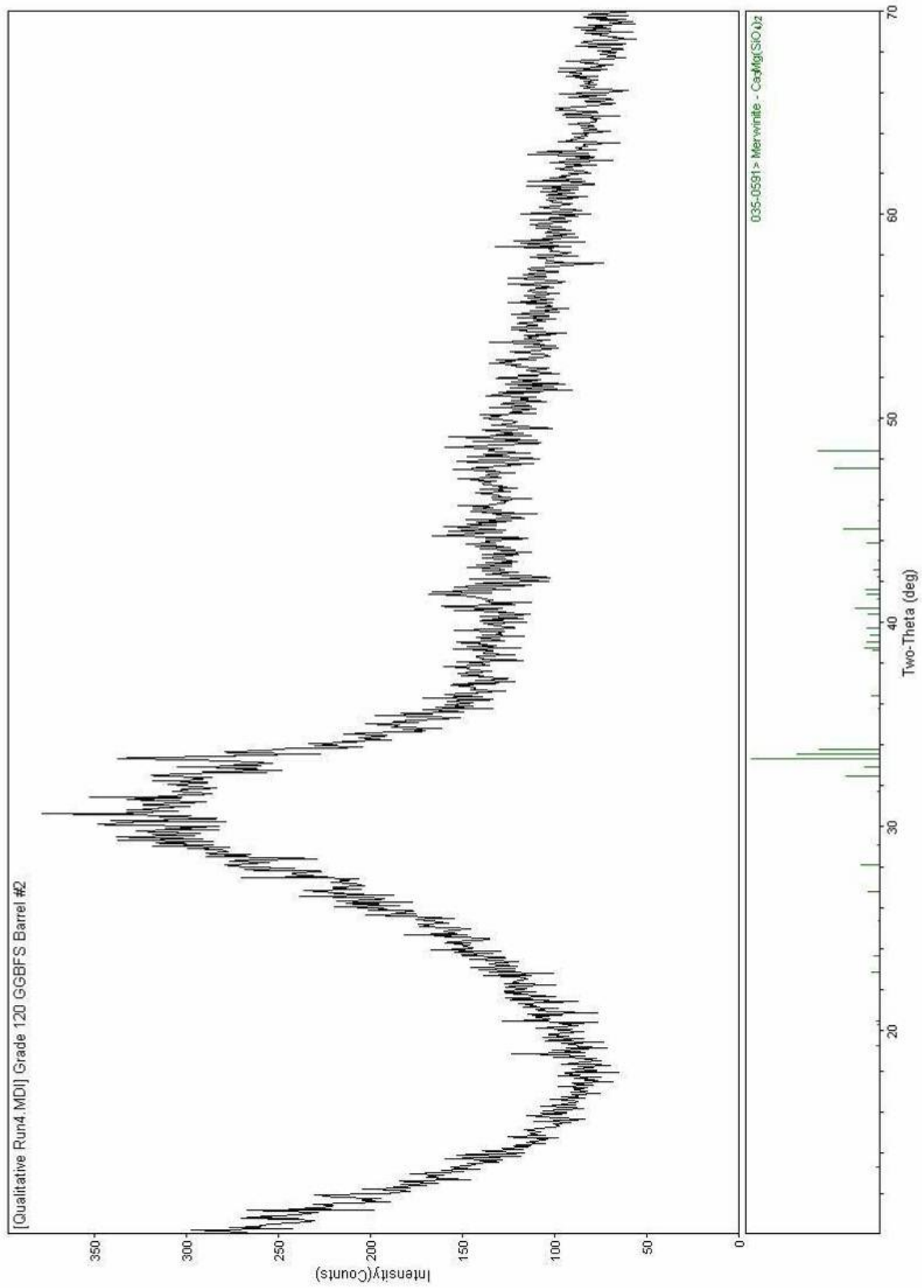

Figure B-11. XRD results for Grade 120 GGBFS

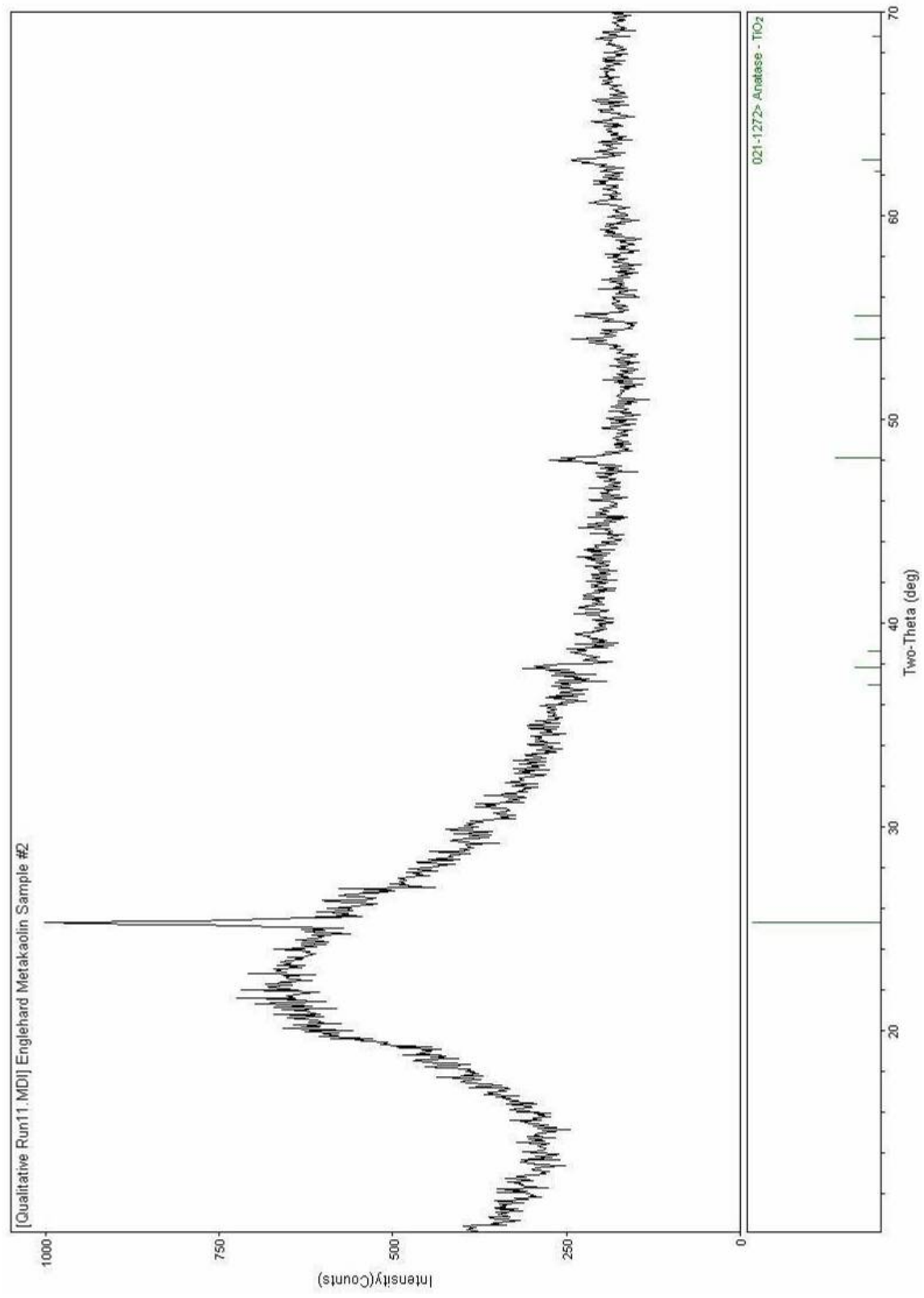

Figure B-12. XRD results for metakaolin

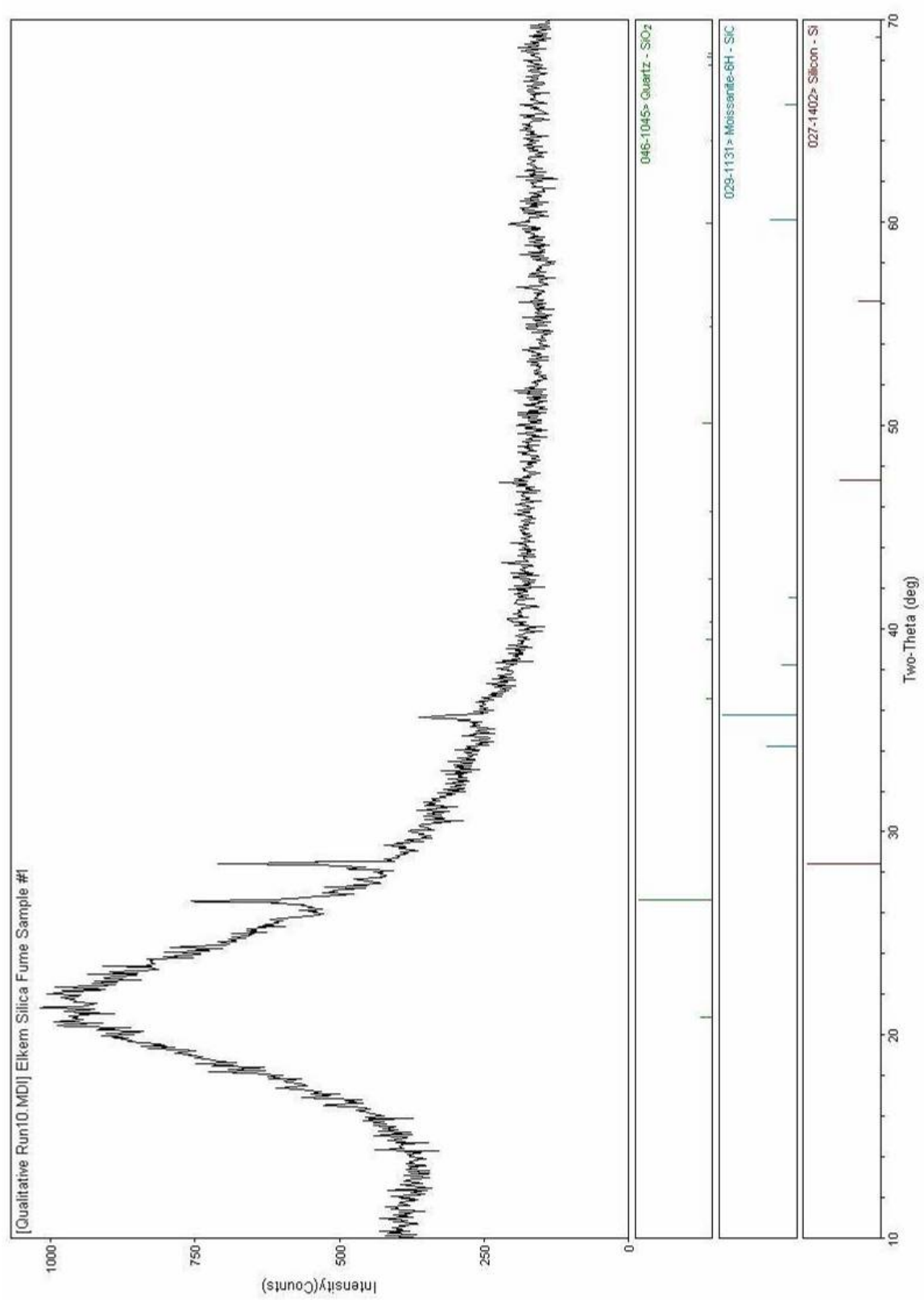

Figure B-13. XRD results for silica fume

APPENDIX C – HEAT SIGNATURE CURVES

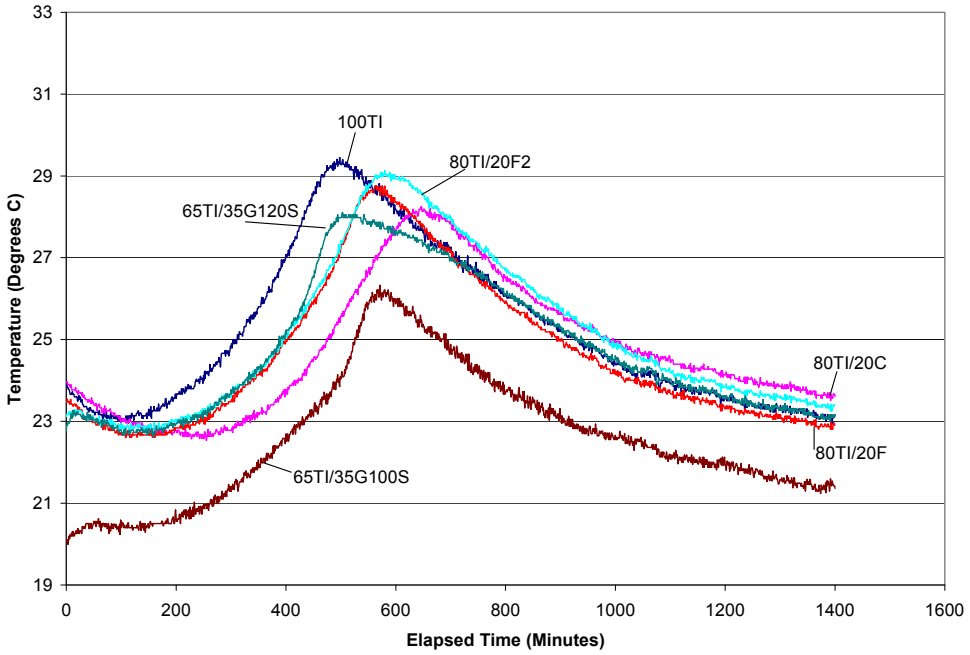

Figure C-1. Heat signature for control mixtures containing Type I PC

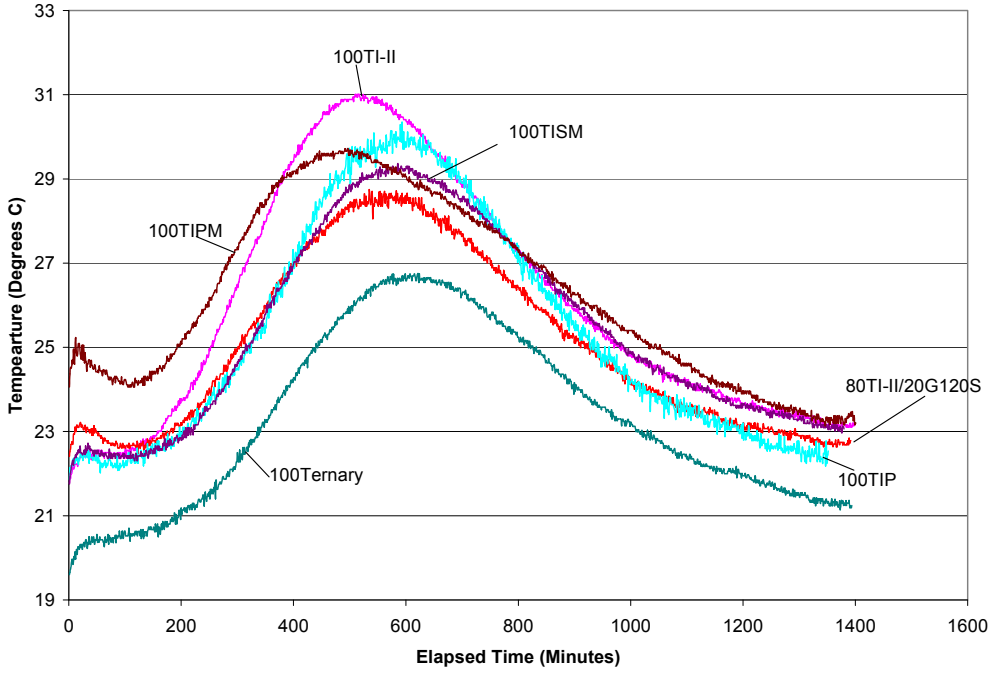

Figure C-2. Heat signature for control mixtures

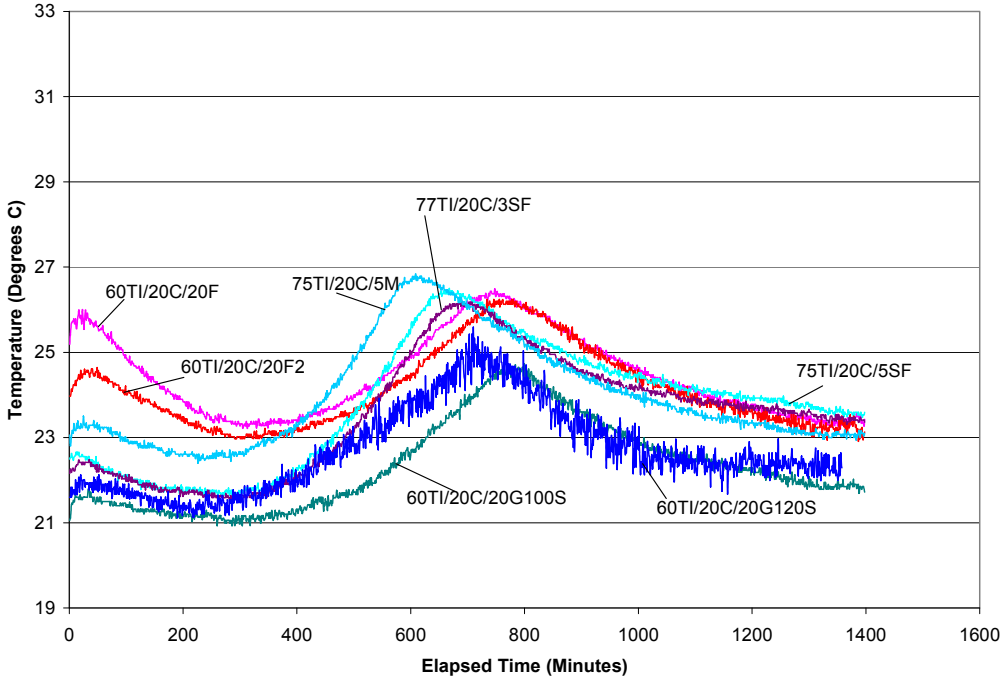

Figure C-3. Heat signature for mixtures containing Type I PC and 20% Class C FA

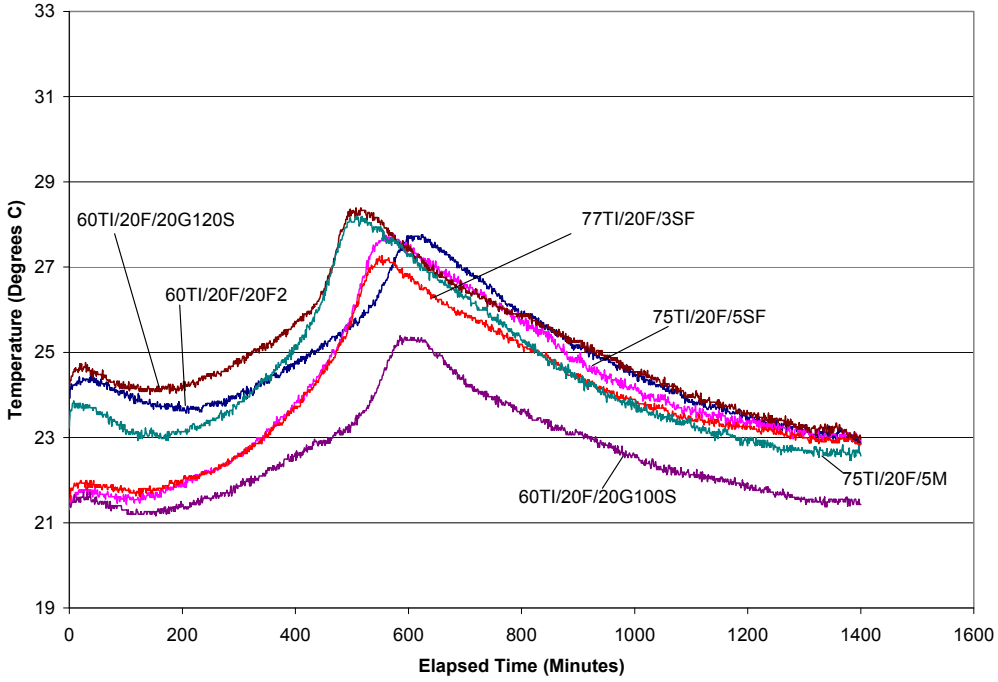

Figure C-4. Heat signature for mixtures containing Type I PC and 20% Class F1 FA

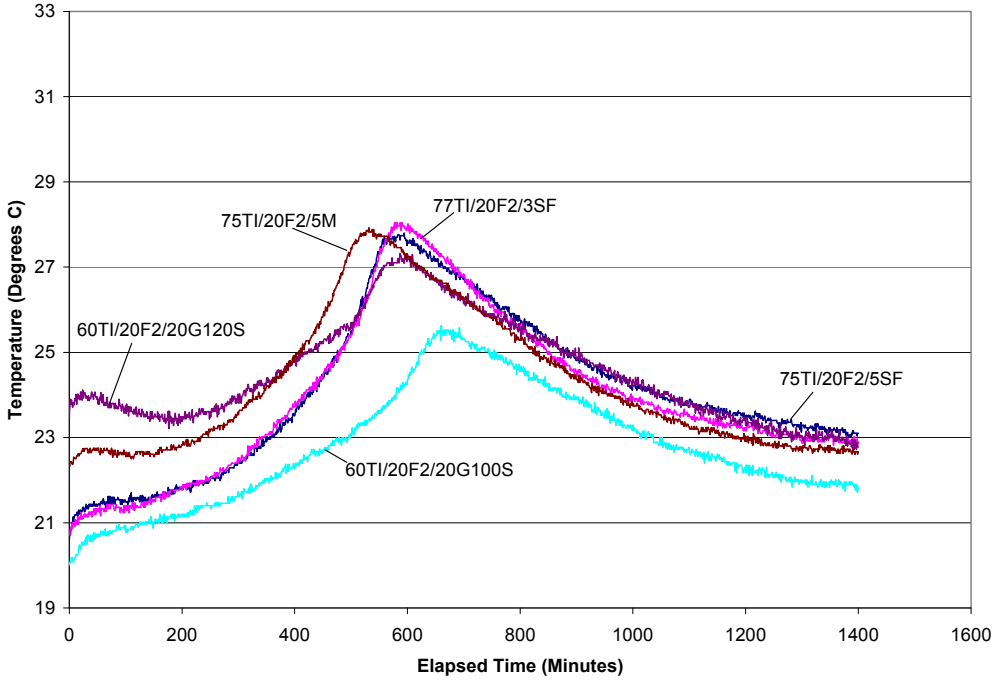

Figure C-5. Heat signature for mixtures containing Type I PC and 20% Class F2 FA

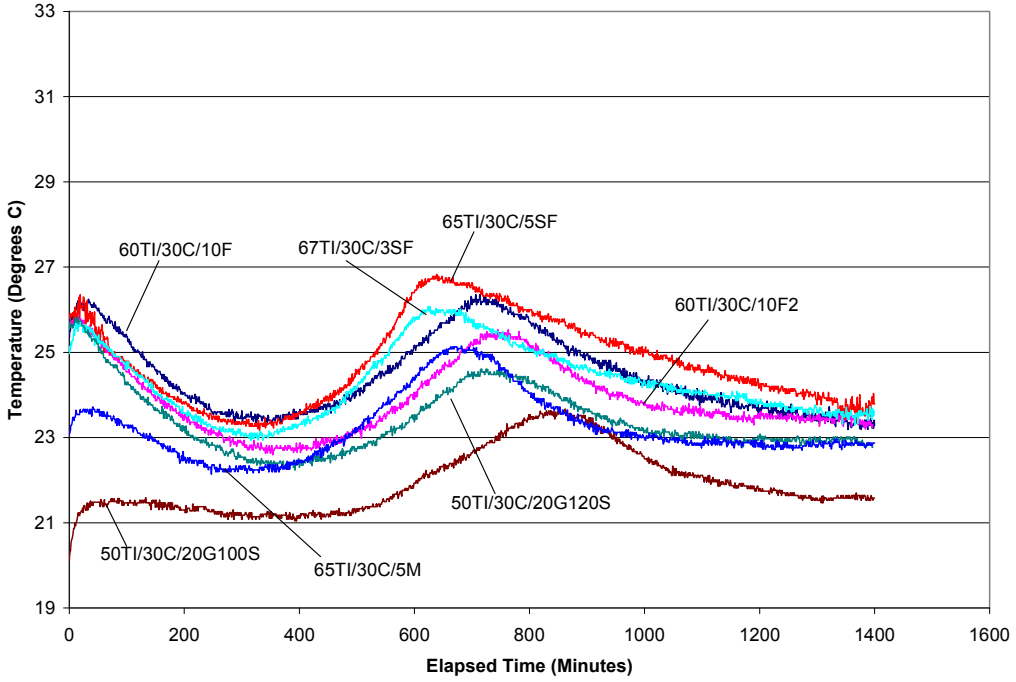

Figure C-6. Heat signature for mixtures containing Type I PC and 30% Class C FA

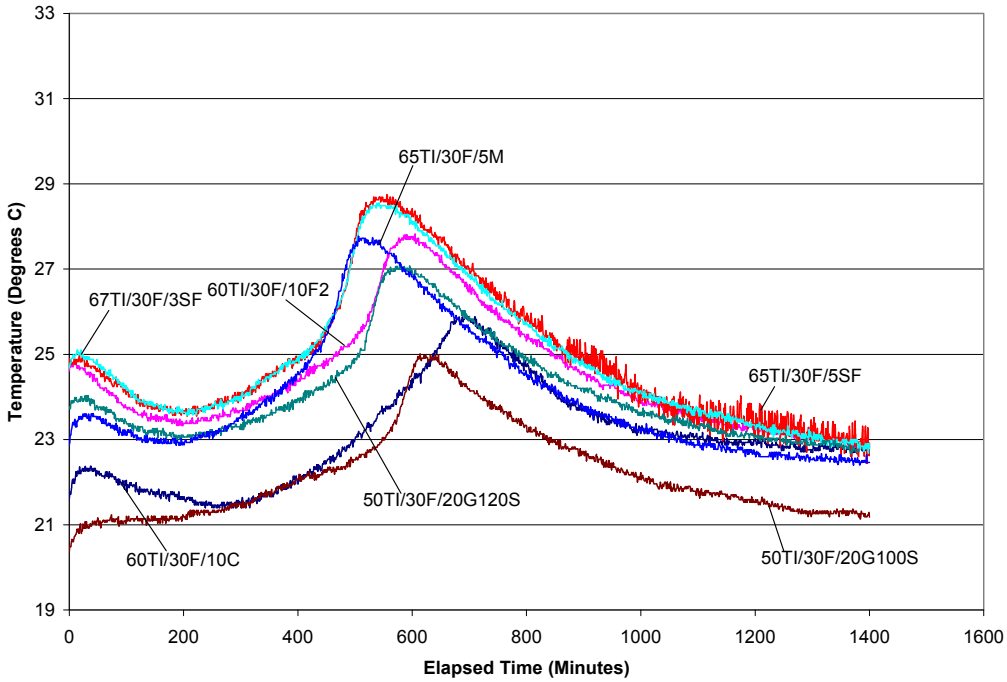

Figure C-7. Heat signature for mixtures containing Type I PC and 30% Class F1 FA

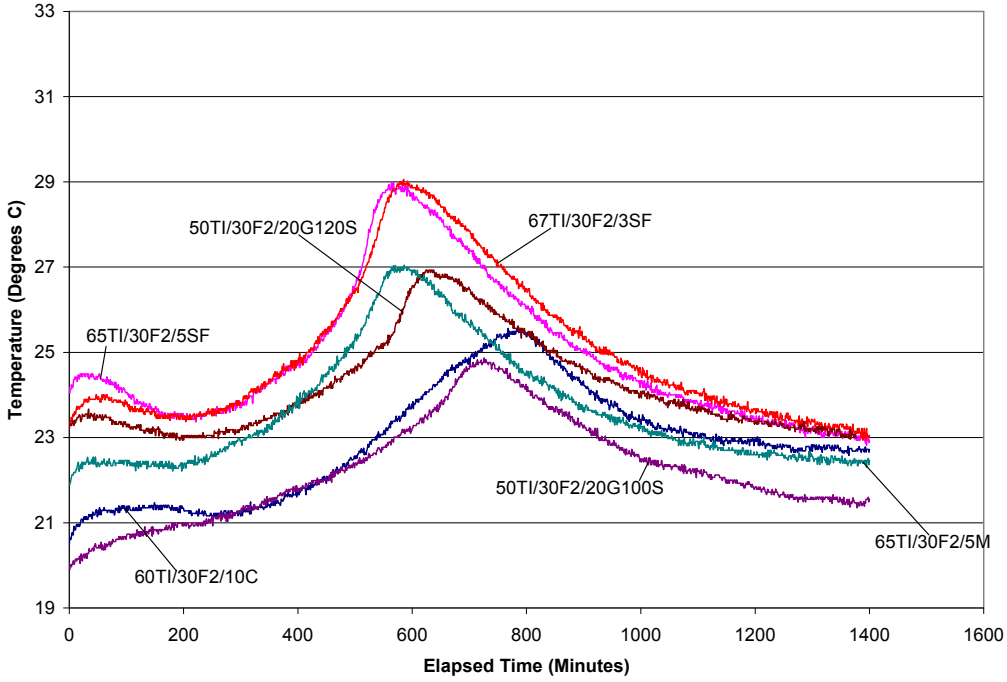

Figure C-8. Heat signature for mixtures containing Type I PC and 30% Class F2 FA

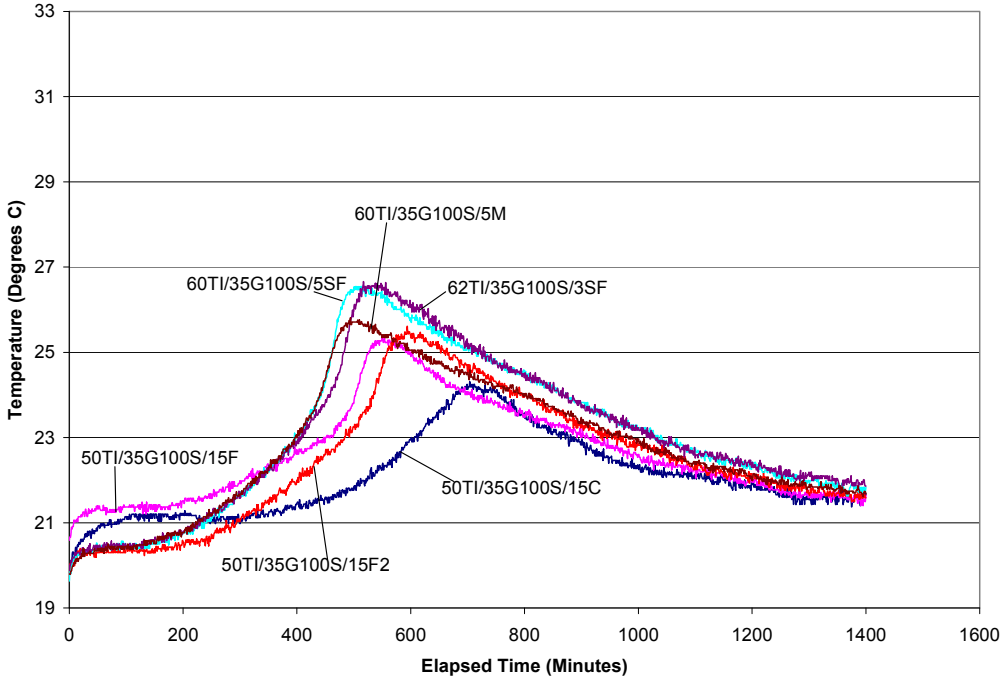

Figure C-9. Heat signature for mixtures containing Type I PC and 35% Grade 100 GGBFS

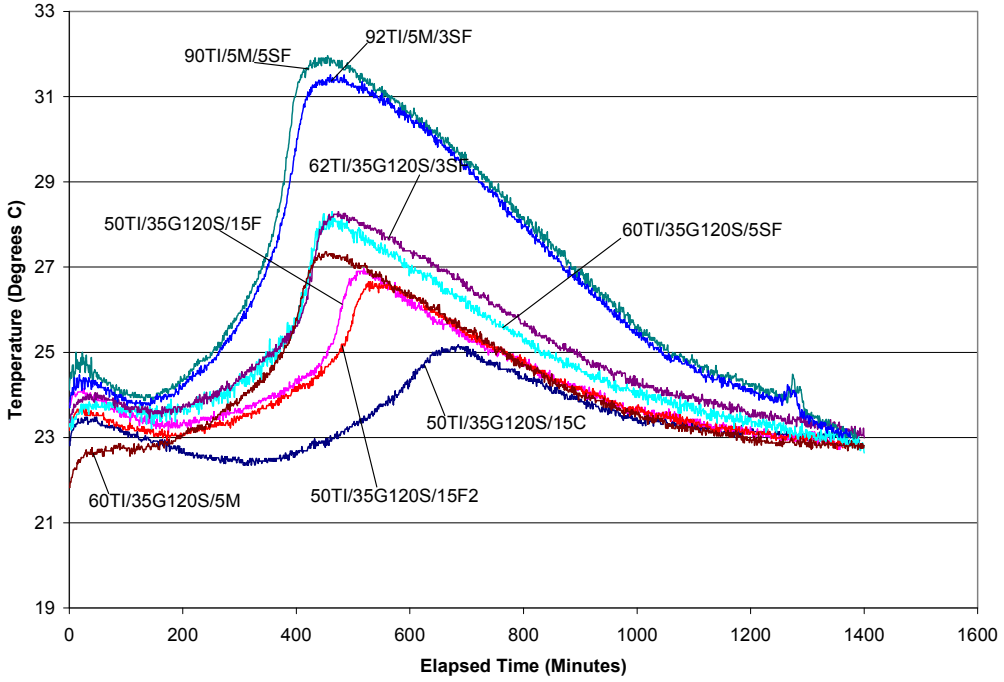

Figure C-10. Heat signature for mixtures containing Type I PC and 35% Grade 120 GGBFS

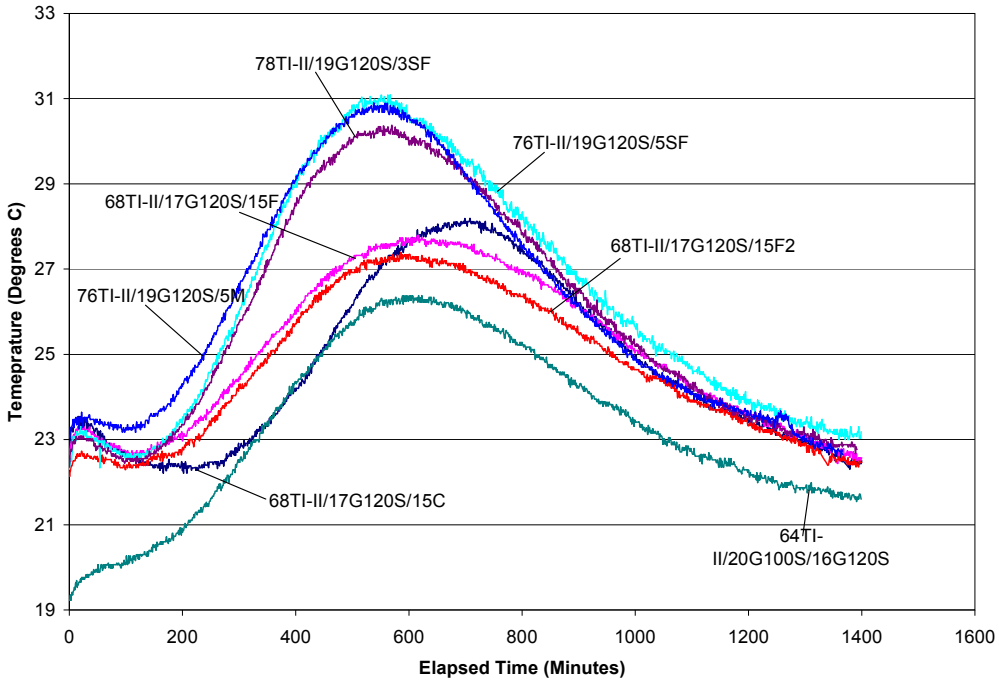

Figure C-11. Heat signature for mixtures containing Type I/II PC and Grade 120 GGBFS

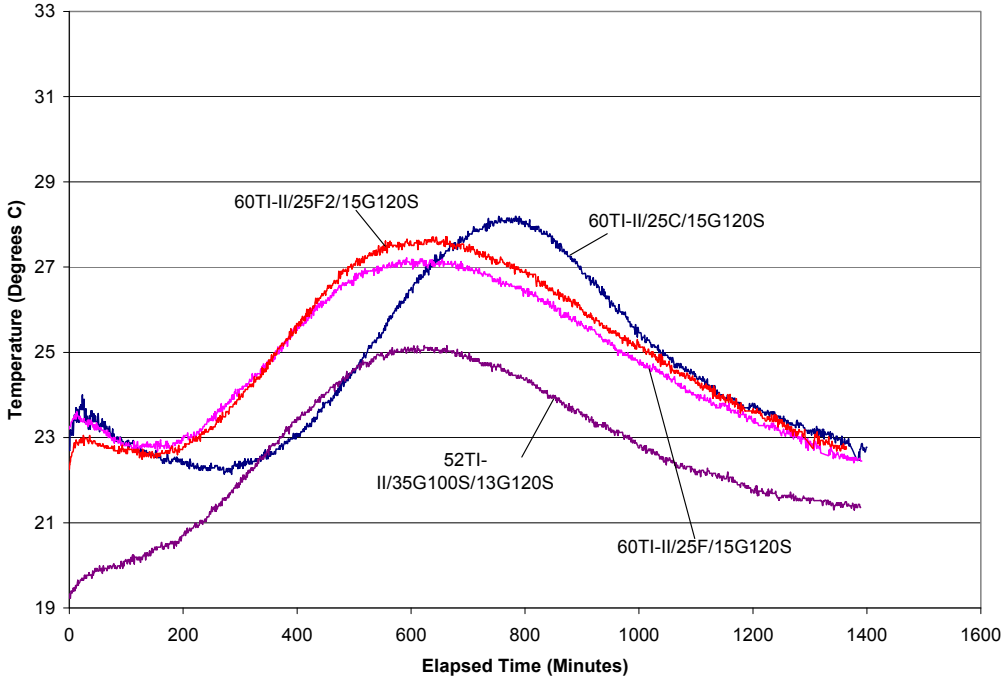

Figure C-12. Heat signature for mixtures containing Type I/II PC

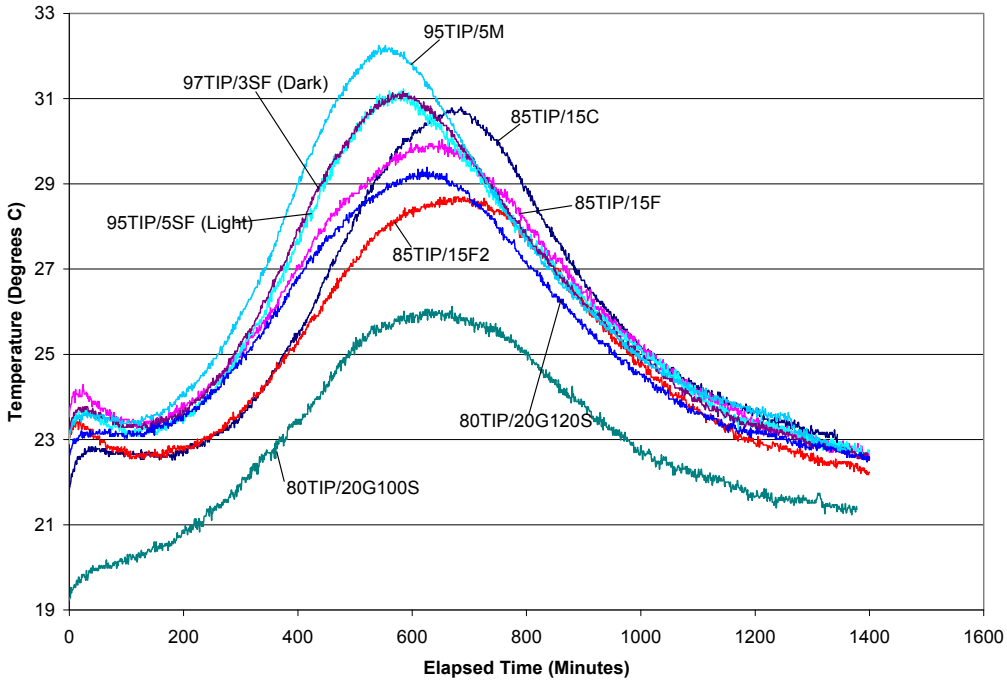

Figure C-13. Heat signature for mixtures containing greater than 80% Type IP PC

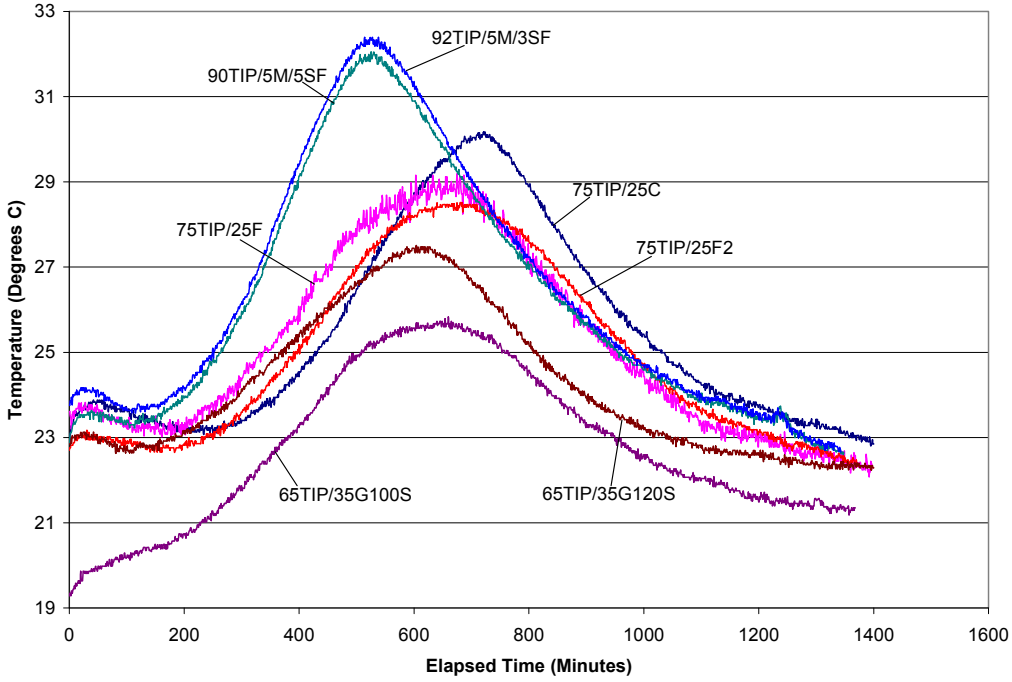

Figure C-14. Heat signature for mixtures containing Type IP PC

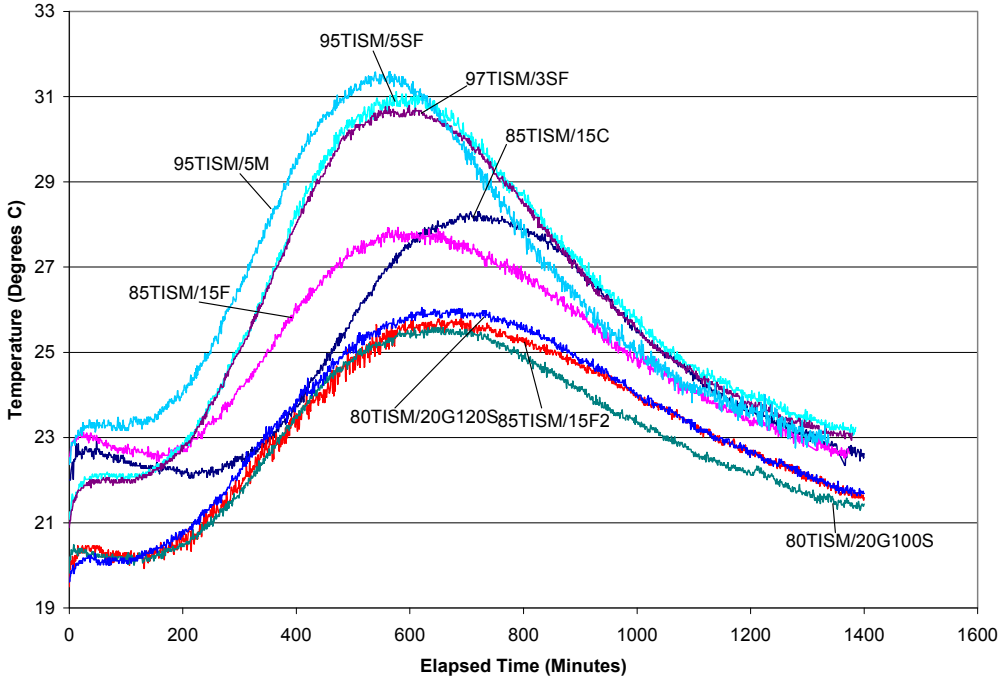

Figure C-15. Heat signature for mixes containing greater than 80% Type ISM PC

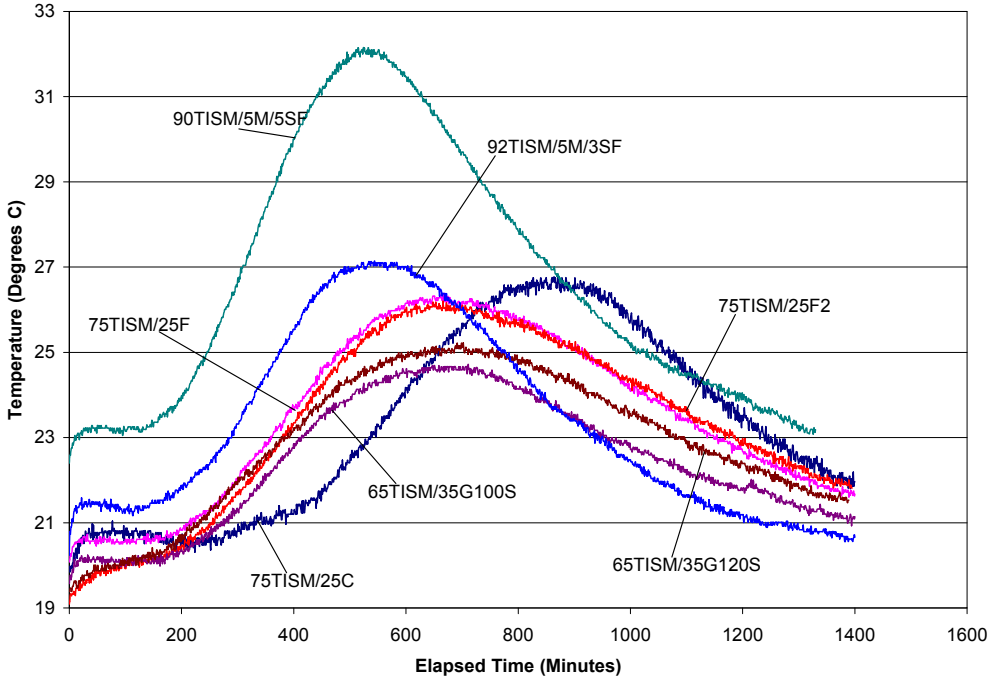

Figure C-16. Heat signature for mixtures containing Type ISM PC

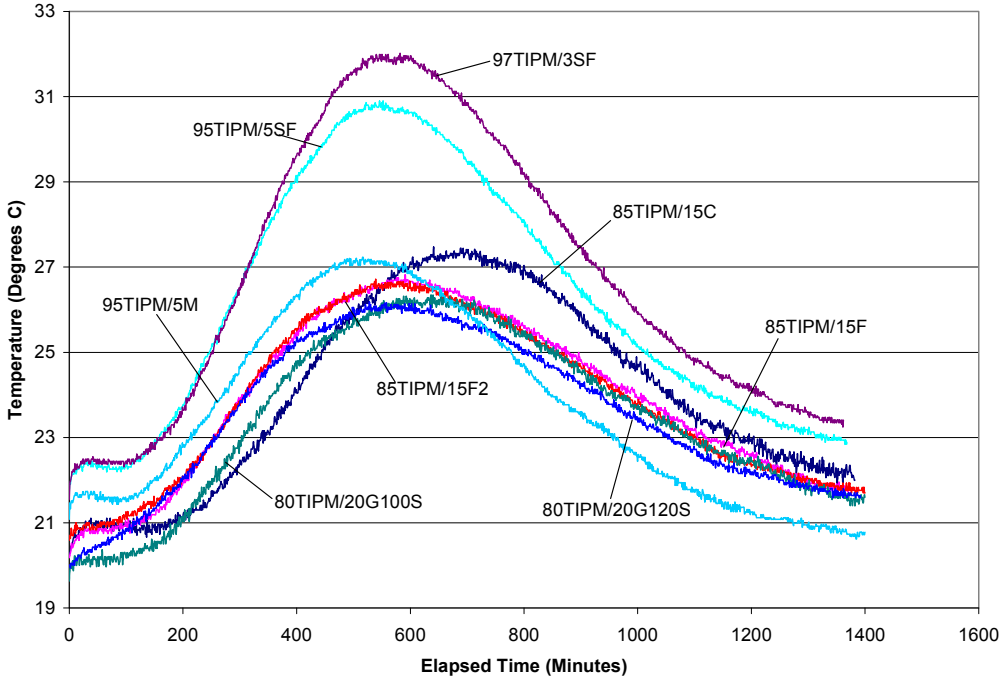

Figure C-17. Heat signature for mixtures containing greater than 80% Type IPM PC

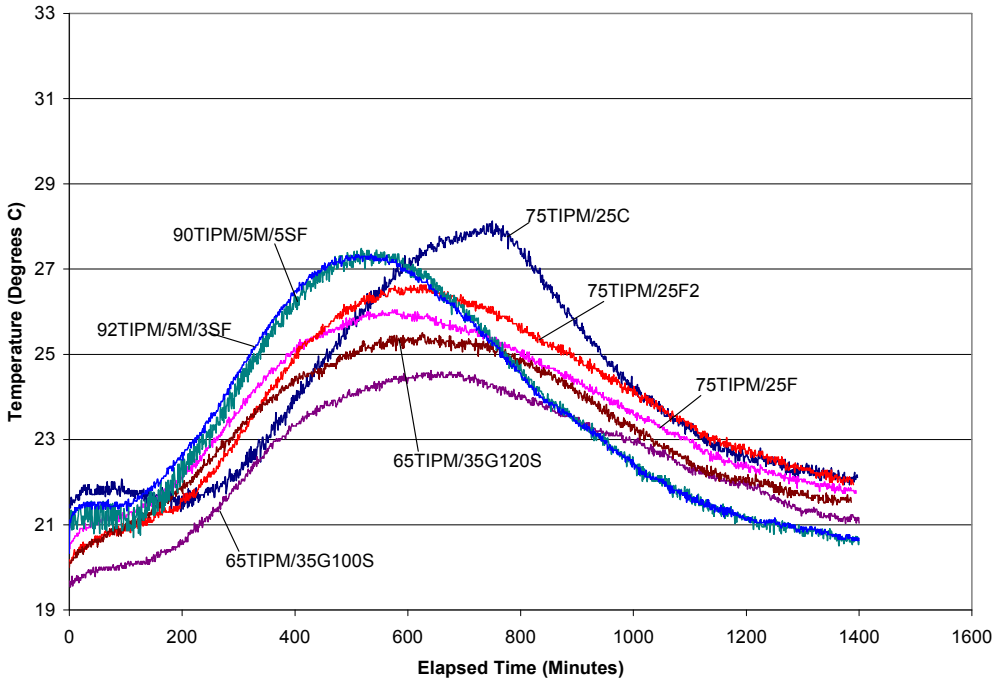

Figure C-18. Heat signature for mixtures containing Type IPM PC

APPENDIX D – SET TIME AND MORTAR FLOW RESULTS

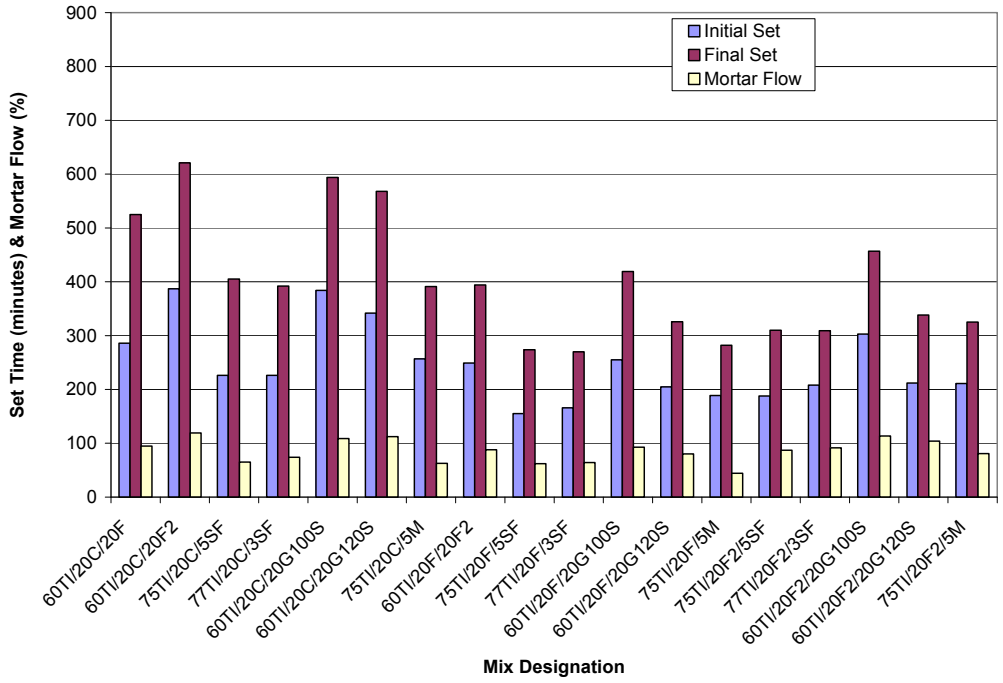

Figure D-1. Set time and mortar flow for mixtures containing Type I PC and 20% FA

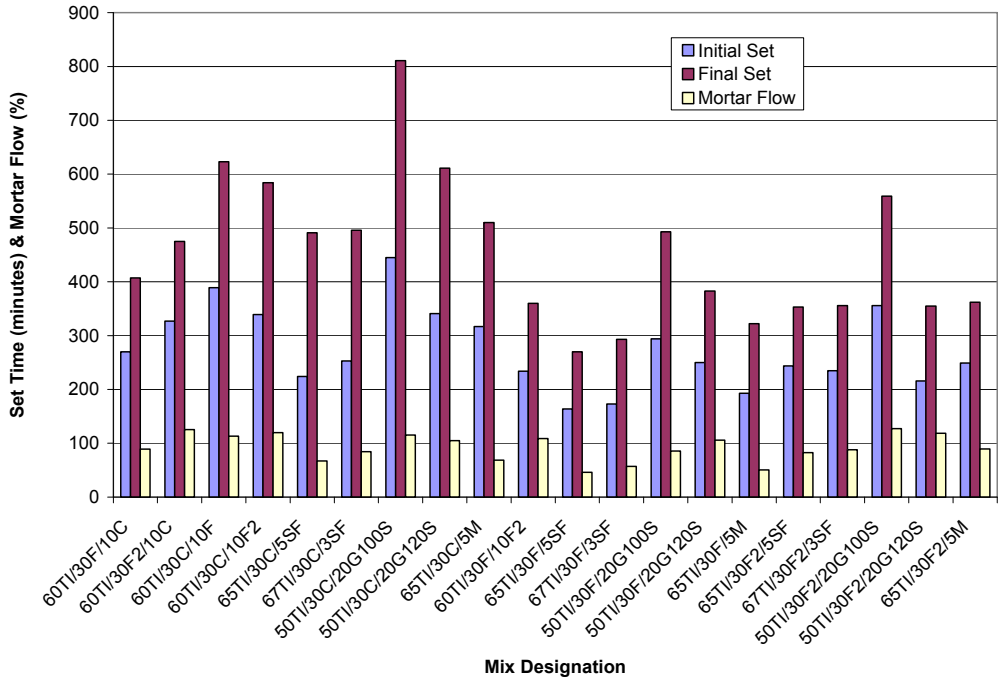

Figure D-2. Set time and mortar flow for mixtures containing Type I PC and 30% FA

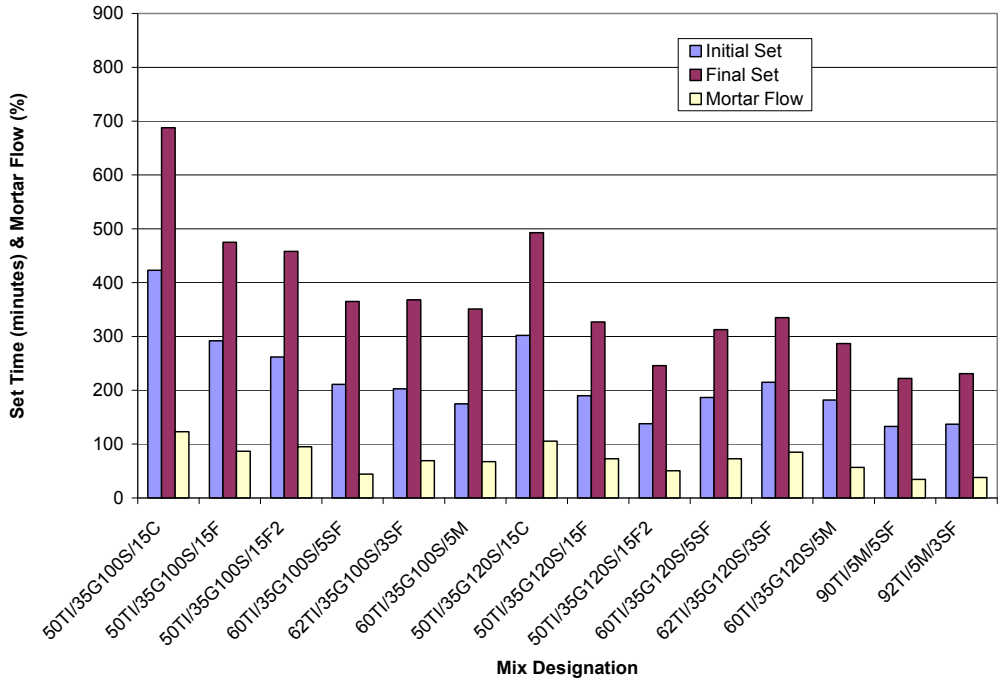

Figure D-3. Set time and mortar flow for mixtures containing Type I PC and 35% GGBFS or Type I PC and 5% metakaolin

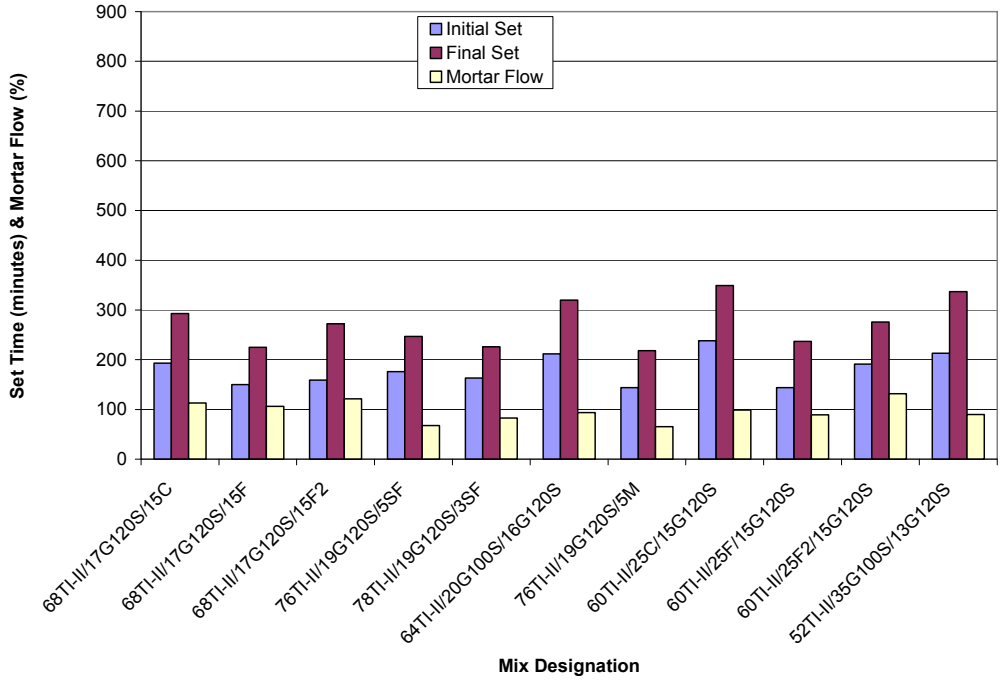

Figure D-4. Set time and mortar flow for mixtures containing Type I/II PC

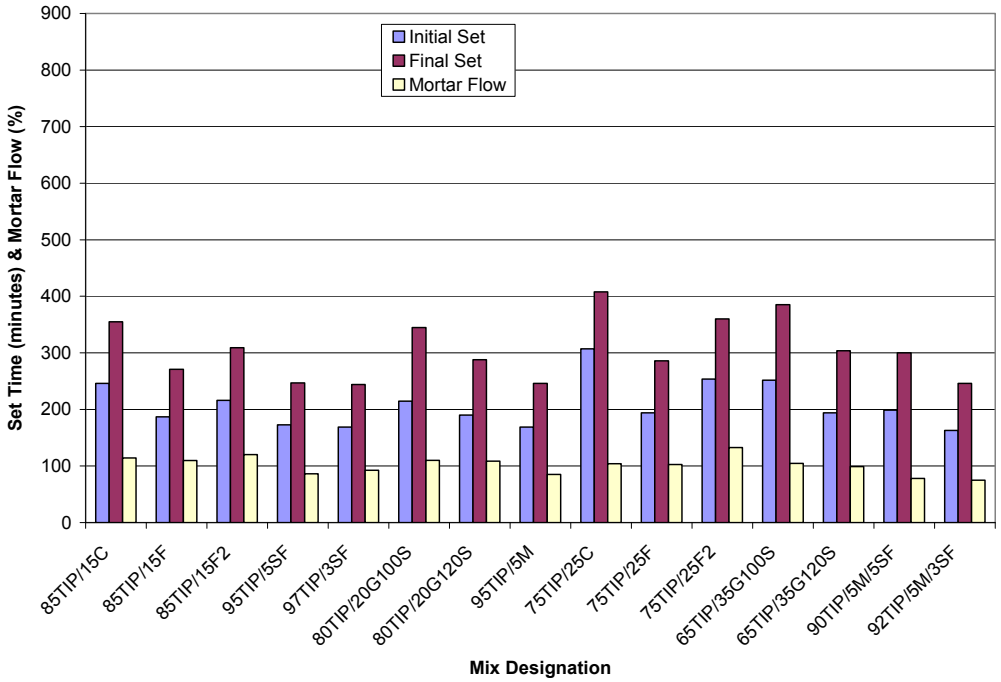

Figure D-5. Set time and mortar flow for mixtures containing Type IP PC

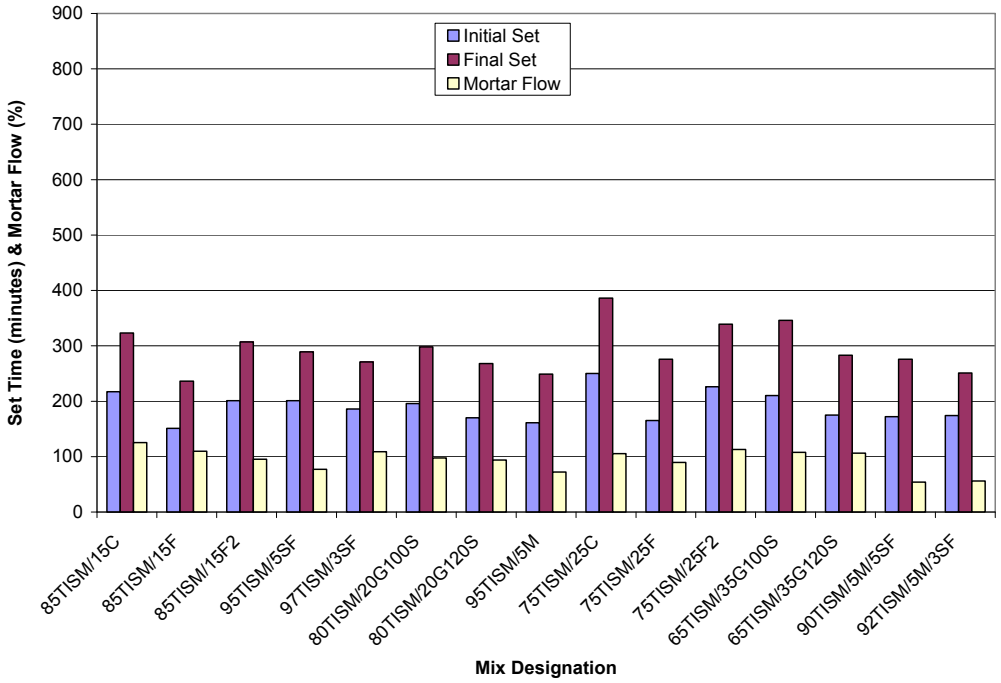

Figure D-6. Set time and mortar flow for mixtures containing Type ISM PC

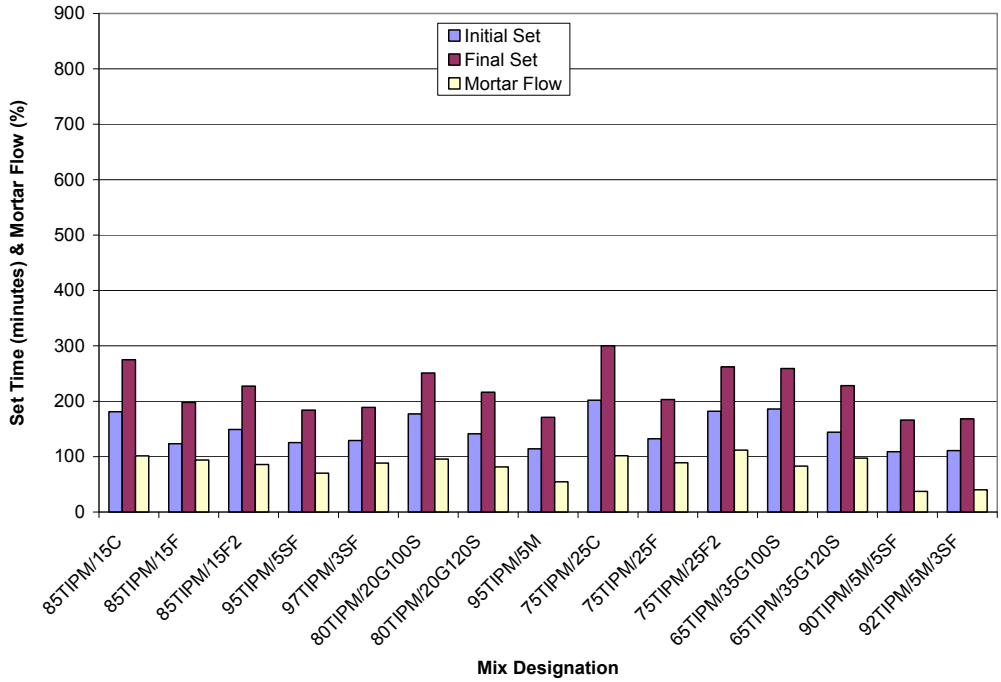

Figure D-7. Set time and mortar flow for mixtures containing Type IPM PC

APPENDIX E – COMPRESSIVE STRENGTH CURVES

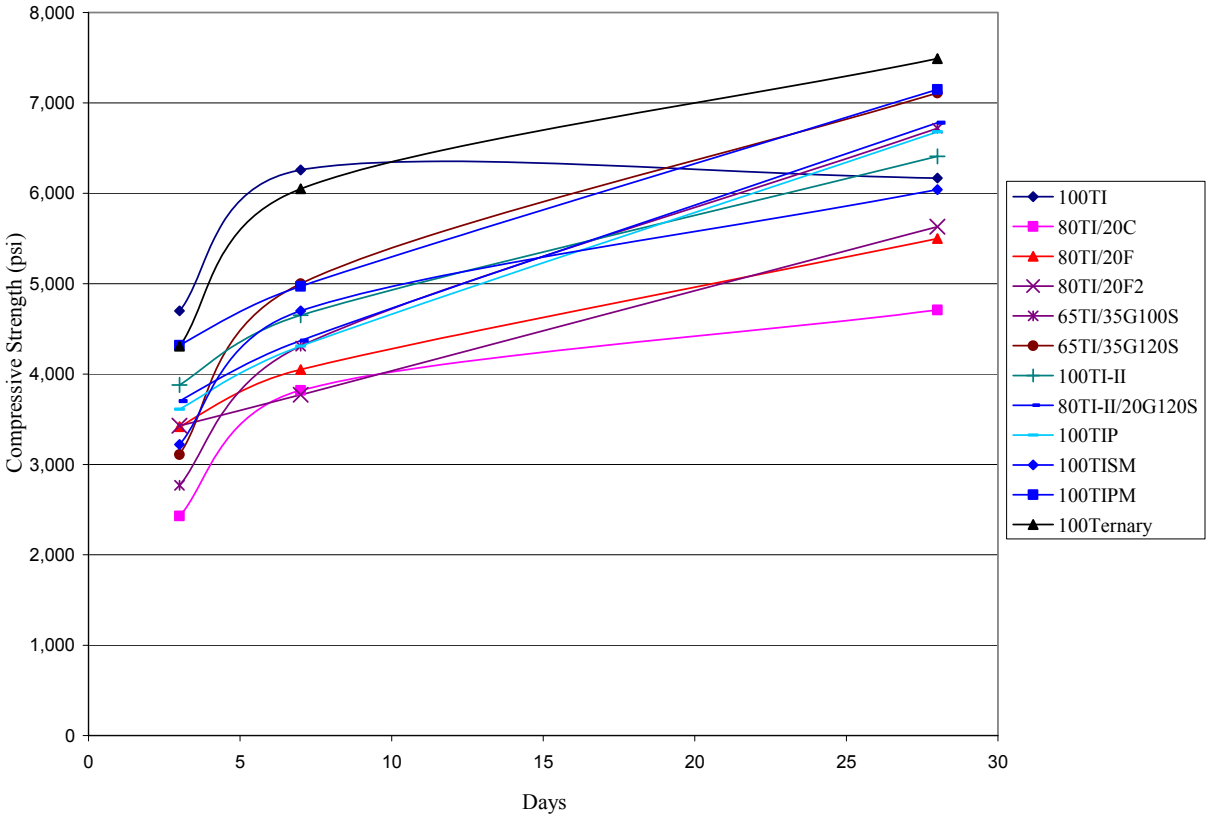

Figure E-1. Strength gain for control mortar mixtures

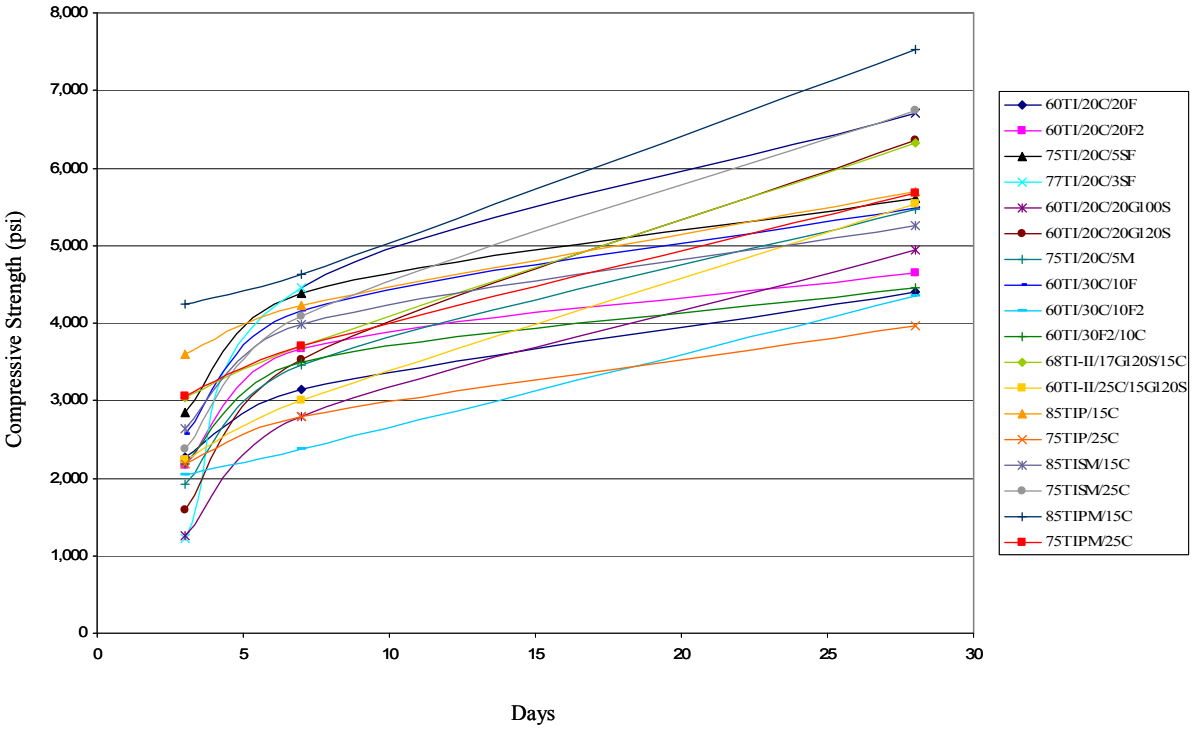

Figure E-2. Strength gain for mortar mixtures containing Class C fly ash

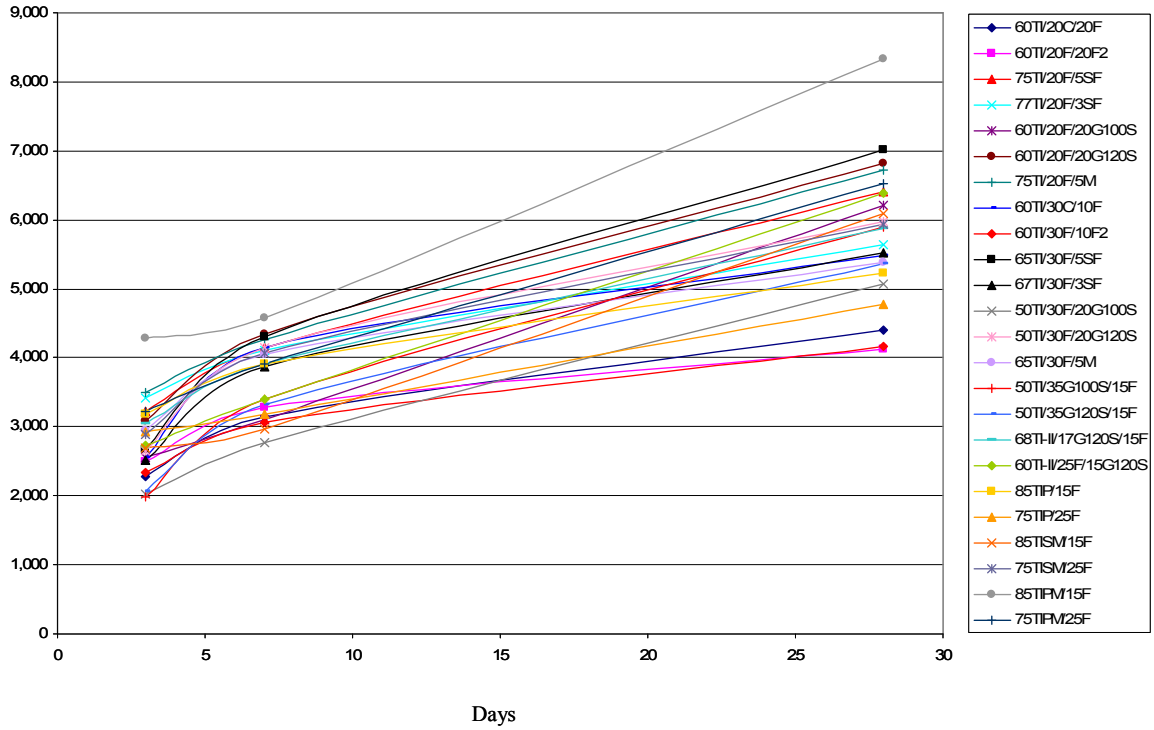

Figure E-3. Strength gain for mortar mixtures containing Class F fly ash

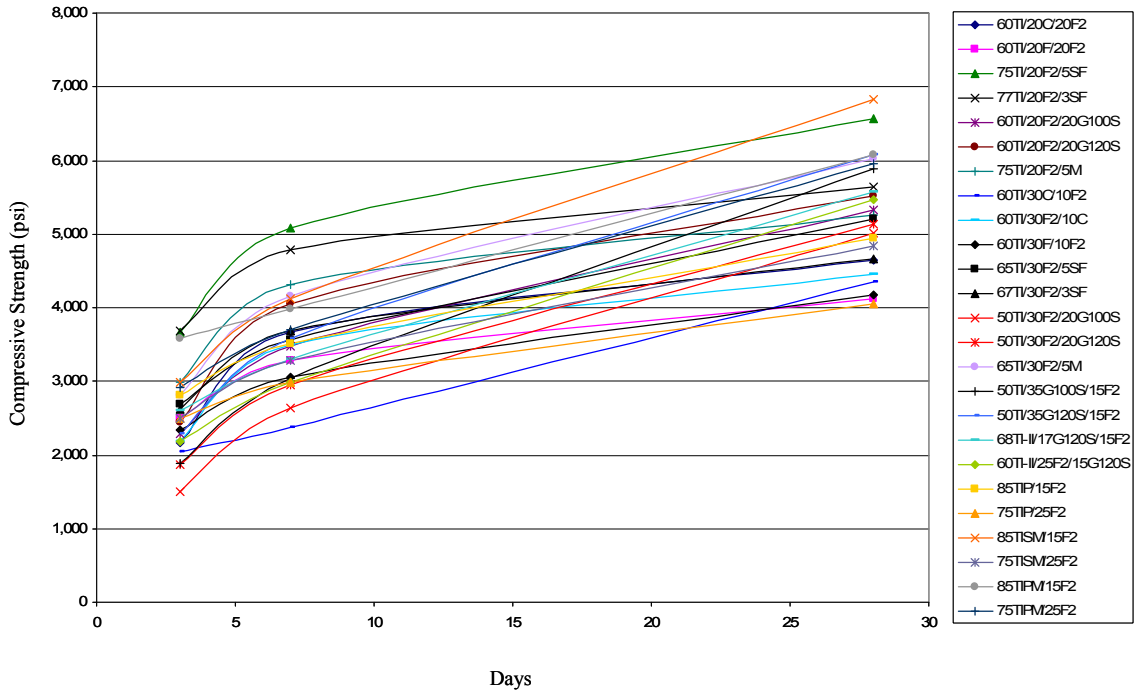

Figure E-4. Strength gain for mortar mixtures containing Class F2 fly ash

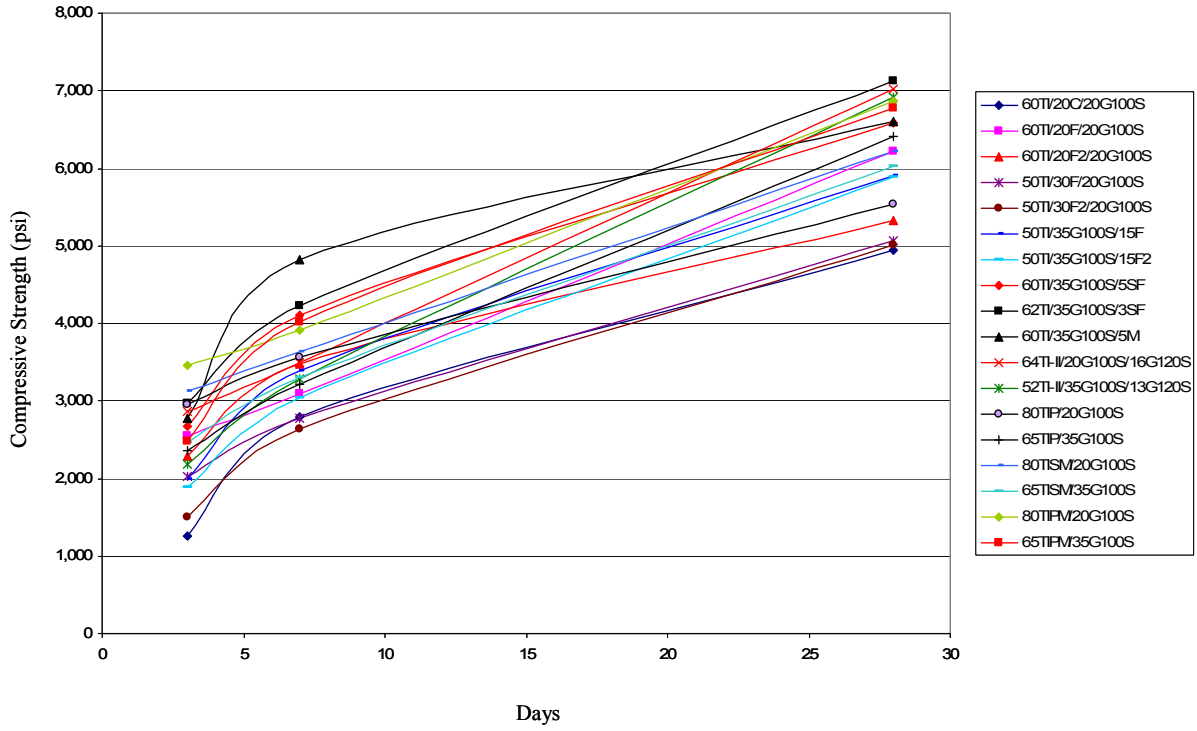

Figure E-5. Strength gain for mortar mixtures containing Grade 100 GGBFS

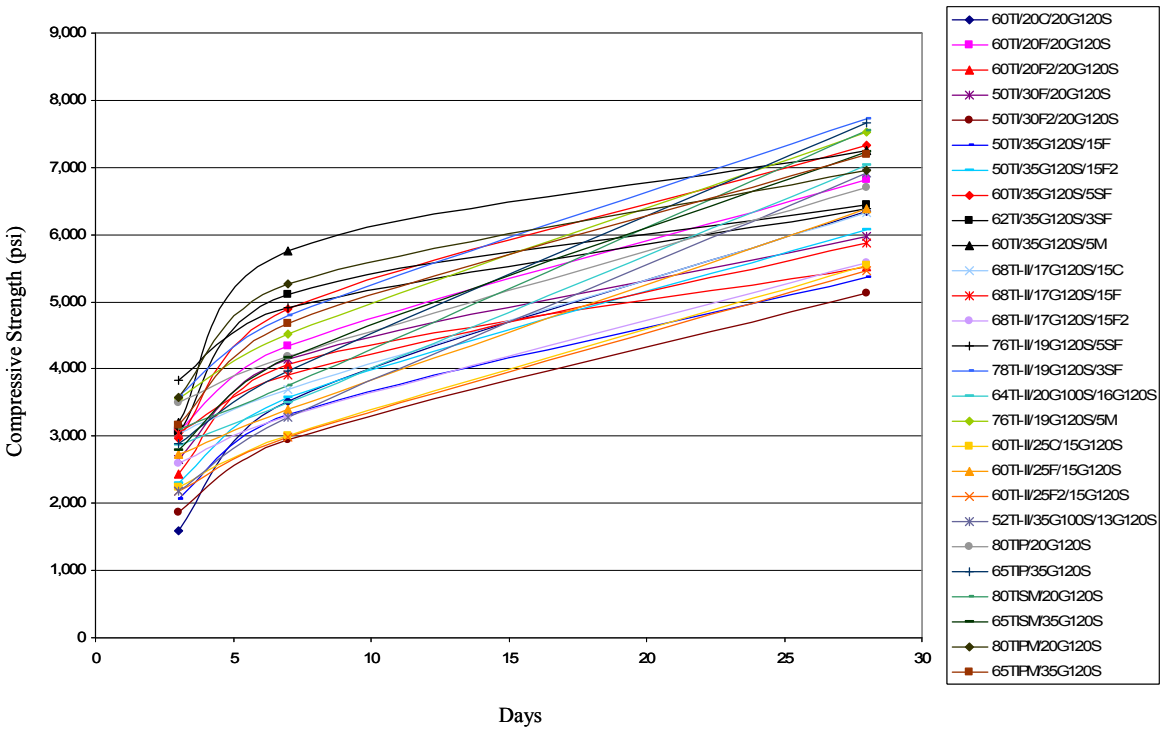

Figure E-6. Strength gain for mortar mixtures containing Grade 120 GGBFS

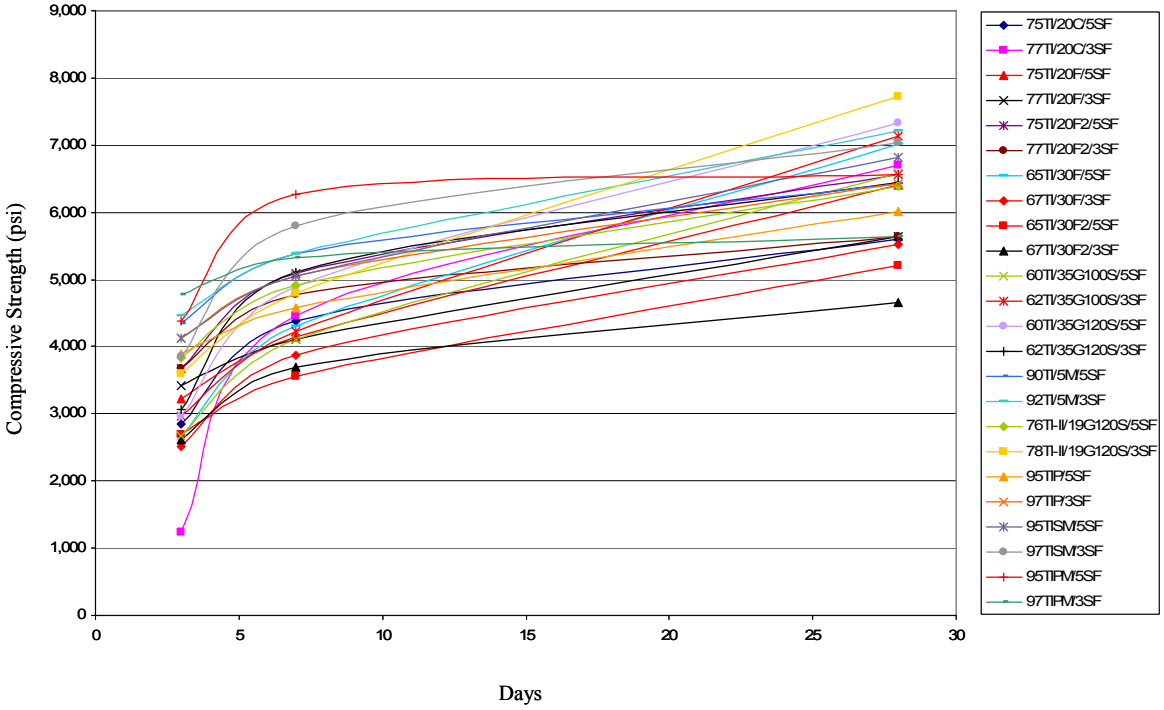

Figure E-7. Strength gain for mortar mixtures containing silica fume

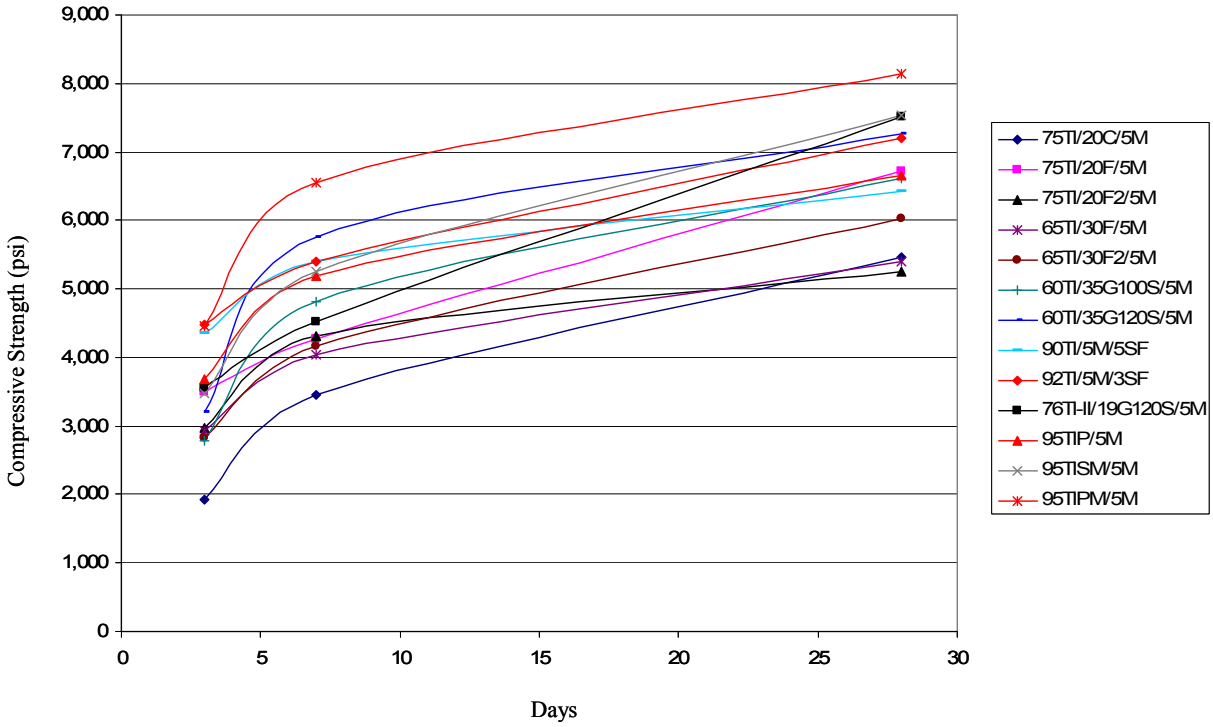

Figure E-8. Strength gain for mortar mixtures containing metakaolin

APPENDIX F – SHRINKAGE RESULTS

Table F-1. Shrinkage for control mixtures

Mixture ID	28 day shrinkage (%)
100TI	-0.1178
80TI/20C	-0.1109
80TI/20F	-0.1006
80TI/20F2	-0.1077
65TI/35G100S	-0.0866
65TI/35G120S	-0.0938
100TI-II	-0.0667
80TI-II/20G120S	-0.0893
100TIP	-0.0834
100TISM	-0.0791
100TIPM	-0.0766
100Ternary	-0.0819

Table F-2. Shrinkage for mortar mixtures containing Class C FA

Mixture ID	28 day shrinkage (%)
60TI/20C/20F	-0.0778
60TI/20C/20F2	-0.0840
75TI/20C/5SF	-0.0803
77TI/20C/3SF	-0.0820
60TI/20C/20G100S	-0.0808
60TI/20C/20G120S	-0.0978
75TI/20C/5M	-0.0713
60TI/30C/10F	-0.0805
60TI/30C/10F2	-0.0870
65TI/30C/5SF	-0.0855
67TI/30C/3SF	-0.0953
50TI/30C/20G100S	-0.0903
50TI/30C/20G120S	-0.0770
65TI/30C/5M	-0.0707
60TI/30F/10C	-0.0873
60TI/30F2/10C	-0.0840
50TI/35G100S/15C	-0.0930
50TI/35G120S/15C	-0.0867
68TI-II/17G120S/15C	-0.0878
60TI-II/25C/15G120S	-0.0813
85TIP/15C	-0.0738
75TIP/25C	-0.0670
85TISM/15C	-0.0803
75TISM/25C	-0.0700
85TIPM/15C	-0.0630
75TIPM/25C	-0.0705

Table F-3. Shrinkage for mortar mixtures containing Class F FA

Mixture ID	28 day shrinkage (%)
60TI/20F/20F2	-0.0765
75TI/20F/5SF	-0.0878
77TI/20F/3SF	-0.0815
60TI/20F/20G100S	-0.0988
60TI/20F/20G120S	-0.0920
75TI/20F/5M	-0.0923
60TI/30C/10F	-0.0805
60TI/30F/10C	-0.0873
60TI/30F/10F2	-0.1020
65TI/30F/5SF	-0.0925
67TI/30F/3SF	-0.0903
50TI/30F/20G100S	-0.1193
50TI/30F/20G120S	-0.0990
65TI/30F/5M	-0.0988
50TI/35G100S/15F	-0.0933
50TI/35G120S/15F	-0.0743
68TI-II/17G120S/15F	-0.0900
60TI-II/25F/15G120S	-0.0855
85TIP/15F	-0.0753
75TIP/25F	-0.0678
85TISM/15F	-0.0730
75TISM/25F	-0.0653
85TIPM/15F	-0.0813
75TIPM/25F	-0.0835

Table F-4. Shrinkage for mortar mixtures containing Class F2 FA

Mixture ID	28 day shrinkage (%)
60TI/20F/20F2	-0.0765
75TI/20F2/5SF	-0.0953
77TI/20F2/3SF	-0.1000
60TI/20F2/20G100S	-0.0920
60TI/20F2/20G120S	-0.0898
75TI/20F2/5M	-0.0853
60TI/30C/10F2	-0.0870
60TI/30F2/10C	-0.0840
60TI/30F/10F2	-0.1020
65TI/30F2/5SF	-0.0943
67TI/30F2/3SF	-0.0965
50TI/30F2/20G100S	-0.0970
50TI/30F2/20G120S	-0.1030
65TI/30F2/5M	-0.0788
50TI/35G100S/15F2	-0.0957
50TI/35G120S/15F2	-0.0798
68TI-II/17G120S/15F2	-0.0895
60TI-II/25F2/15G120S	-0.0910
85TIP/15F2	-0.0738
75TIP/25F2	-0.0730
85TISM/15F2	-0.0758
75TISM/25F2	-0.0720
85TIPM/15F2	-0.0660
75TIPM/25F2	-0.0770

Table F-5. Shrinkage for mortar mixtures containing Grade 100 GGBFS

Mixture ID	28 day shrinkage (%)
60TI/20F/20G100S	-0.0988
60TI/20F2/20G100S	-0.0920
50TI/30C/20G100S	-0.0903
50TI/30F/20G100S	-0.1193
50TI/30F2/20G100S	-0.0970
50TI/35G100S/15C	-0.0930
50TI/35G100S/15F	-0.0933
50TI/35G100S/15F2	-0.0957
60TI/35G100S/5SF	-0.0798
62TI/35G100S/3SF	-0.0813
60TI/35G100S/5M	-0.0790
64TI-II/20G100S/16G120S	-0.0875
52TI-II/35G100S/13G120S	-0.0888
80TIP/20G100S	-0.0938
65TIP/35G100S	-0.0968
80TISM/20G100S	-0.0753
65TISM/35G100S	-0.0735
80TIPM/20G100S	-0.0768
65TIPM/35G100S	-0.0763

Table F-6. Shrinkage for mortar mixtures containing Grade 120 GGBFS

Mixture ID	28 day shrinkage (%)
60TI/20F/20G120S	-0.0920
60TI/20F2/20G120S	-0.0898
50TI/30C/20G120S	-0.0770
50TI/30F/20G120S	-0.0990
50TI/30F2/20G120S	-0.1030
50TI/35G120S/15C	-0.0867
50TI/35G120S/15F	-0.0743
50TI/35G120S/15F2	-0.0798
60TI/35G120S/5SF	-0.0880
62TI/35G120S/3SF	-0.0865
60TI/35G120S/5M	-0.0738
68TI-II/17G120S/15C	-0.0878
68TI-II/17G120S/15F	-0.0900
68TI-II/17G120S/15F2	-0.0895
76TI-II/19G120S/5SF	-0.0823
78TI-II/19G120S/3SF	-0.0933
64TI-II/20G100S/16G120S	-0.0875
76TI-II/19G120S/5M	-0.0723
60TI-II/25C/15G120S	-0.0813
60TI-II/25F/15G120S	-0.0855
60TI-II/25F2/15G120S	-0.0910
52TI-II/35G100S/13G120S	-0.0888
80TIP/20G120S	-0.0853
65TIP/35G120S	-0.0840
80TISM/20G120S	-0.0750
65TISM/35G120S	-0.0790
80TIPM/20G120S	-0.0828
65TIPM/35G120S	-0.0853

Table F-7. Shrinkage for mortar mixtures containing silica fume

Mixture ID	28 day shrinkage (%)
77TI/20C/3SF	-0.0820
75TI/20F/5SF	-0.0878
77TI/20F/3SF	-0.0815
75TI/20F2/5SF	-0.0953
77TI/20F2/3SF	-0.1000
65TI/30C/5SF	-0.0855
67TI/30C/3SF	-0.0953
65TI/30F/5SF	-0.0925
67TI/30F/3SF	-0.0903
65TI/30F2/5SF	-0.0943
67TI/30F2/3SF	-0.0965
60TI/35G100S/5SF	-0.0798
62TI/35G100S/3SF	-0.0813
60TI/35G120S/5SF	-0.0880
62TI/35G120S/3SF	-0.0865
90TI/5M/5SF	-0.0980
92TI/5M/3SF	-0.1005
76TI-II/19G120S/5SF	-0.0823
78TI-II/19G120S/3SF	-0.0933
95TIP/5SF	-0.0955
97TIP/3SF	-0.0903
95TISM/5SF	-0.0705
97TISM/3SF	-0.0823
95TIPM/5SF	-0.0783
97TIPM/3SF	-0.0800

Table F-8. Shrinkage for mortar mixtures containing metakaolin

Mixture ID	28 day shrinkage (%)
75TI/20F/5M	-0.0923
75TI/20F2/5M	-0.0853
65TI/30C/5M	-0.0707
65TI/30F/5M	-0.0988
65TI/30F2/5M	-0.0788
60TI/35G100S/5M	-0.0790
60TI/35G120S/5M	-0.0738
90TI/5M/5SF	-0.0980
92TI/5M/3SF	-0.1005
76TI-II/19G120S/5M	-0.0723
95TIP/5M	-0.0823
95TISM/5M	-0.0738
95TIPM/5M	-0.0798